

HW1 Solutions

See MATLAB demonstration

Solution

Given whole 3D coordinates of a specific anatomical object such as an amygdala, there are several ways to calculate total surface area comprised of triangular meshes but only two concepts would be introduced in this document as following.

1) In three dimensions, the area of a general triangle $\{A = (X_A, Y_A, Z_A), B = (X_B, Y_B, Z_B), C = (X_C, Y_C, Z_C)\}$ is the **Pythagorean sum of the areas** of the respective projections on the three principle planes

$$S = \frac{1}{2} \sqrt{\left(\det \begin{pmatrix} Y_B - Y_A & Z_B - Z_A \\ Y_C - Y_A & Z_C - Z_A \end{pmatrix}\right)^2 + \left(\det \begin{pmatrix} X_B - X_A & Z_B - Z_A \\ X_C - X_A & Z_C - Z_A \end{pmatrix}\right)^2 + \left(\det \begin{pmatrix} X_B - X_A & Y_B - Y_A \\ X_C - X_A & Y_C - Y_A \end{pmatrix}\right)^2}$$

2) The shape of the triangle is determined by the lengths of the sides alone. Therefore the area S also can be derived from the lengths of the sides. **By Heron's formula**,

$$S = \sqrt{s(s-a)(s-b)(s-c)}$$

where $S = \frac{1}{2}(a+b+c)$ is the semiperimeter of half of the triangle's perimeter.

To implement these concepts as a matlab code (including only the essential part),

```

for i=1:2536
    p=coord(tri(i,:),:);
    % algorithm 1 [x1 y1 z1; x2 y2 z2; x3 y3 z3]
    % 0.5 x sqrt(pow(det([y2-y1 z2-z1; y3-y1 z3-z1]),2)
    %           + pow(det([x2-x1 z2-z1; x3-x1 z3-z1]),2)

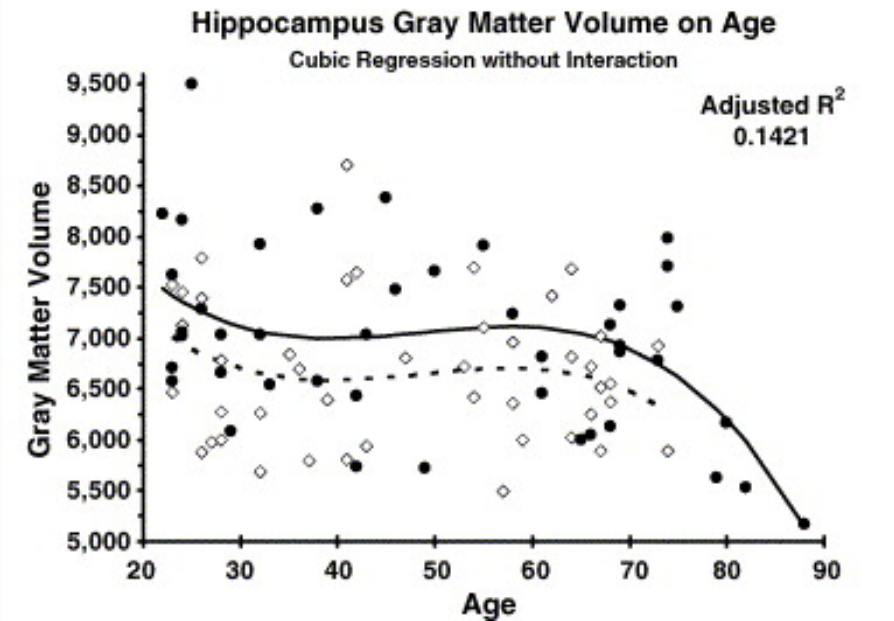
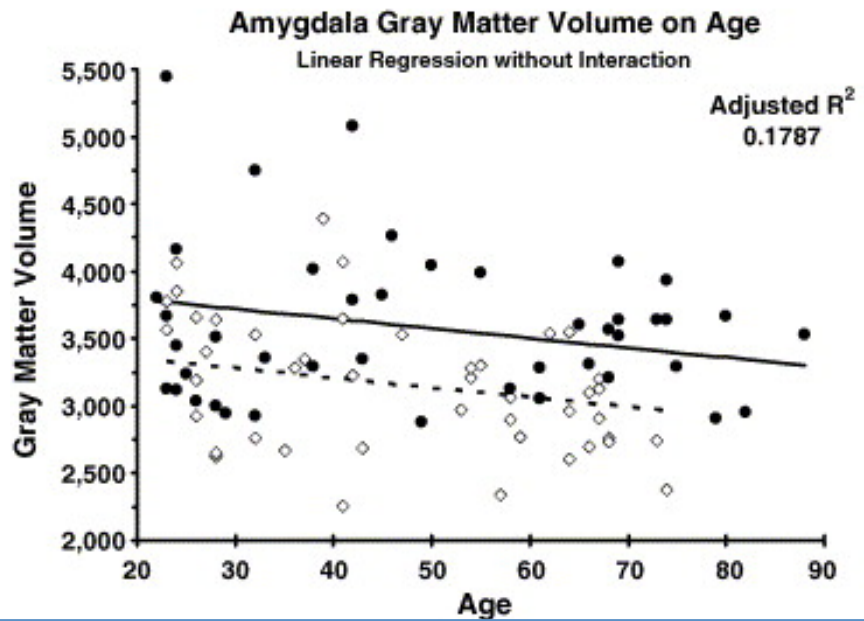
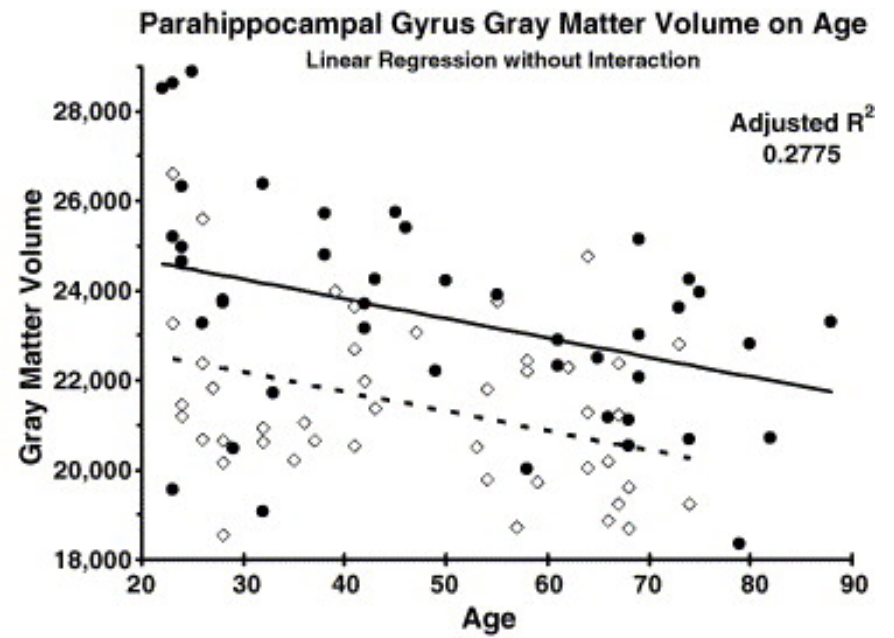
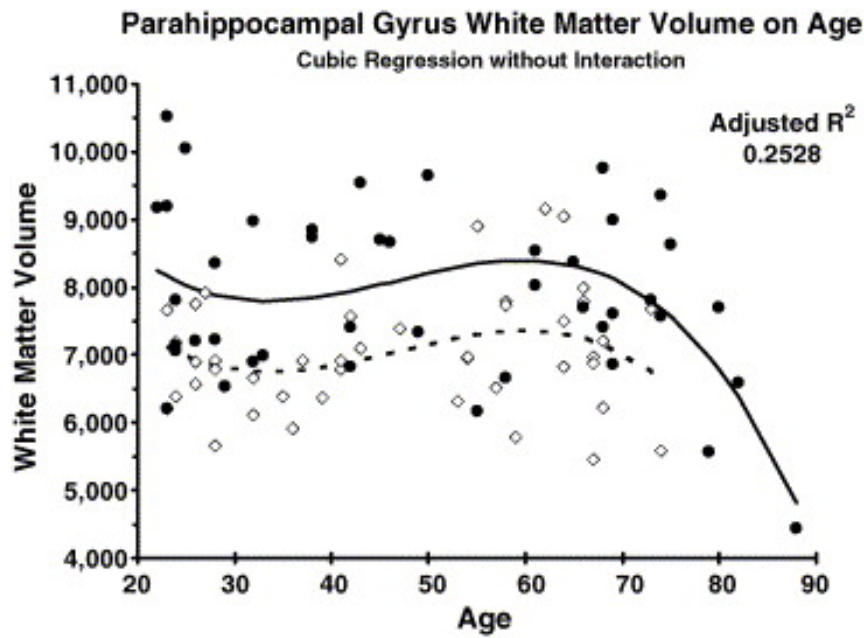
```

HW2 Solutions

For a normal population, does amygdala volume increase or decrease with age? Discuss the problem with the sufficient number of references.

Jiwon Hur

The significant and irreversible loss of volume in amygdala with aging is observed because all neurons in the brain do not regenerate (Rakic, 1985). The amygdala shows decreased patterns in volume with age in a linear fashion (presumably through the steady loss of neurons over the lifespan) (Mu et al., 1999). The amygdala as well as gray matter in the parahippocampal gyrus as a whole decreased linearly with age (Allen et al., 2005). Jack Jr (1997) also reported the average amygdala volume decline of $20.75\text{mm}^3/\text{year}$.



Most studies use fixed effect model

Allen et al., 2005

@article{jack1997medial, title={{Medial temporal atrophy on MRI in normal aging and very mild Alzheimer's disease}}, author={Jack Jr, C.R. and Petersen, R.C. and Xu, Y.C. and Waring, S.C. and O'Brien, P.C. and Tangalos, E.G. and Smith, G.E. and Ivnik, R.J. and Kokmen, E.}, journal={Neurology}, volume={49}, pages={786}, year={1997}}

@article{allen2005normal, title={{Normal neuroanatomical variation due to age: the major lobes and a parcellation of the temporal region}}, author={Allen, J.S. and Bruss, J. and Brown, C.K. and Damasio, H.}, journal={Neurobiology of Aging}, volume={26}, pages={1245--1260}, year={2005}}

@article{rakic1985limits, title={{Limits of neurogenesis in primates}}, author={Rakic, P.}, journal={Science}, volume={227}, pages={1054}, year={1985}}

@article{mu1999quantitative, title={{A quantitative MR study of the hippocampal formation, the amygdala, and the temporal horn of the lateral ventricle in healthy subjects 40 to 90 years of age}}, author={Mu, Q. and Xie, J. and Wen, Z. and Weng, Y. and Shuyun, Z.}, journal={American Journal of Neuroradiology}, volume={20}, pages={207--211}, year={1999}}

Hansem Sohn

It was observed that the amygdala volume increases during typical childhood and adolescence (Ostby et al., J Neuro, 2009). It might be that temporal lobes including the amygdala and hippocampus play a role in emotion, language, and memory and these cognitive functions become pronounced between ages of 4 and 18 years (Giedd, J of Adolescent Health, 2008).

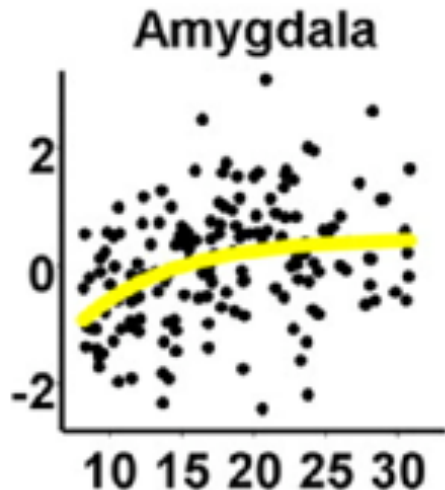
Sex-specific maturational volume changes in the amygdala have been shown (Giedd et al., J Comp Neurol, 1996).

For adults, the amygdala volume with its adjacent hippocampus was relatively preserved compared to the global loss of the brain volume by ages (Good et al., Neuroimage, 2001).

No correlation between the amygdala volume and age was found after controlling for other factors (Cherubini et al., Neuroimage, 2009).

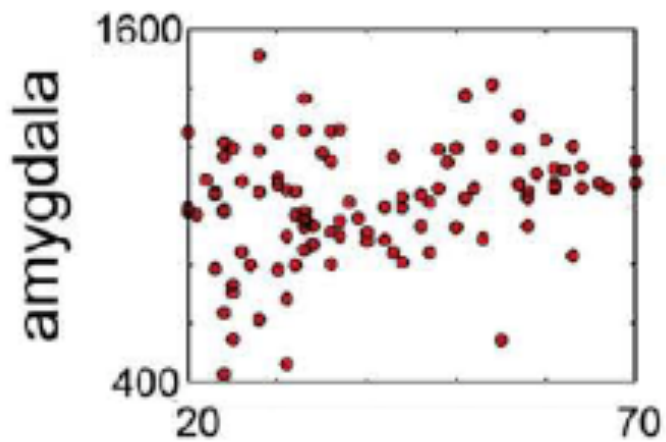
Most likely improper processing and analysis or possibly biased sampling

Seok Jun Hong



Ylva Ostby et al., 2007. J. Neurosci.

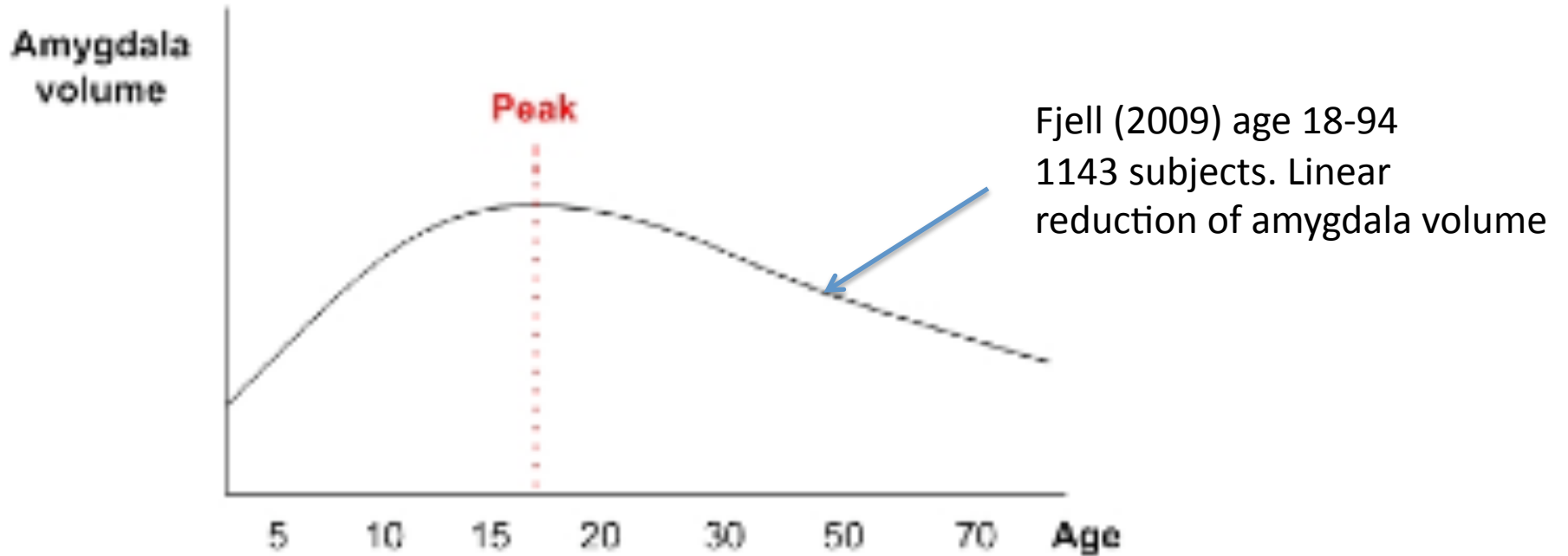
1~18y age group, both boys and girls, shows the positive correlation between age and an amygdala volume regardless of whether they have psychiatric disorders or not (Brendon MN et al. Arch Gen Psych 2006; Matthew WM et al. Arch Gen Psych 2009).



Andrea Cherubini et al., 2009. NeuroImage

However entering the post-adolescence, it has reported that such a trend become to converge into a specific volume (2000~2100mm³) (Hilary PB et al. Arch Gen Psych 2003). It is thought that this convergence might be due to the saturation of rapid brain development and relatively increased white matter tissue.

Dajung Kim



Note 1. Specify sample size. There is huge difference between a 40-subject study vs. a 1143-subject study.

Note 2. Amount of gray matter directly correspond to the amount of fMRI activation. So for fMRI analysis in amygdala regions, you may want to covariate fMRI signal with amygdala volume (see Oaks et al., 2007, NeuroImage)

HW 3

Using the code developed in HW1, compute the surface area of both inner and outer cortical surfaces for all subjects. Then determine the significance of the group effect on cortical thickness while accounting for total cortical surface area and age for all mesh vertices. What is the maximum F statistic value and the corresponding p-value?

Provide MATLAB codes.

The inner surface areas of autistic subjects are significantly smaller than those of controls and to a lesser extent, outer surface areas exhibit similar pattern as well (two sample t-test was used).

It requires computing the areas of 4 different surfaces:

1. outer cortical surface of control
2. inner cortical surface of control
3. outer cortical surface of autism
4. inner cortical surface of autism

Some students wrote extremely lengthy code repeating doing Heron's formula. Make a function call like

Function `a=compute_area(surface)`

This function should compute the surface area of the given surface. Then simply call this function 4 times.

What does it mean by covarying with cortical surface area?

You should have asked yourself at least two questions when you saw this problem.

1. Which surface area to covariate?

Inner and outer cortical surface areas are highly correlated. So it does not make any sense to add two highly correlated variables in the GLM. So simply put the either outer or inner surface area into a model but not both.

Correct models:

$\text{thickness} = \lambda_1 + \lambda_2 * \text{age} + \lambda_3 * \text{group} + \beta_1 * \text{inner_surface}$

$\text{thickness} = \lambda_1 + \lambda_2 * \text{age} + \lambda_3 * \text{group} + \beta_1 * \text{outer_surface}$

$\text{thickness} = \lambda_1 + \lambda_2 * \text{age} + \lambda_3 * \text{group} + \beta_1 * (\text{inner_surface} + \text{outer_surface})$

$\text{thickness} = \lambda_1 + \lambda_2 * \text{age} + \lambda_3 * \text{group} + \beta_1 * (\text{inner_surface} + \text{outer_surface}) / 2$

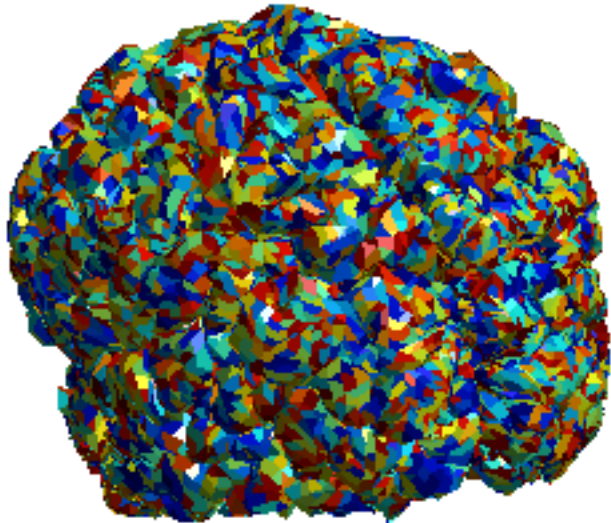
Incorrect model:

$\text{thickness} = \lambda_1 + \lambda_2 * \text{age} + \lambda_3 * \text{group} + \beta_1 * \text{inner_surface} + \beta_2 * \text{outer_surface}$

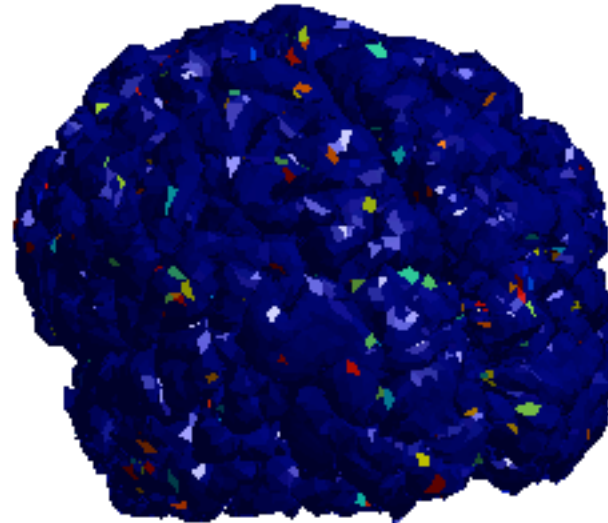
2. *Why covarying with cortical surface?*

Since there is no information about brain size, cortical surface serves as the only available global index for the brain size.

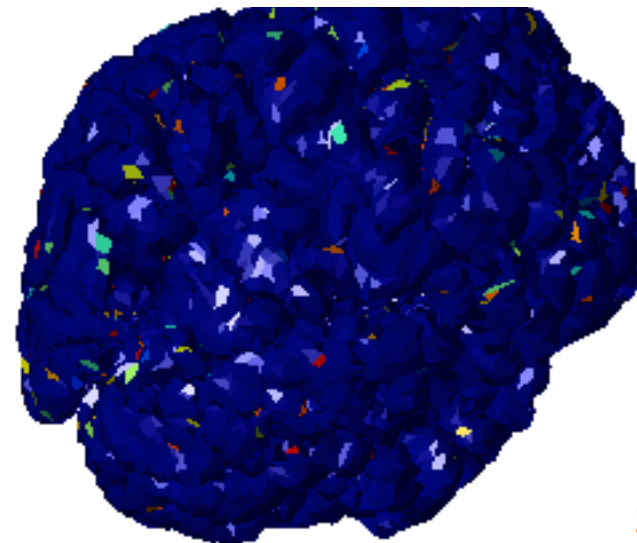
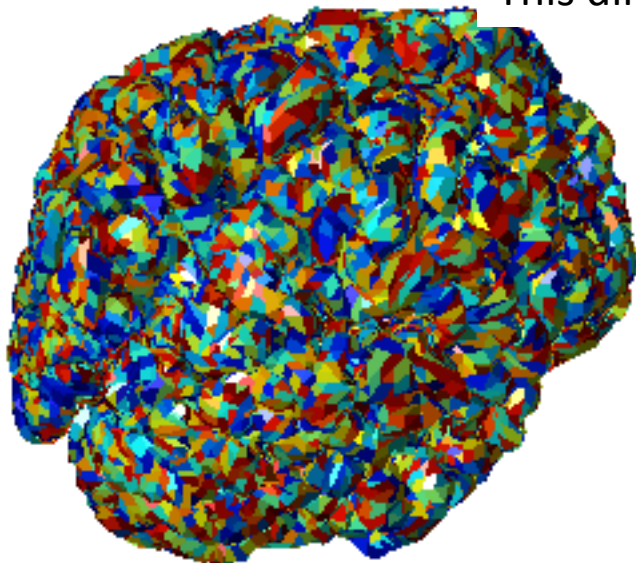
Raw result mapping p-value



Thresholded with p-value < 0.05



There are a lot of signals that are not clustered together.
All these can't possibly be signal. So there is a need for smoothing
This directly demonstrates the need for surface-based smoothing



HW4 Solutions

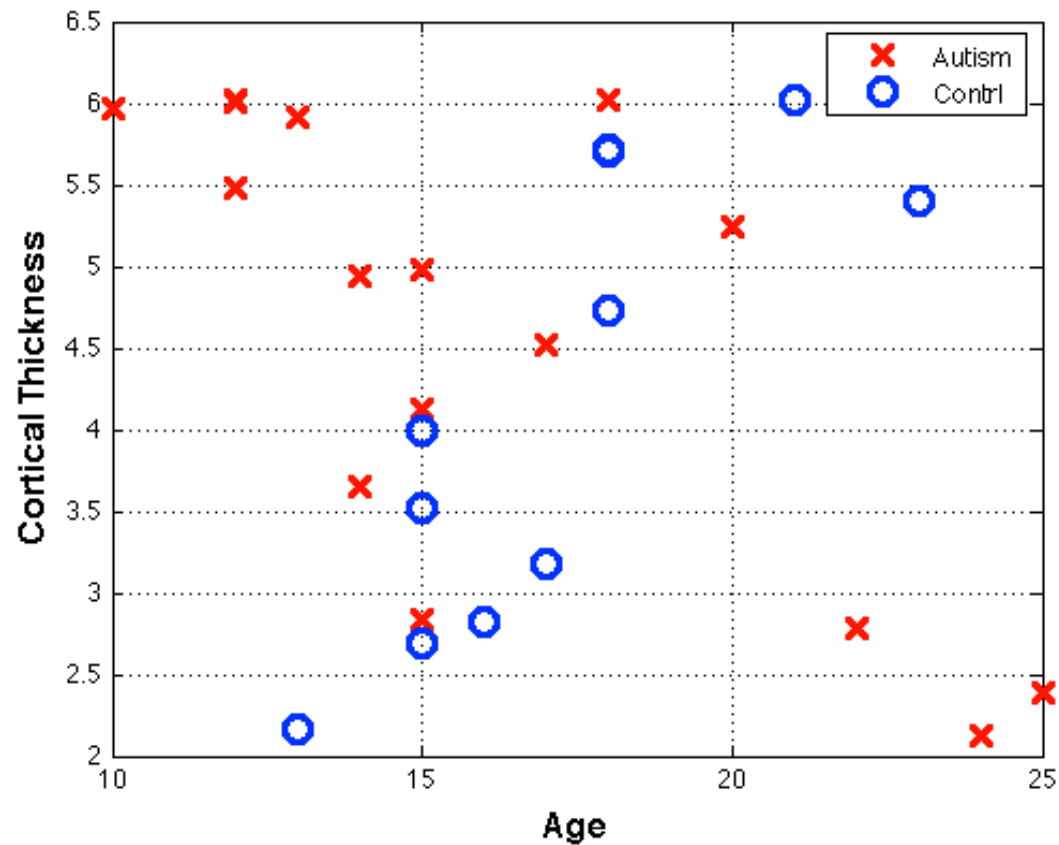
Set up the general linear model testing for interaction between the group and age for all mesh vertices. That is, you need to test the significance of the coefficient β_1 in the model:

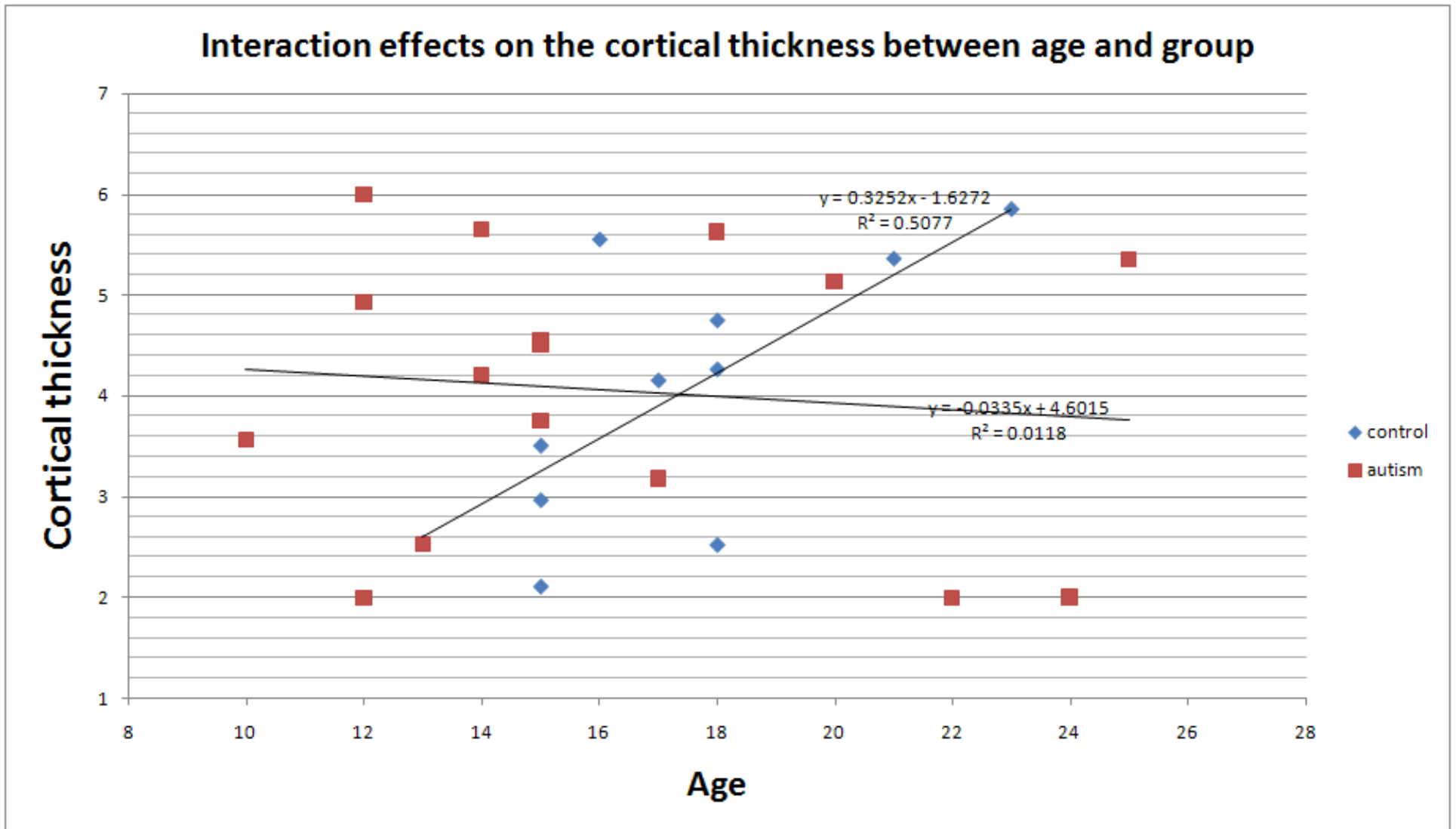
$$\text{thickness} = \lambda_1 + \lambda_2 * \text{age} + \lambda_3 * \text{group} + \beta_1 * \text{age} * \text{group}$$

What vertex gives you the most significant interaction?
How will you interpret your result?

Hansem Sohn

The interaction term in the GLM test whether the effect of age varies between the autism patients and healthy subjects. In other words, the sign and/or magnitude of the age effect on the cortical thickness can be different in the two groups.





If you simply shown this plot, there is no need to even explaining what interaction term really means. But in order to be able to draw this plot, you had to know what interaction term really means.

HW5 Solutions

Following Chung et al. NI 2004 paper, perform Gaussian kernel smoothing and perform a two sample t-test on white matter density. Discuss your result. There is no need to do multiple comparisons.

The problem ask you to find out why people do smoothing before any statistical analysis.

Dajung Kim

Grid lines were drawn to identify the region of significant signal.

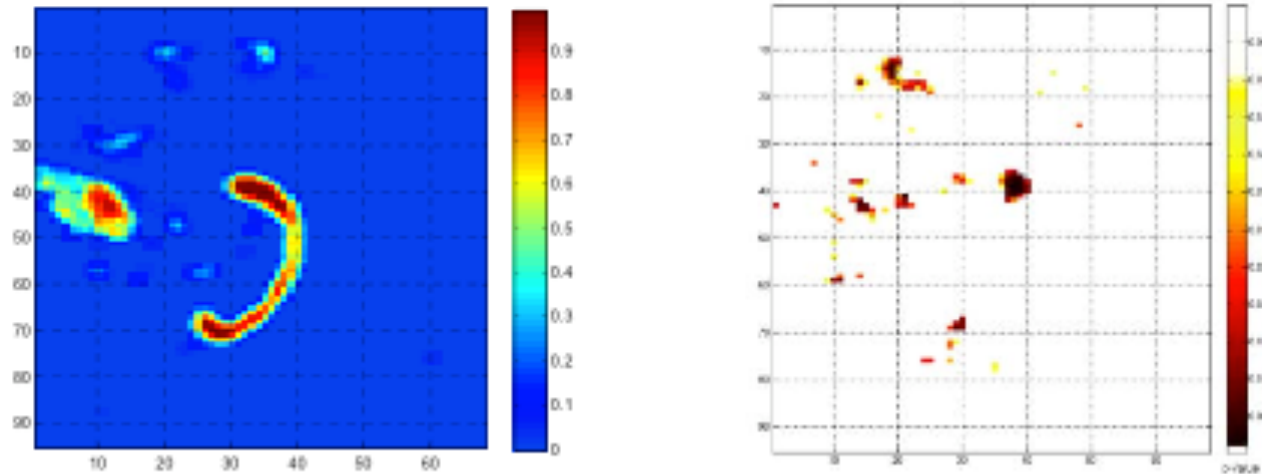
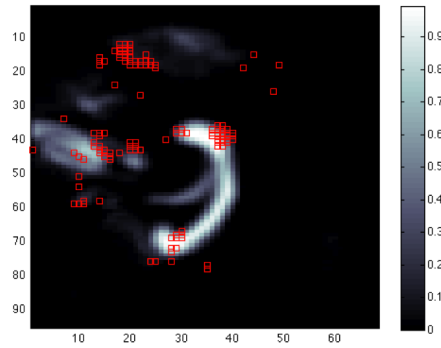


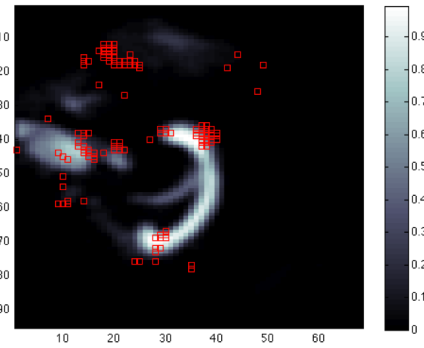
Figure 2. The mean white matter density of control group (left). The second figure represents p -value map from t-test. Gridline is drawn for detection of the statistically significant regions with structure of the corpus callosum.

Statistically significant region is near or outside of the boundary of the splenium. The observed group difference might be the result of mis-registration. Whitwell (2009) pointed out that VBM cannot differentiate the real volume change from group difference due to mis-registration.

<Control>

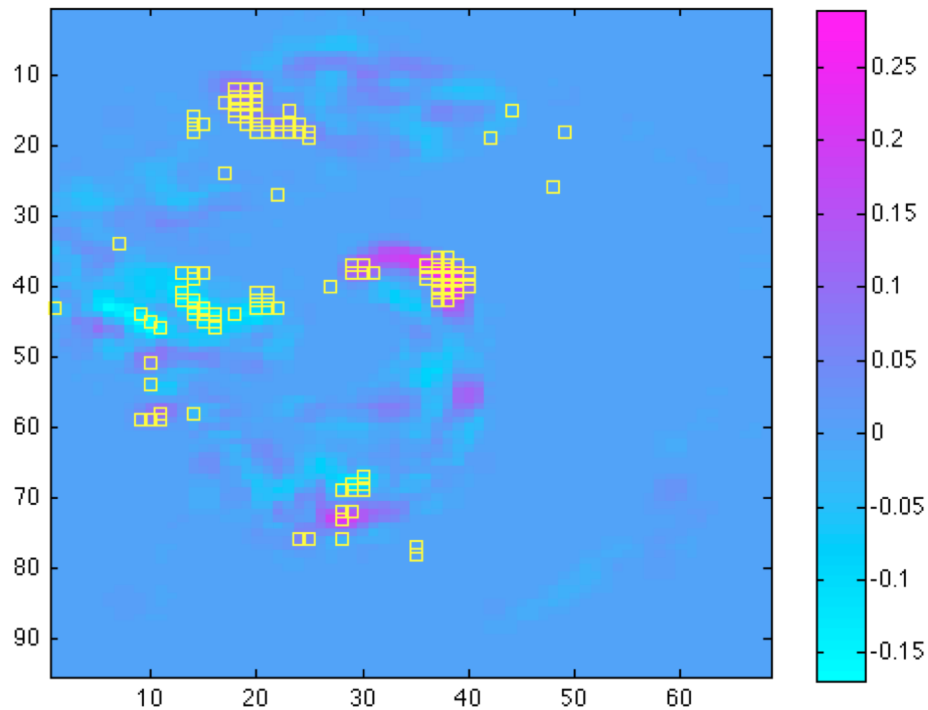


<Autism>



Hansem Sohn

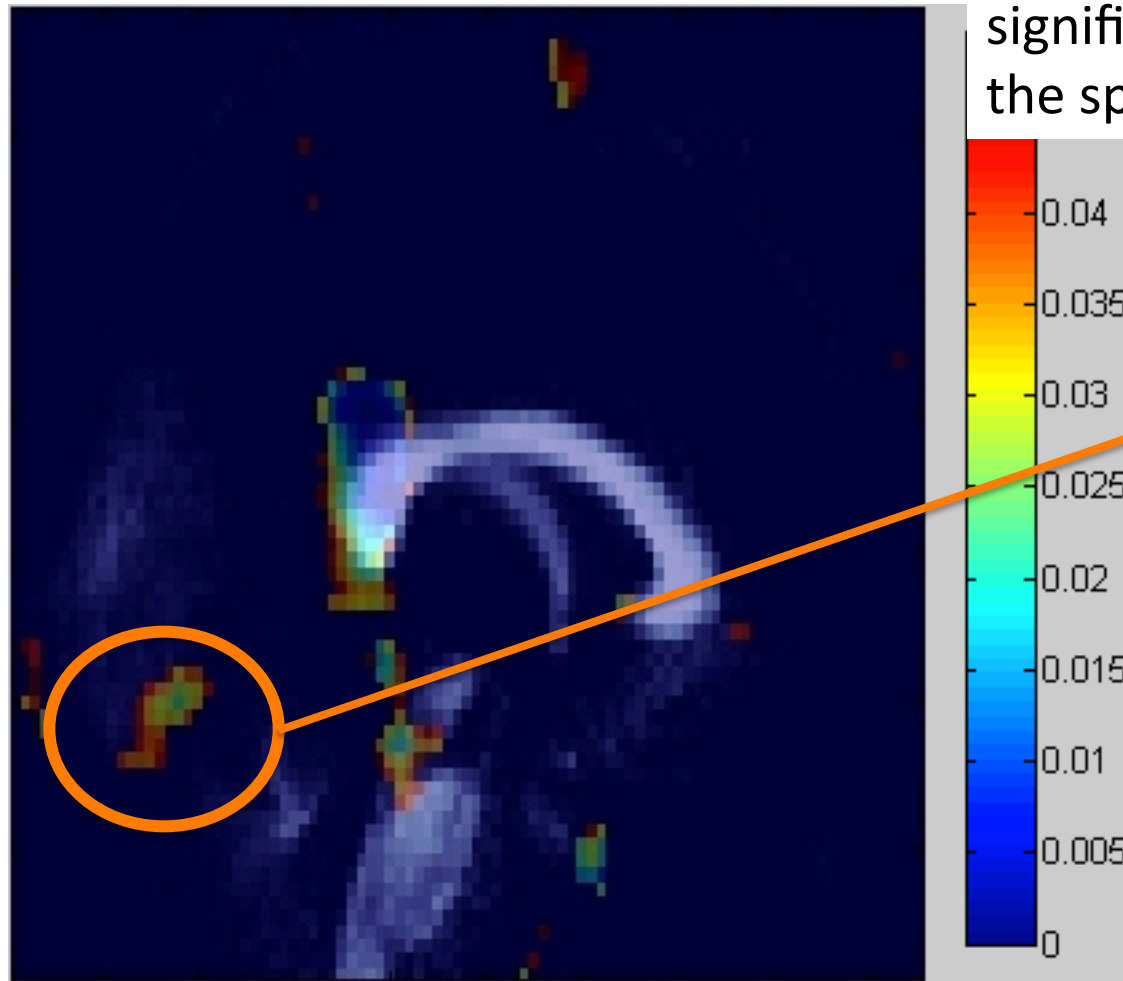
Difference map



Two sample t-test is testing for the significant of the difference

Seok Jun Hong

The p-values of the two-sample t-test are overlaid on the average anatomical density map of the corpus callosum (CC). The most significant signal is observed in the splenium of CC.



Why there are signal outside of the brain?

Mainly image processing artifacts. Simply you should not try to over interpret or over analyze these.

If you know the issue of multiple comparison corrections, you may unnecessarily worry about this. But there is no need.

HW6 Solutions

Write an EM algorithm for estimating 2 unknown parameters μ_1 and μ_2 assuming the mixing proportion p_1 and p_2 , and s.d. σ_1 and σ_2 are known. Need to go through the textbook for detail.

Seok Jun Hong

The underlying principle of this algorithm is to estimate the parameters of a model which maximizes the likelihood of data approximately by the repeated two step (expectation and maximization steps) since the direct analytical estimation of the model parameters are not feasible.

Repeat until convergence: {

(E-step) For each i, j , set

$$w_j^{(i)} := p(z^{(i)} = j | x^{(i)}; \phi, \mu, \Sigma)$$

(M-step) Update the parameters:

$$\phi_j := \frac{1}{m} \sum_{i=1}^m w_j^{(i)},$$

$$\mu_j := \frac{\sum_{i=1}^m w_j^{(i)} x^{(i)}}{\sum_{i=1}^m w_j^{(i)}},$$

$$\Sigma_j := \frac{\sum_{i=1}^m w_j^{(i)} (x^{(i)} - \mu_j)(x^{(i)} - \mu_j)^T}{\sum_{i=1}^m w_j^{(i)}}$$

}

Trick to the this problem is to fix the mixing proportions and variance in the full version of EM algorithm, which are given in many textbooks and simply iterate with respect to the formula involving the means.

$$\text{Log } p(Y|\mu_1, \mu_2) = \sum_i \log(p_1 * f_1(y_i|\mu_1) + p_2 * f_2(y_i|\mu_2))$$

By setting the partial derivative of the above equation with respect to μ_1 and μ_2 to 0, we can obtain the following equation.

$$-\sum_i \{p_k * f_k(y_i|\mu_k) / (\sum_m p_m * f_m(y_i|\mu_m)) * \sigma_k * (y_k - \mu_k)\} = 0 \text{ for each } k$$

Rearranging for μ_k lead to the next equation.

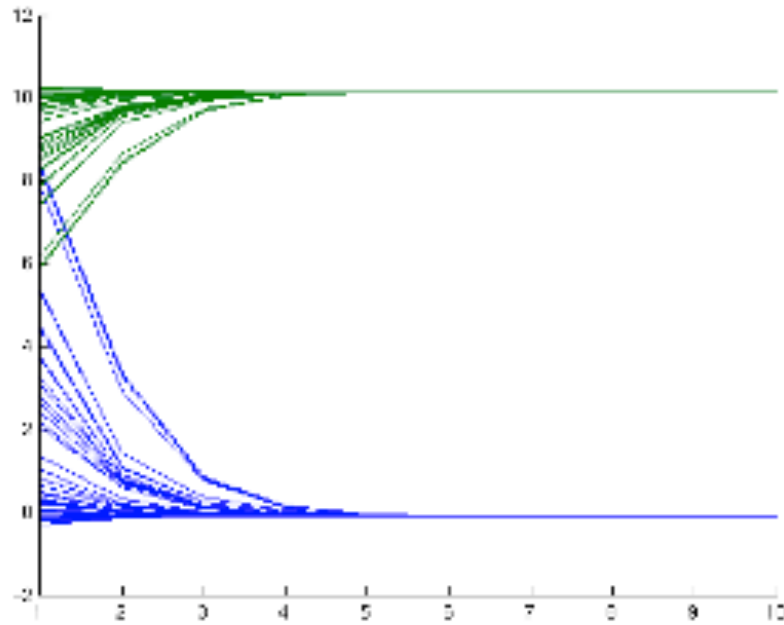
$$\mu_k = \{\sum_i (R_{ik} * y_i)\} / (\sum_i R_{ik})$$

Where $R_{ik} = p_k * f_k(y_i|\mu_k) / (\sum_m p_m * f_m(y_i|\mu_m))$. Using this equation iteratively with the other known parameters, μ_1 and μ_2 can be estimated. The EM algorithm can be summarized as below.

- (1) Initialize μ_1 , μ_2 and evaluate the initial log likelihood.
- (2) E step: Evaluate R_{ik} using the current parameters.
- (3) M step: Re-estimate μ_1 and μ_2 using R_{ik}
- (4) Check for convergence.

Reference: Pattern recognition and machine learning by Christopher M. Bishop (2006)

Seung-goo Kim



<X-axis: # of iteration; Y-axis: estimation for means>

Demonstration of EM algorithm showing the convergence to the estimated means.

Another reference:
Martinez & Martinez (2002)

HW7 Solutions

Redo HW5 with at least three different bandwidths (suggestions: 5, 10, 15, 20mm) and discuss the effect of different bandwidth on the final result (after performing t-test). There are a couple of NeuroImage papers out there that discuss this important issue.

The problem ask you to determine the effect of smoothing on the final statistical result.

Dajung Kim

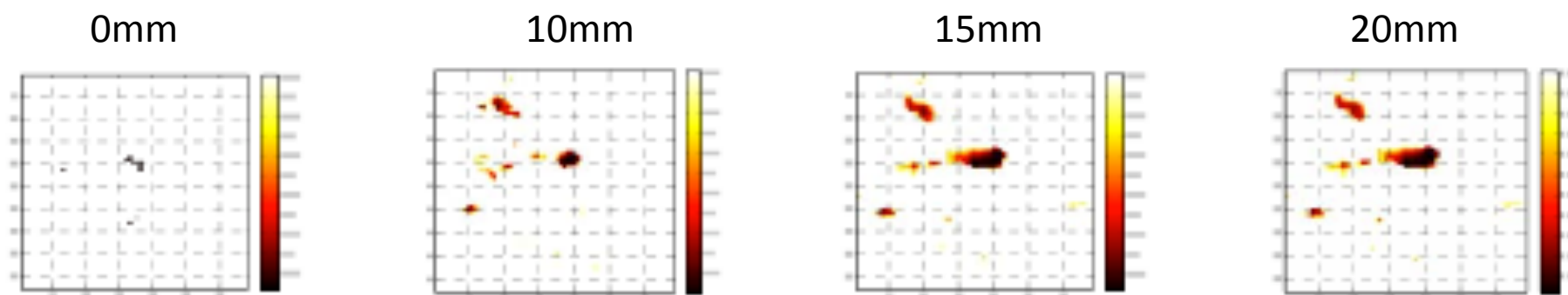
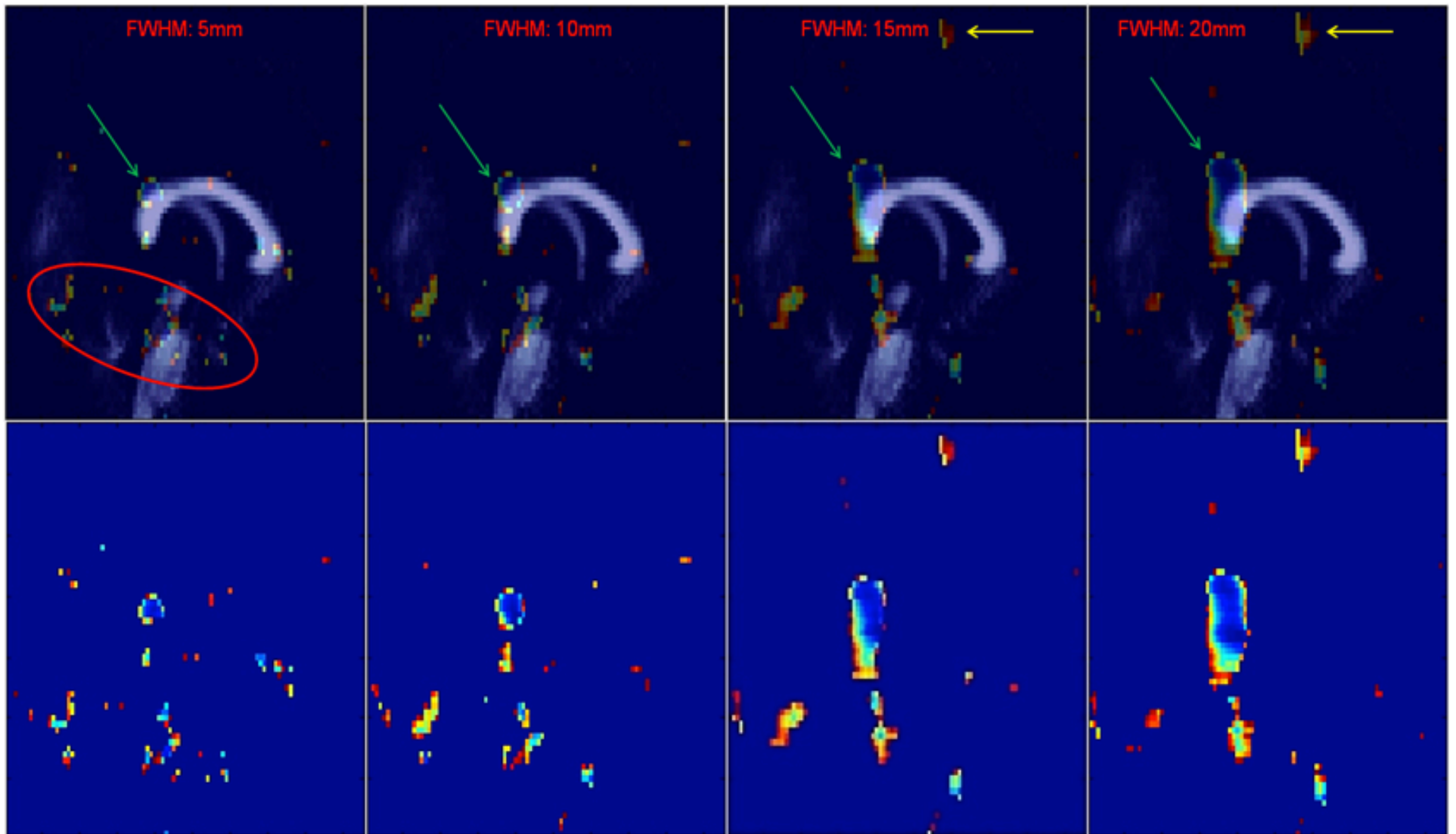


Figure 3. A two sample t -test results comparing the white matter density of CC. (a) smoothing bandwidth = 0mm, (b) 10mm, (c) 15mm, (d) 20mm. Color bar indicates the p -value. The maximum t -statistic is on the splenium of the CC.

There is not much difference

Rametti (2007) pointed out in his hippocampal VBM analysis that small smoothing kernel (4- 8mm) in small structure increased sensitivity. Salmond (2002) reported that with 4mm FWHM kernel size, normality is sufficiently guaranteed to test valid in balanced design. The CC used in this study is relatively small compared to whole-brain, it is appropriate to use a small kernel size below 10mm.

Seok Jun Hong



I wanted to observe what really happens when you change the FWHM on your final statistical analysis result. It can change your inference.

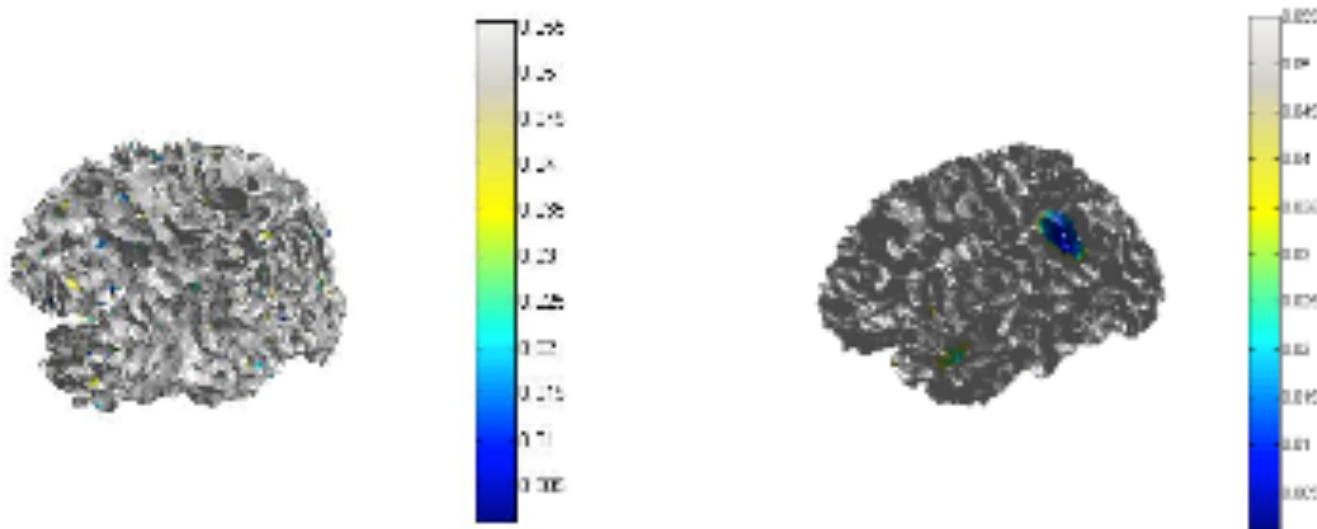
Hansem Sohn

Smoothing, low-pass filtering, has shown several advantages for image processing such as improvement in SNR and increased sensitivity in statistical analyses. In addition, the increase in the FWHM of the Gaussian kernel reduces the number of non-normality voxels (Jones et al., Neuroimage, 2005).

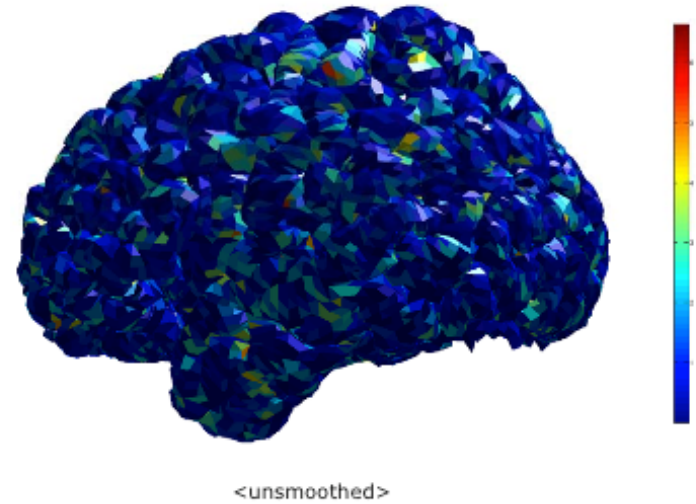
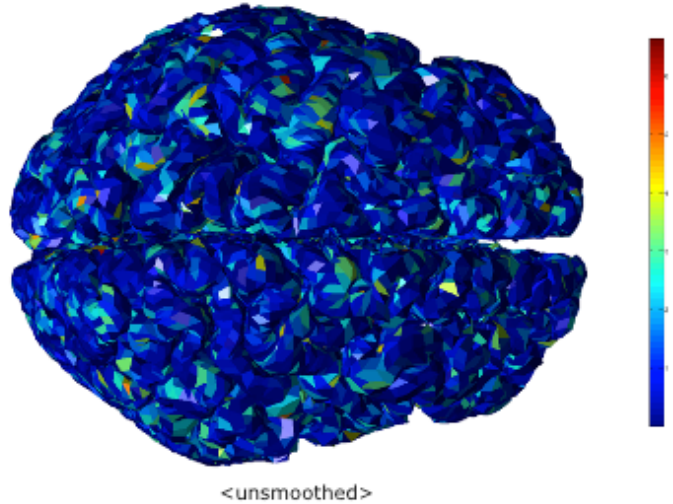
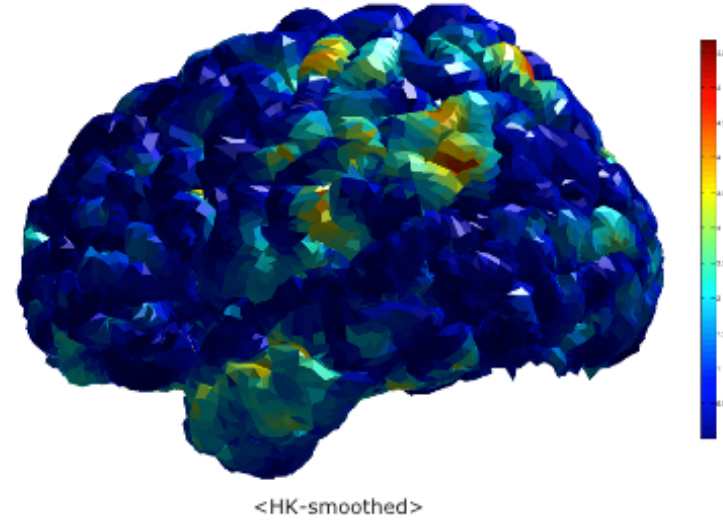
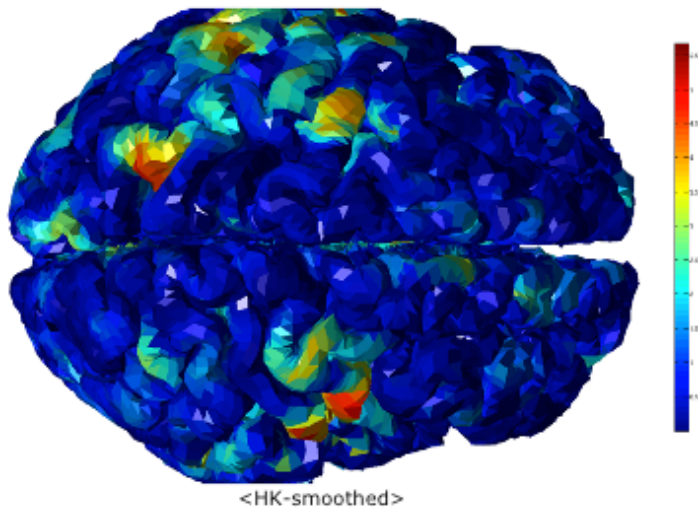
HW8 Solutions

Redo HW3 after heat kernel smoothing. Discuss your results with and without smoothing. Reading Chung et al., NeuroImage 2005 will help you understand the problem.

Dajung Kim



This is what I wanted to see and demonstrate to me!
Many students didn't have clue why I was asking this
particular a bit tedious problem.

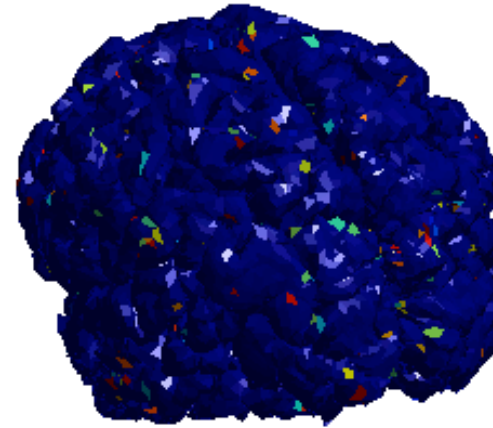
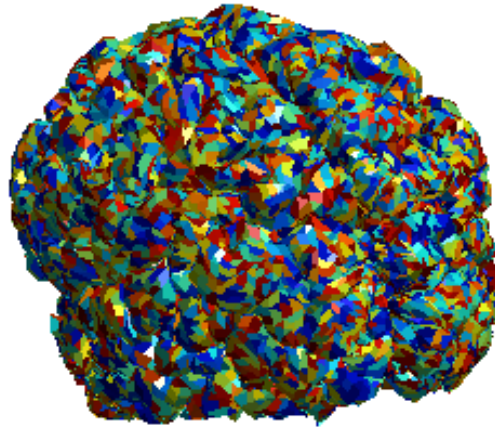


Seung-goo Kim

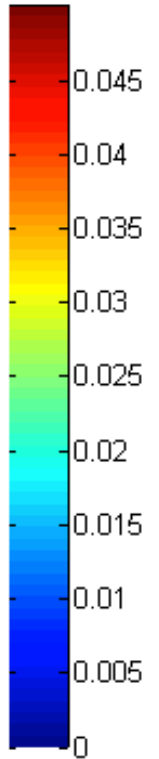
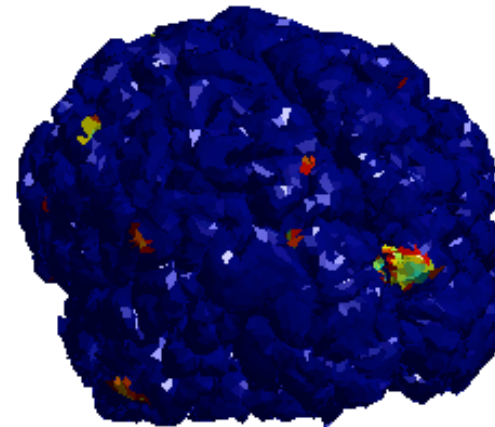
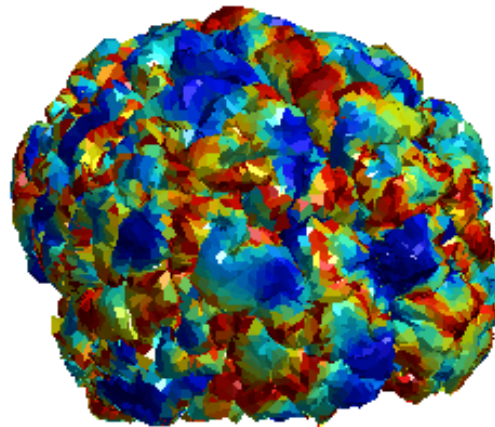
Raw result mapping p-value

Thresholded with p-value < 0.05

Not smoothed by
heat kernel



Smoothed by
heat kernel



Seok Jun Hong

You get less number of clusters and much
larger cluster → easier interpretation

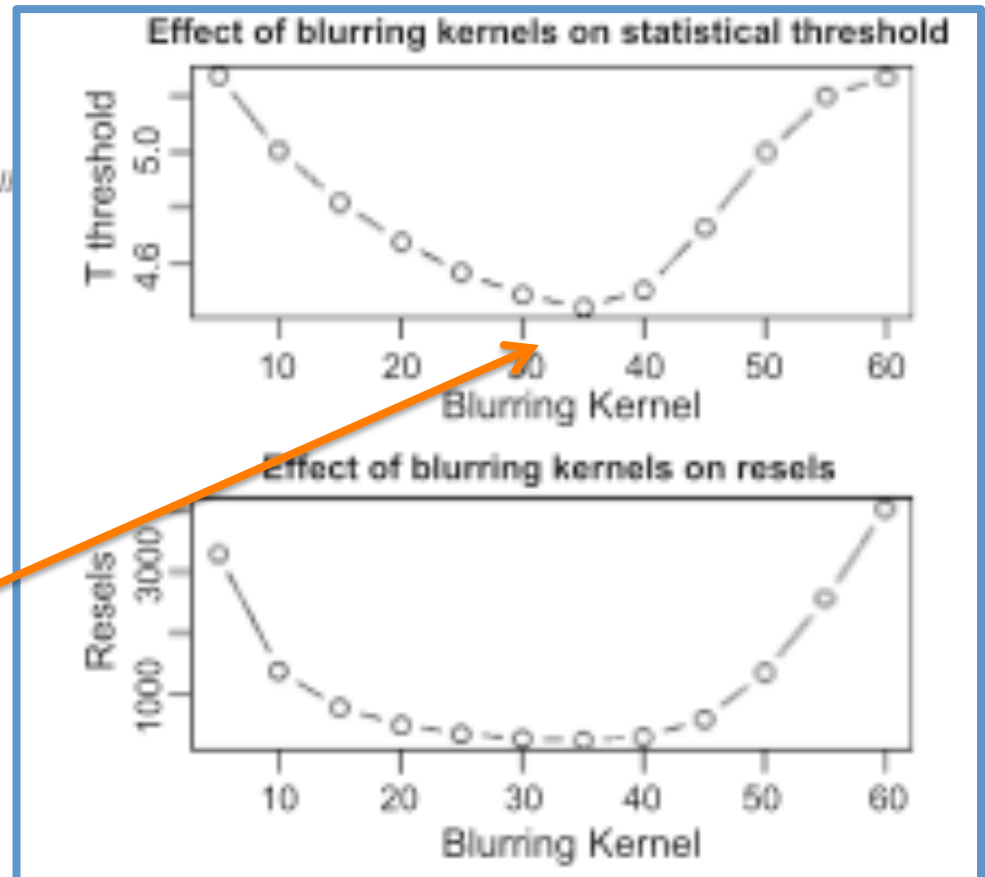
Cortical thickness analysis examined through power analysis and a population simulation

Jason P. Lerch and Alan C. Evans*

McCowell Brain Imaging Centre, Montreal Neurological Institute, McGill

Received 23 March 2004; revised 27 June 2004; accepted 12 July 2004
Available online 18 November 2004

Optimal smoothing FWHM
can be determined somehow

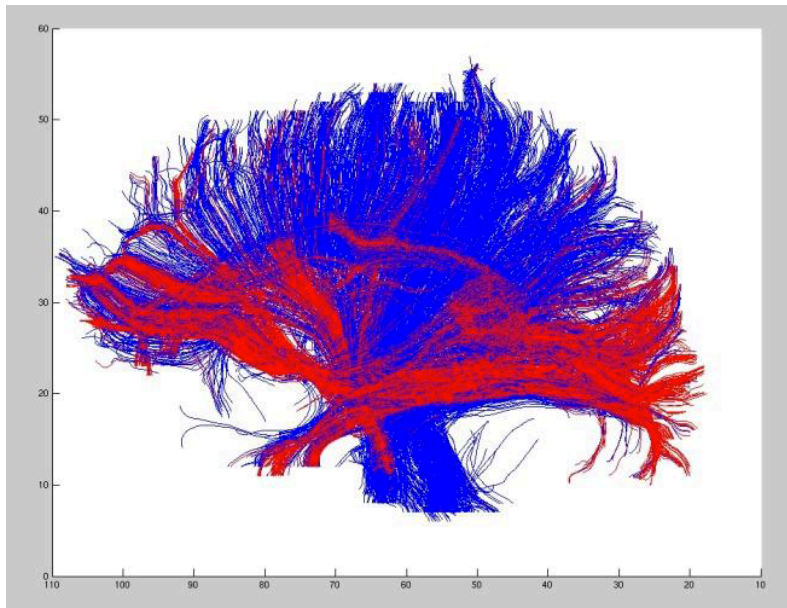


HW9 Solutions

Compute the length of 10000 tracts and plot the histogram. Threshold the histogram at upper 10% and determine the longest 10% tracts. What tracts are likely to be longer than other tracts. Discuss your result.

1 Point deducted if you did KS-test on kernel density estimate blindly without the discussion of the optimal amount of smoothing and tail distribution issues.

The **superior longitudinal fascicle**, microscopically indentified in the postmortem human brains by Burgel et al. (2005, NeuroImage), connects mainly occipital lobes with frontal association cortices which is located medial to the corticospinal fibers.



Schuz & Braitenberg (2002) indentified two group of white matter; “**short-distance (10~30 mm) fibers** below the gray matter that follows its contours, and **long distance (30~170 mm) fibers** that are bundled into fascicle in the deep white matter.

“As a rough rule, the number of fibres of a certain range of lengths is inversely proportional to their length”

Schuz & Braitenberg (2002) The human cortical white matter: Quantitative aspects of cortico-cortical long-range connectivity. *Cortical Areas: Unity and Diversity, Conceptual Advances in Brain Research*. pp 377–386, Taylor and Francis London

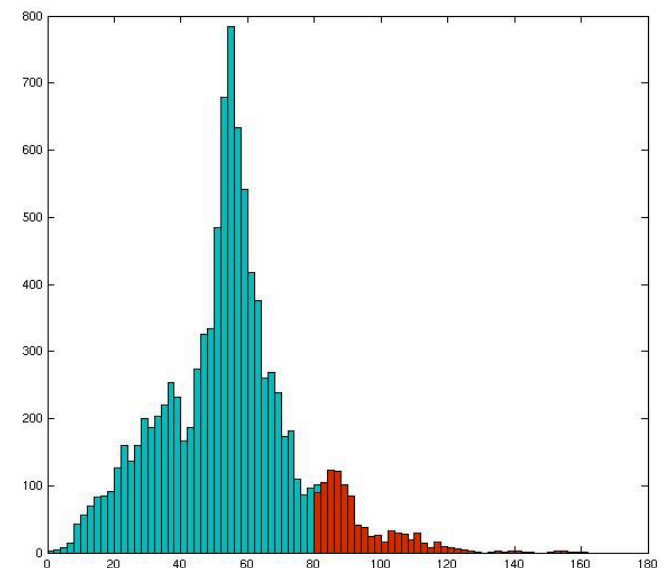

```
% 10% tracts.  
prctile(lnth(1,:),90)  
% the length of the 90th percentile  
is 80.211.  
upper10_tract=find(lnth(1,:)  
>prctile(lnth(1,:),90));  
% get upper 10% length indices.
```

```
figure;  
bin=[1:2:180];  
hist(lnth,bin); hold on;  
hist(lnth(upper10_tract),bin);  
GG=get(gca,'children')  
set(GG(6),'FaceColor',[1 1 1])  
set(GG(5),'FaceColor',[.85 .16 0])
```

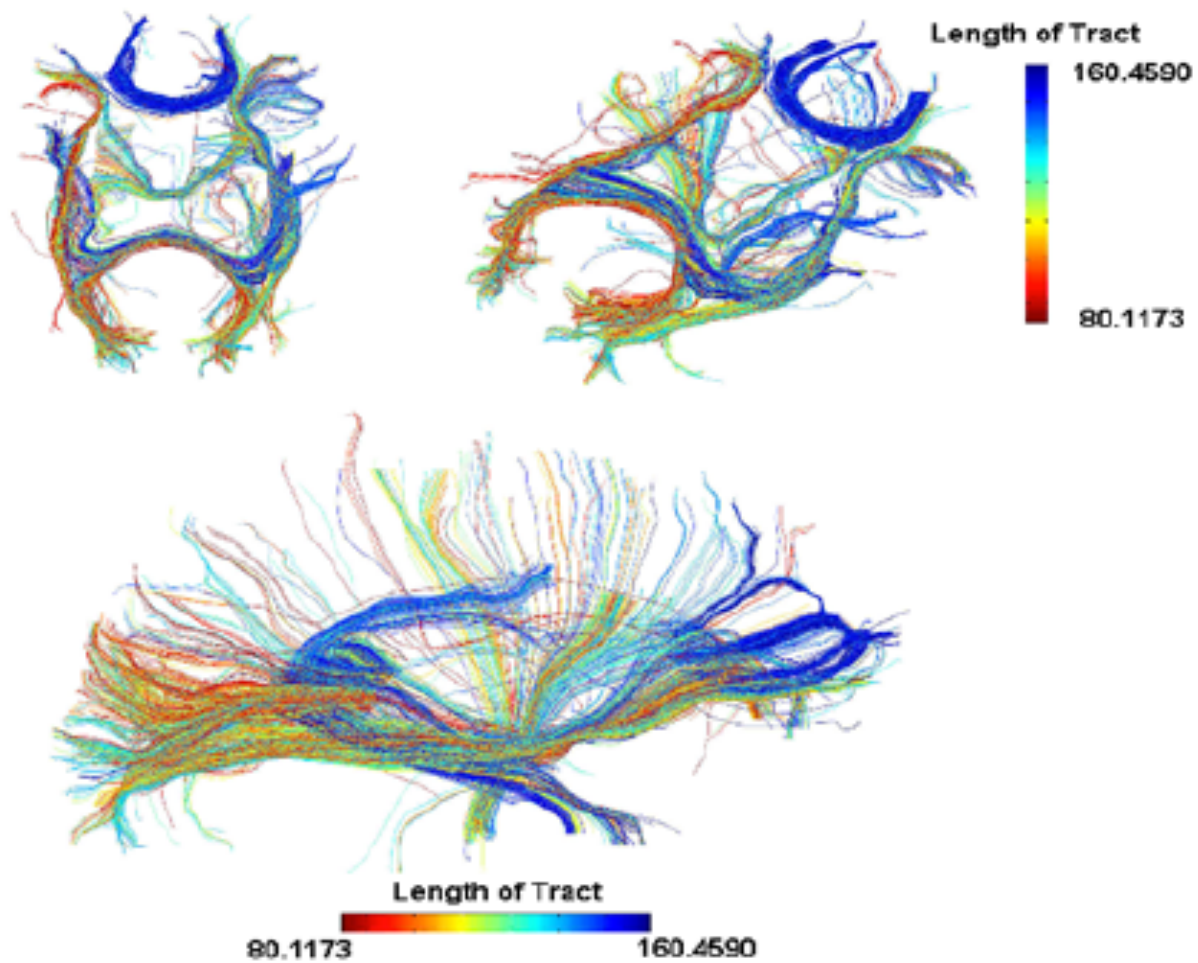
Ehhhhh....

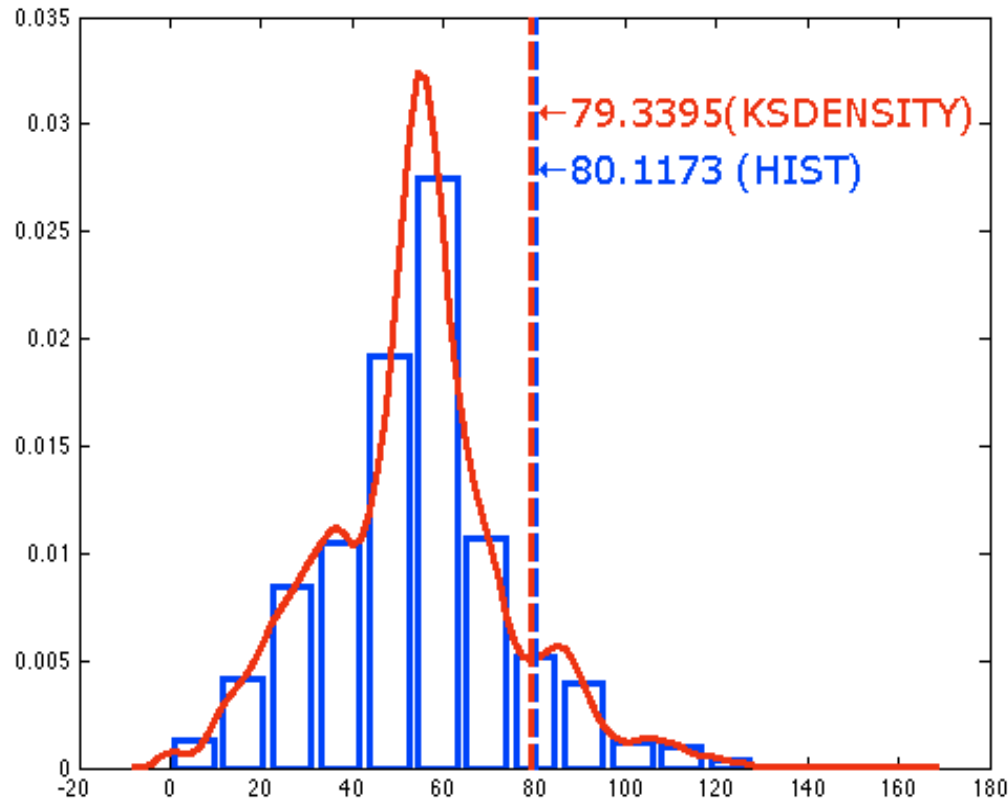
*Few students worked
so hard to write
prctile command.*

*This is actually easier
than you think. All
you need is to sort
measurements.*



Seok Jun Hong



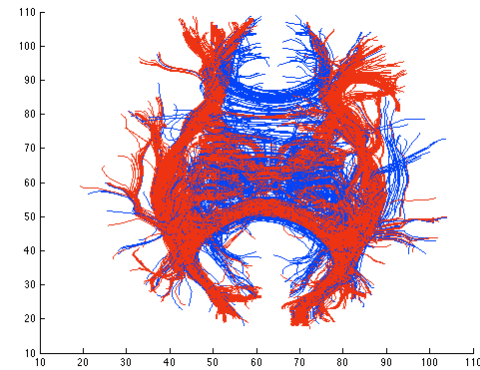
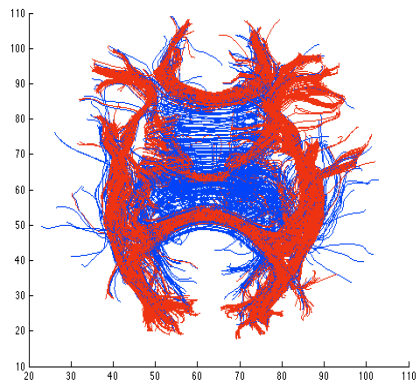
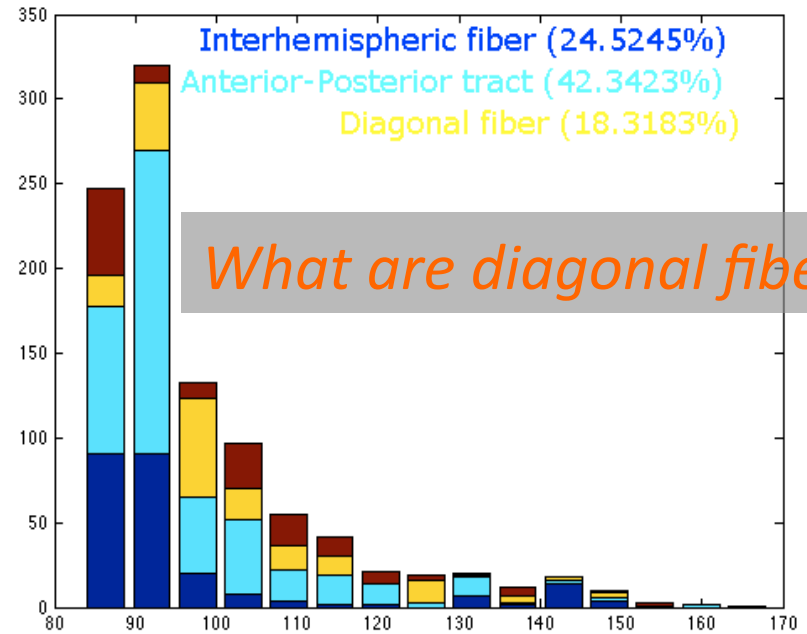
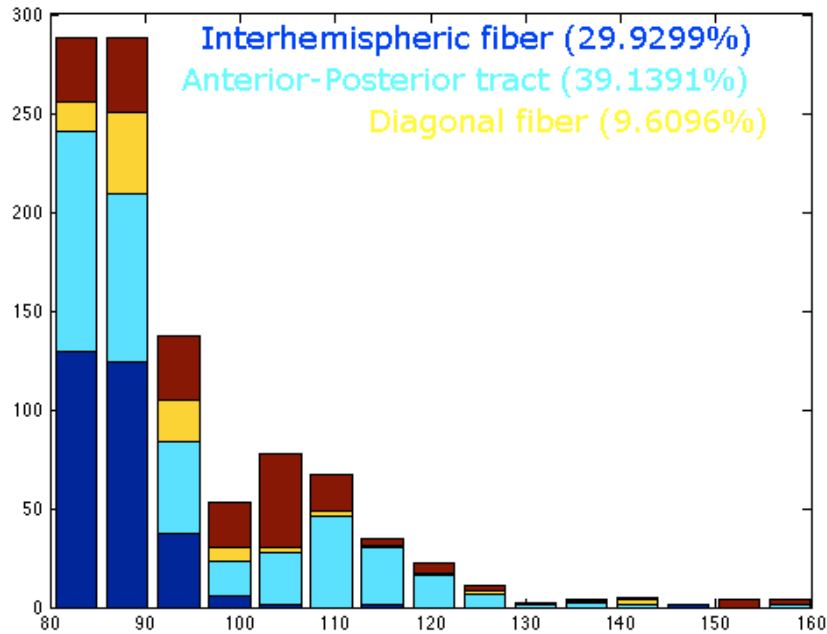


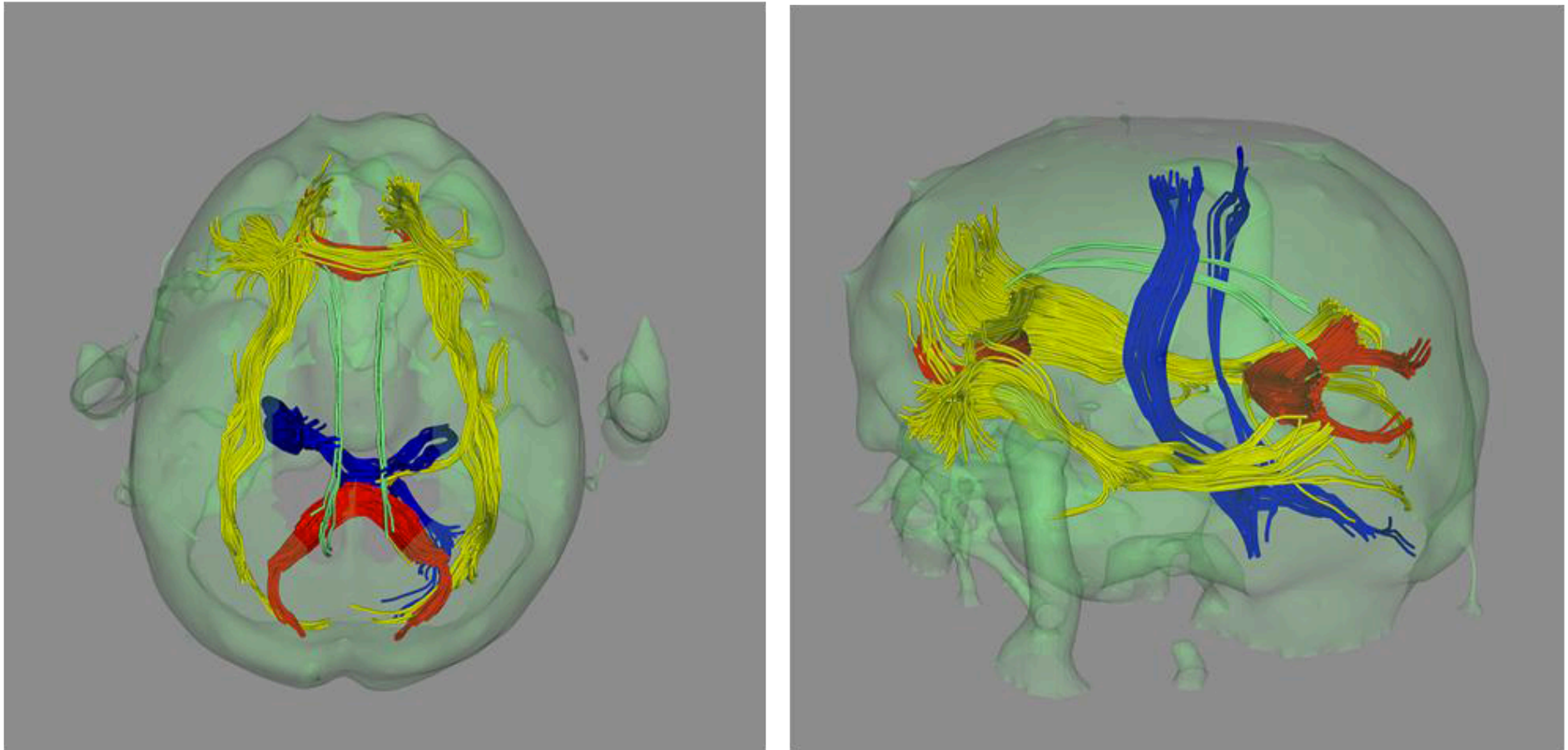
See lecture notes on
quantile and percentile.
Chapter 2.1 of the
textbook

Kernel density estimation
= can smooth out histogram
= 1D version of heat kernel smoothing

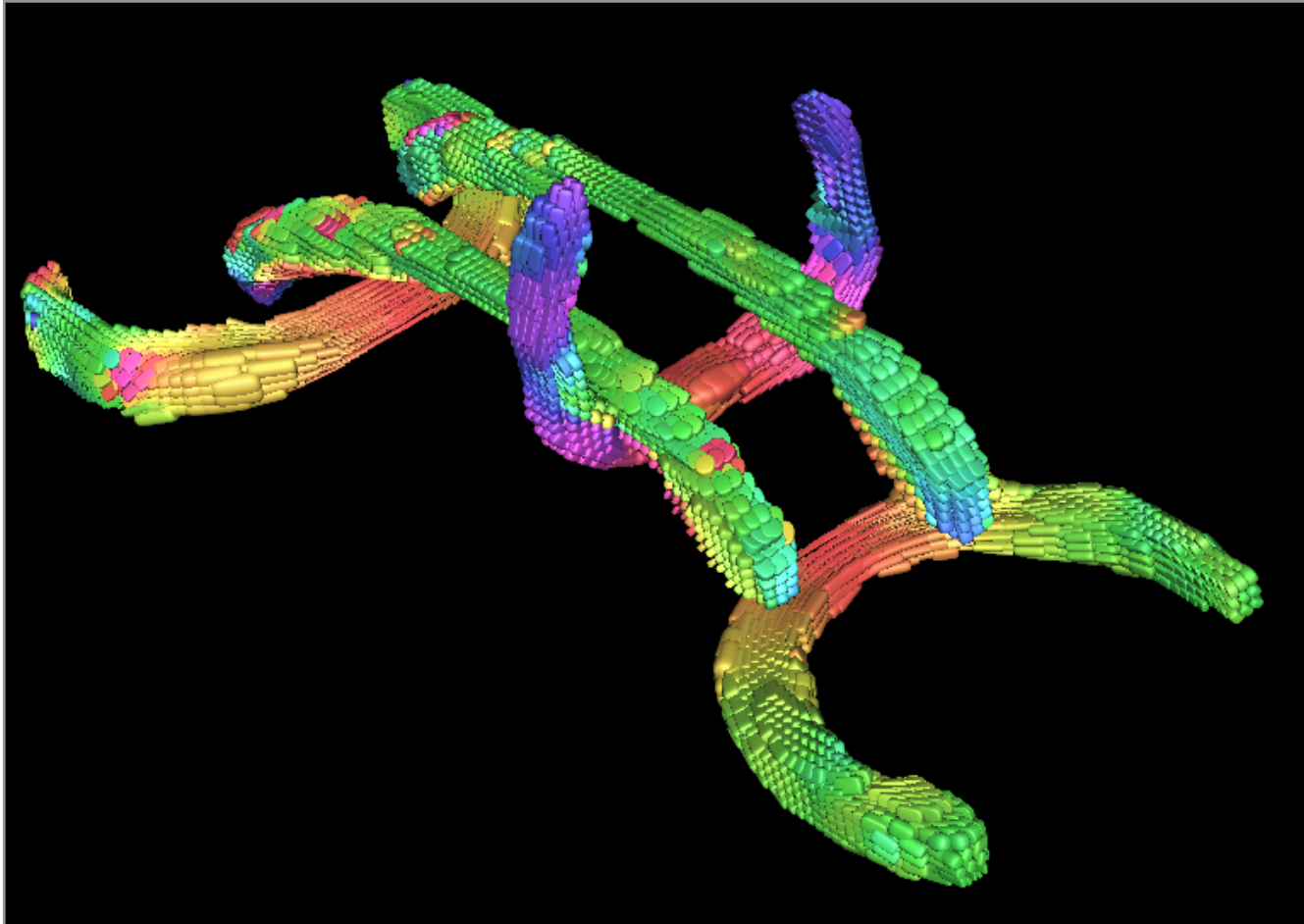
Read Chapter 2.1 and
MATLAB demonstration

The most of the long-range tracts are for remote interaction between anterior and posterior parts of the brain or across the midline.





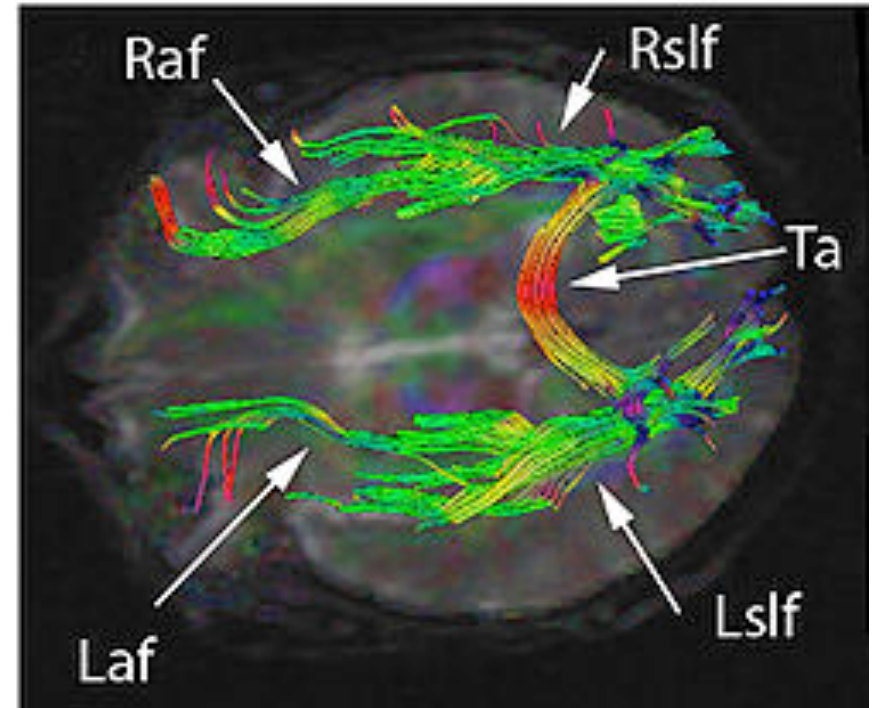
Four major fibers tracts: cortico-spinal tract (blue), transversal tracts through splenium and genu of corpus callosum (red), cingulate (green), longitudinal fasciculi (yellow). (Fillard & Gerig, 2003)



Whitaker: Volumetric tracts, computed interactively using the method of [Jeong et. al 2007], displayed as ellipsoidal glyphs, colored with orientation.

Ji Won Hur

right and left arcuate fasciculus (Raf & Laf),
the right and left superior longitudinal
fasciculus (Rslf & Lslf), and tapetum of
corpus callosum (Ta).



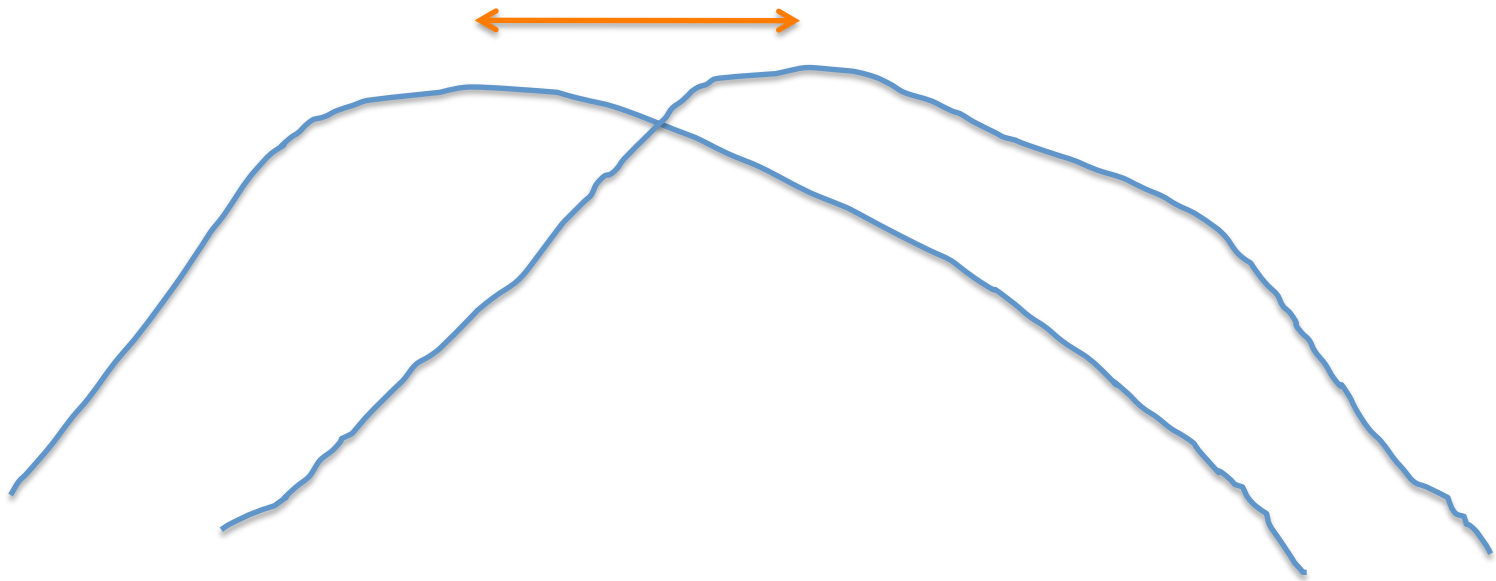
The longer fiber tracts are fasciculus, a bundle of nerve fibers, and corpus callosum. Above red tracts indicate Superior longitudinal fasciculus (Arcuate fasciculus; the neural pathway connecting the posterior part of the temporoparietal junction with the frontal cortex in the brain), Dorsal longitudinal fasciculus (myelinated axon bundles carrying information between neurons. The ascending and descending DLF fibers, conveys visceral motor and sensory signals) and Medial longitudinal fasciculus (carrying information about the direction that the eyes should move). The corpus callosum is a structure connects the left and right cerebral hemispheres. It facilitates communication between the two hemispheres. It is the largest white matter structure in the brain, consisting of 200-250 million contralateral axonal projections.

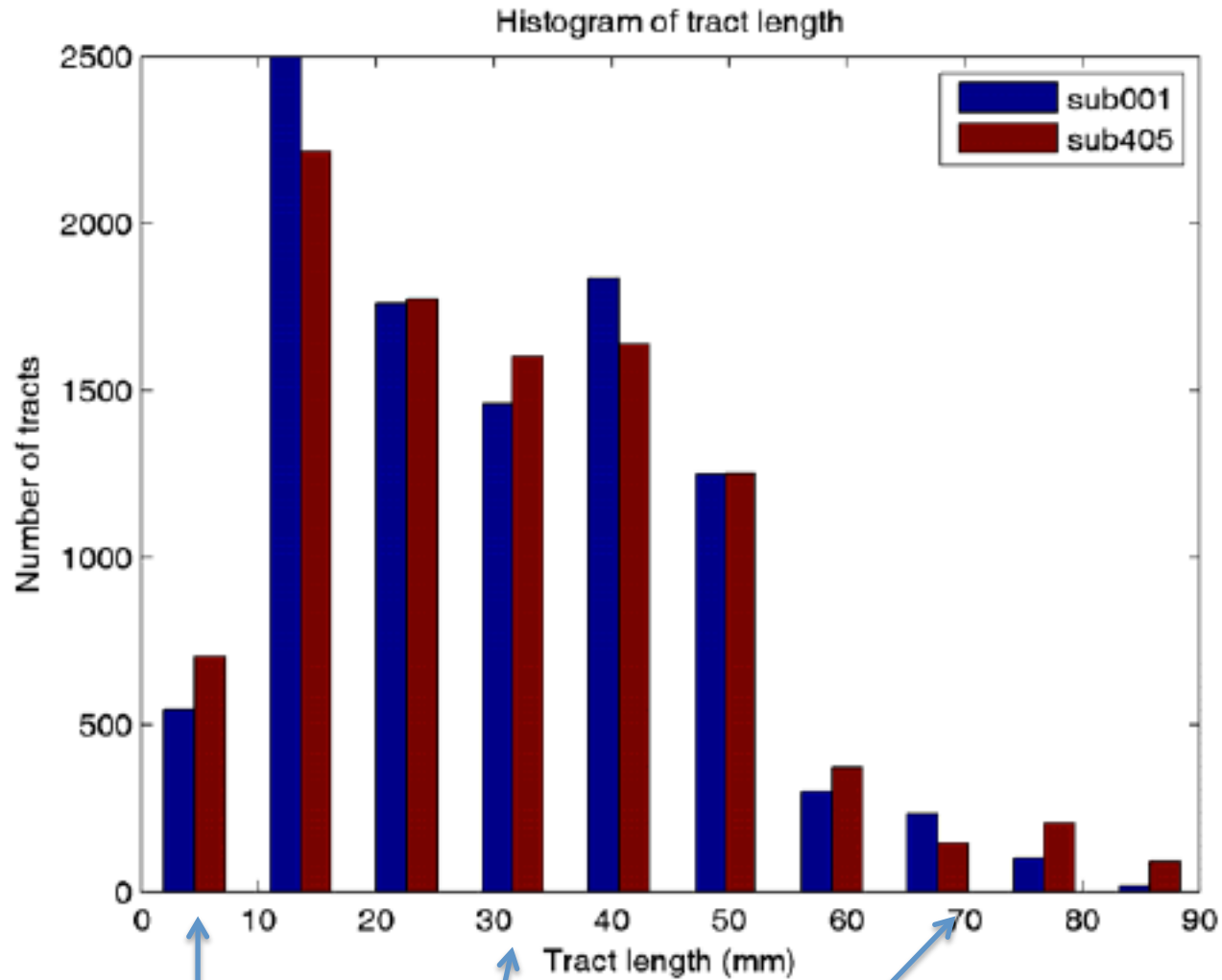
HW10 Solutions

Based on the length of tracts, determining if there is any tract length difference between two subjects. There can be many different solutions to this particular problem.

Why you should not use the two sample t-test for this problem?

Two sample t-statistic only tests for the group mean difference





Apply t-test at each interval

Localized tract length comparison

Seung-goo Kim

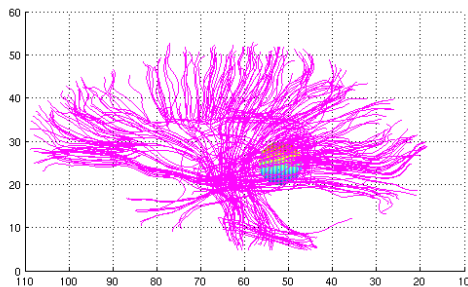
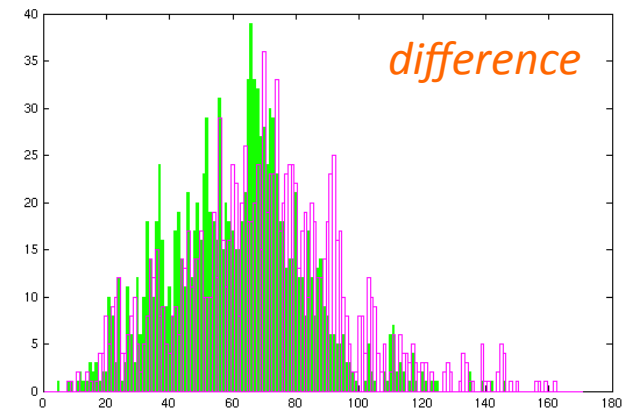
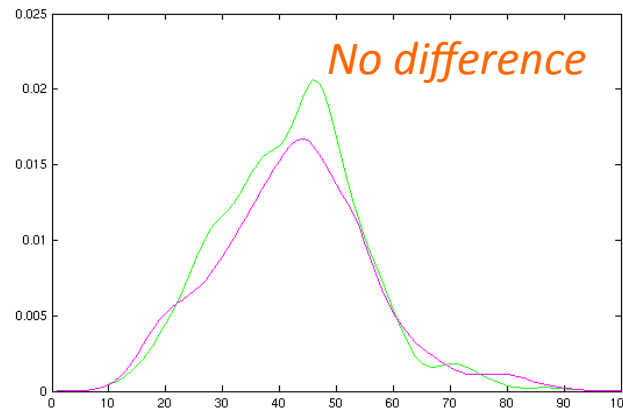
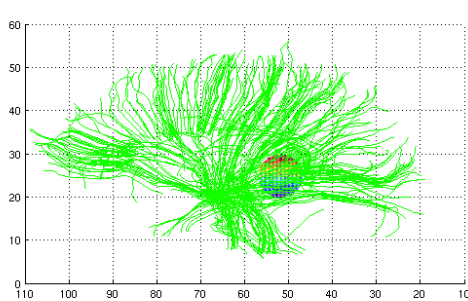
The splenium of the corpus callosum was manually defined as a ball of radius 5mm originating (62, 52, 25) in the given coordinate system and visually checked for both two subjects (Fig. 6).

After the origin (x_0, y_0, z_0) of the sphere had been defined, the tracts passing through it were identified for any point (x, y, z) consisting a tract;

$$(d_i' d_i) < r$$

$$d_i = [(x_i - x_0), (y_i - y_0), (z_i - z_0)]$$

where r is the radius of the sphere.



Care should be taken using kernel-density estimation. See MATLAB demo.

Two sample KS-test

The test statistic is:

$$D(x_1, x_2) = \max_x |F_1(x) - F_2(x)|$$

where $F_1(x)$ is the proportion of x_1 values less than or equal to x and $F_2(x)$ is the proportion of x_2 values less than or equal to x .

The null hypothesis is rejected at level α if

$$\sqrt{\frac{n_1 * n_2}{n_1 + n_2}} D(n_1, n_2) > K_\alpha$$

Where n_1 and n_2 are the numbers of iid observations and K_α is found from

$$Pr(K \leq K_\alpha) = 1 - \alpha$$

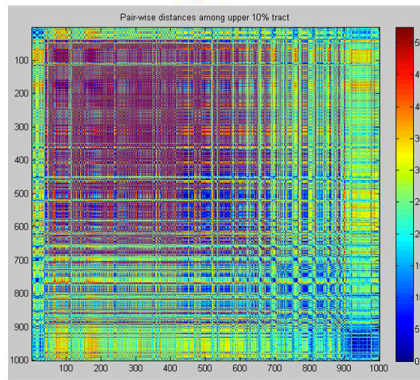
Tract clustering

Jarang Ham

Euclidean distance between the center of mass of tracts

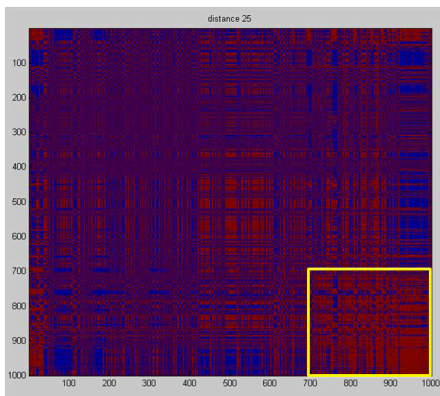


subject 01

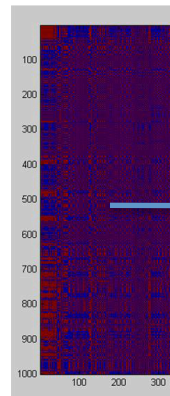


Adjacency matrix

Adjacency matrix of distance



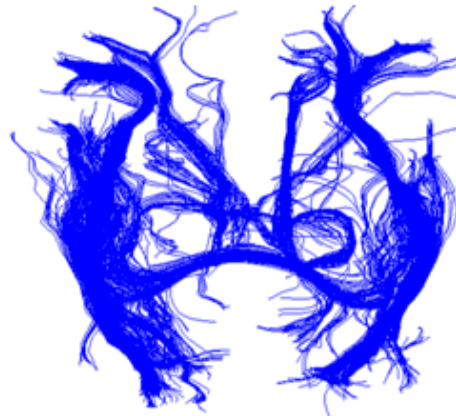
subject 01



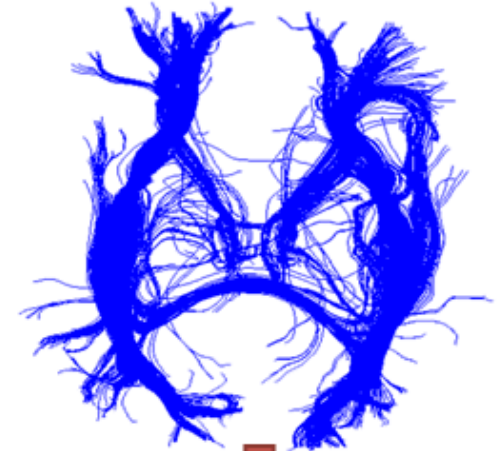
s



[subject 01]



[subject 02]

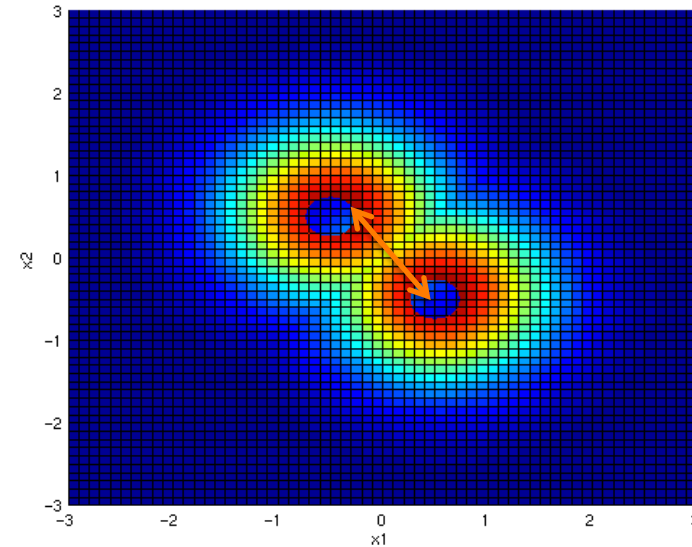
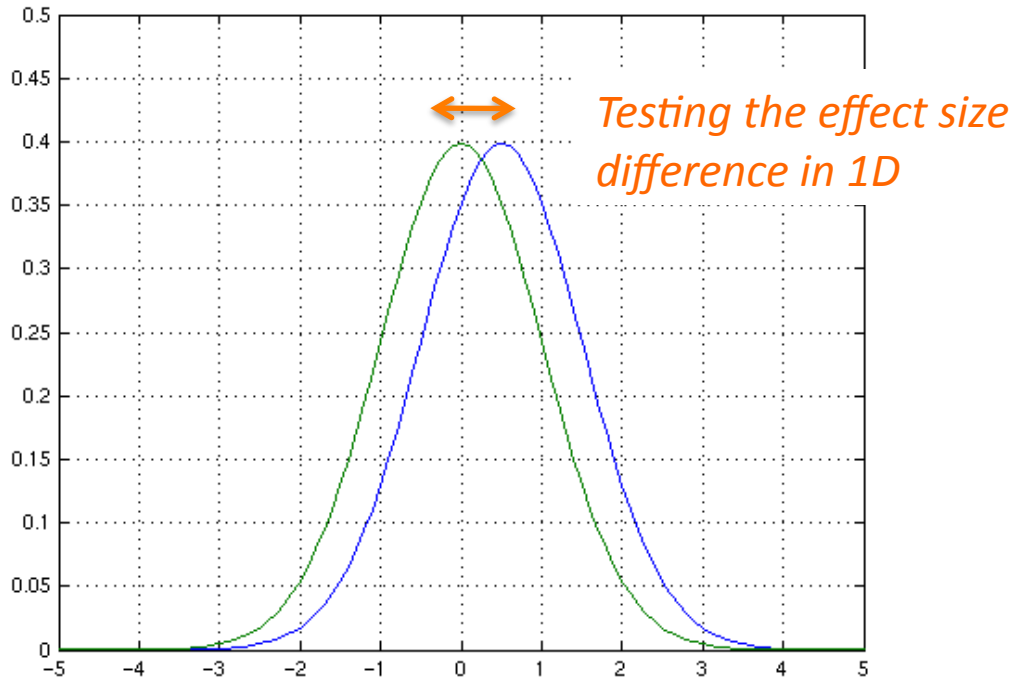


After clustering to bundles
-superior view-

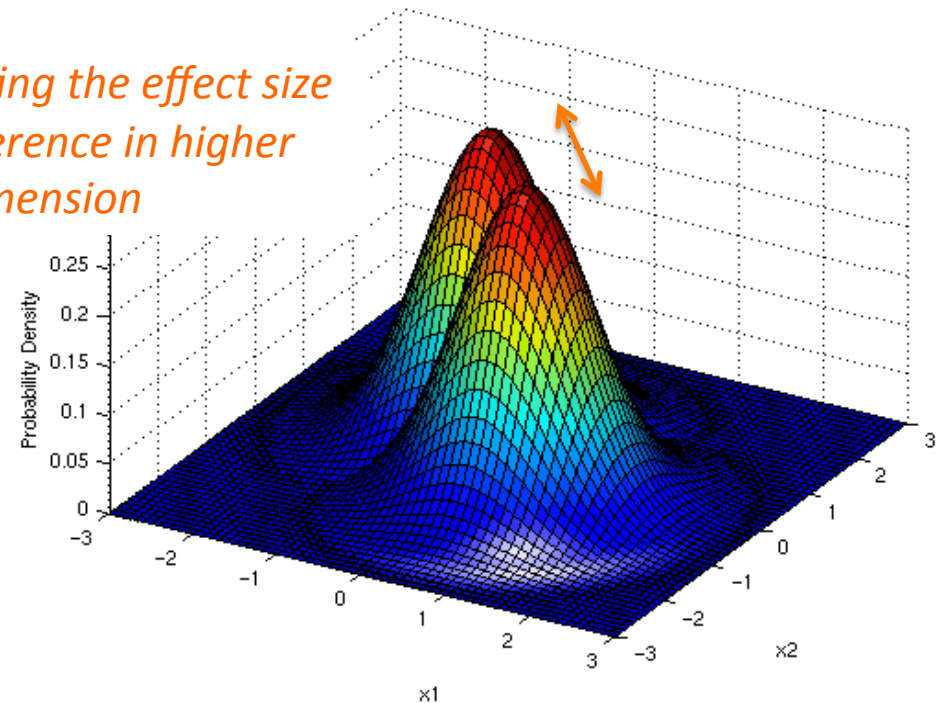
HW11 Solutions

Clearly describe what Hotelling's T-square test procedure is. What are the underlying statistical assumptions in Hotelling's T-square test procedure? Are these assumptions satisfied in the above example? Why we are not using the two-sample t-test in Chung et al., 2010 and the above example.

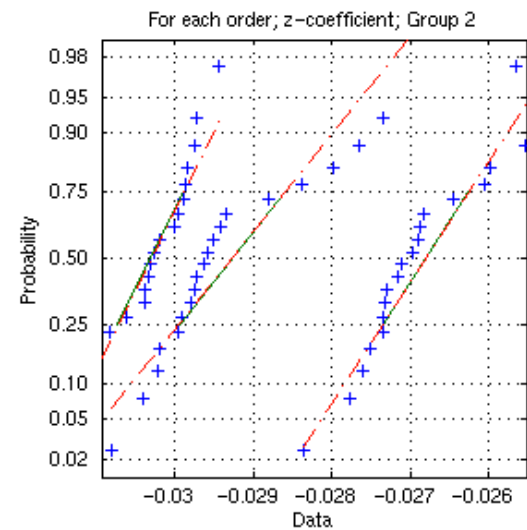
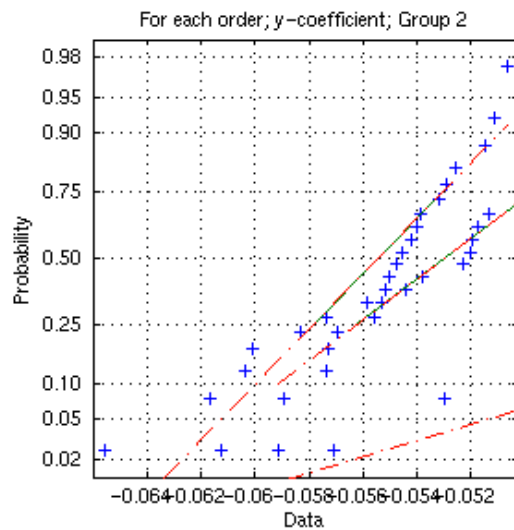
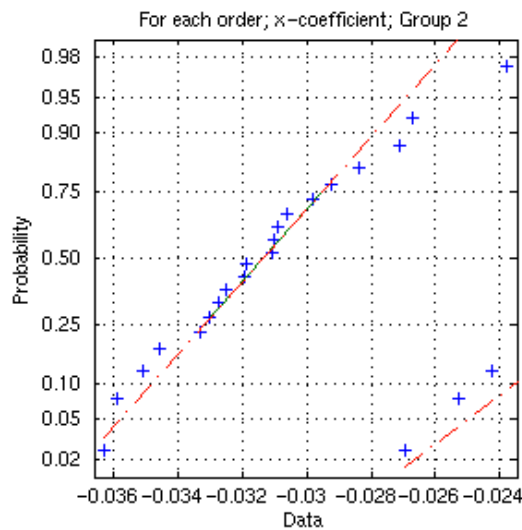
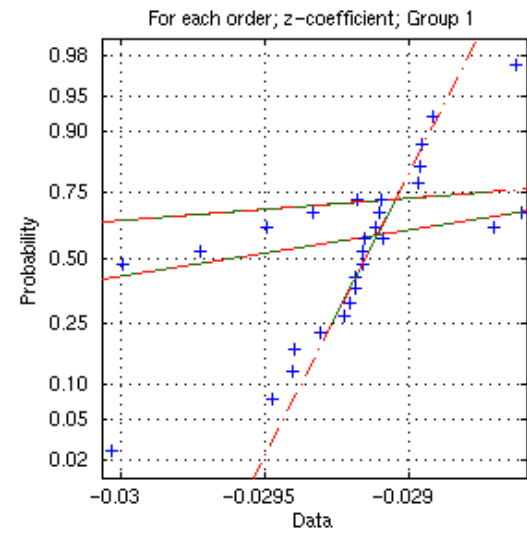
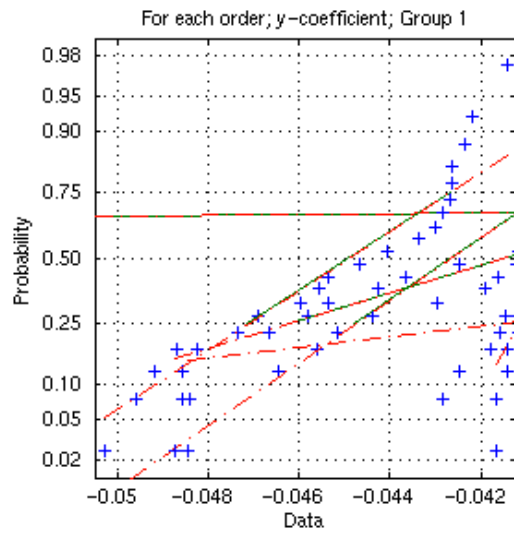
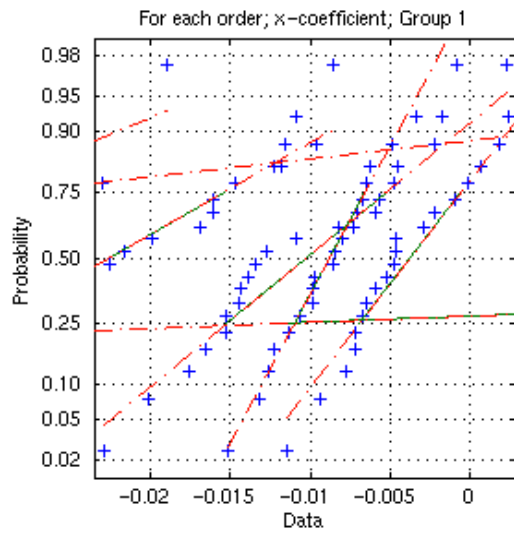
Sample covariance matrix needs to be computed for Hotelling's T-square statistic. Explain what covariance matrix is. Covariance matrix is usually modeled as Wishart distribution.



Testing the effect size difference in higher dimension



Hotelling's T-square assumption:
Two samples are assumed to have
identical covariance structures.



Normal probability plots

Read Chapter 2.1

MATLAB Demonstration

HW12 Solutions

Literature review. Given the 3D graph model of structural connectivity, discuss how others performed the network complexity analysis. A certain clinical population may have over- or under-connectivity of brain compared normal controls.

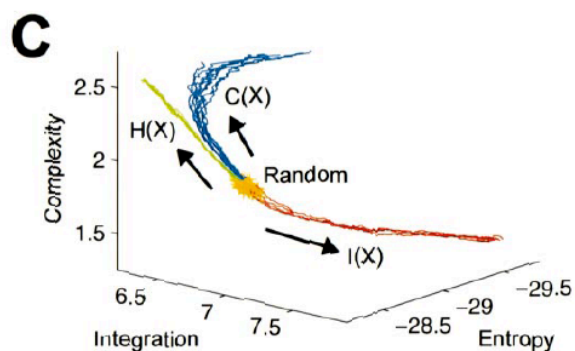
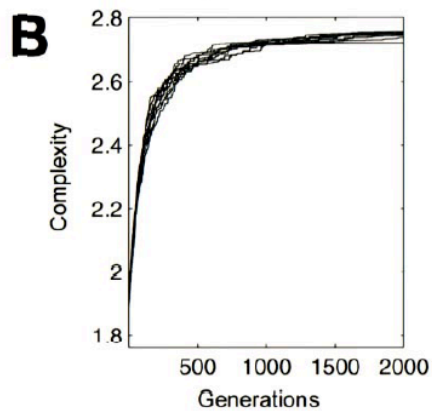
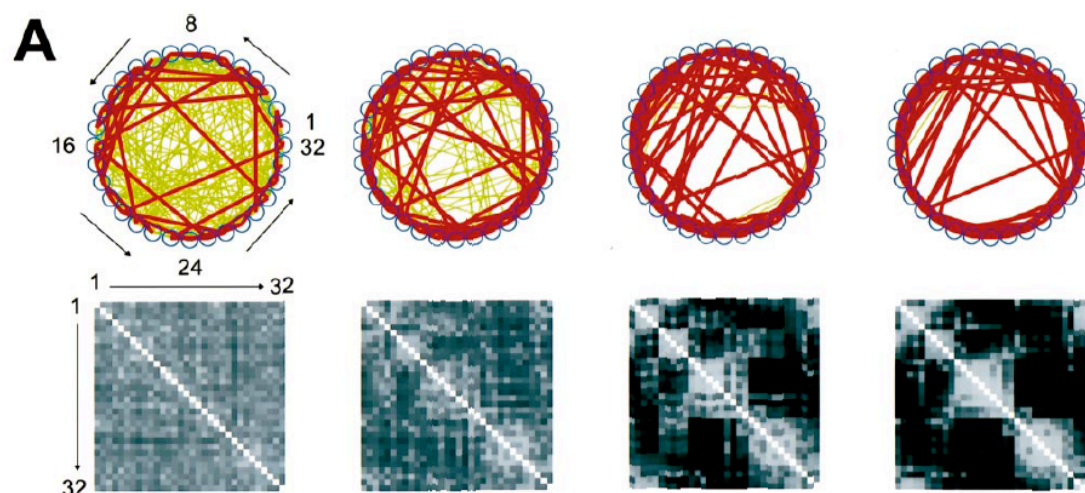
Discuss how you will test over- and over-connectivity hypothesis.

Then using the 3D graph model given in NIP.lecture05.dti.m, determine which subject has more complex brain network.

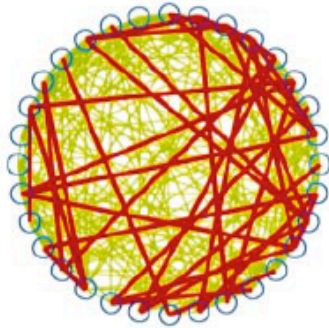
Theoretical Neuroanatomy: Relating Anatomical and Functional Connectivity in Graphs and Cortical Connection Matrices

O. Sporns, G. Tononi and G.M. Edelman

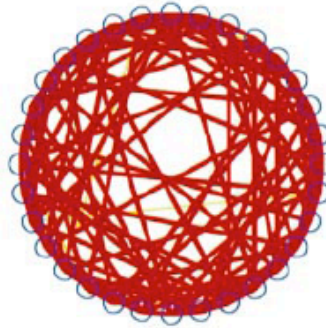
The Neurosciences Institute, 10640 John Jay Hopkins Drive,
San Diego, CA 92121, USA



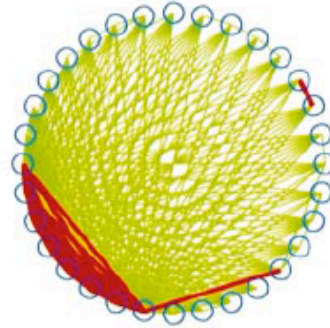
A Random



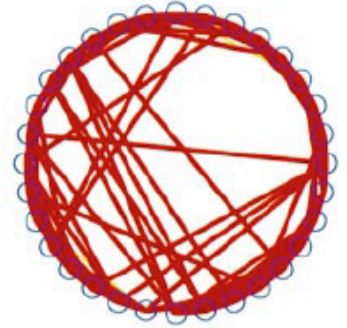
B Entropy



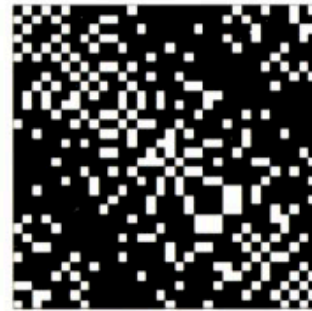
C Integration



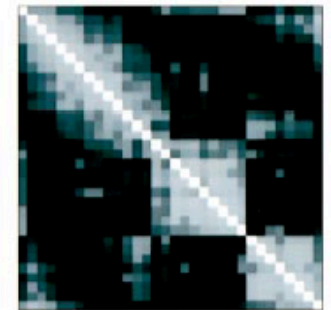
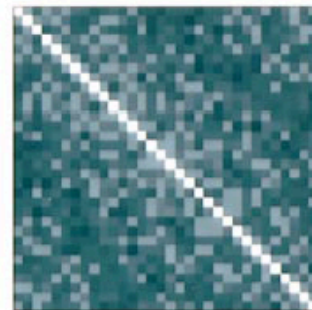
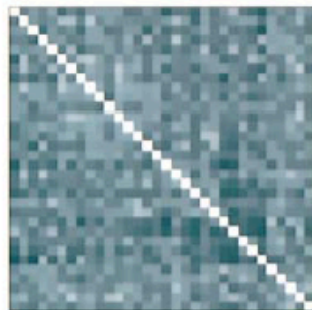
D Complexity



Adjacency matrix



Covariance matrix

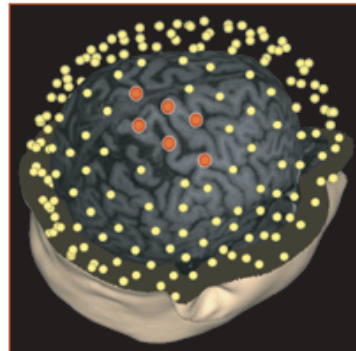
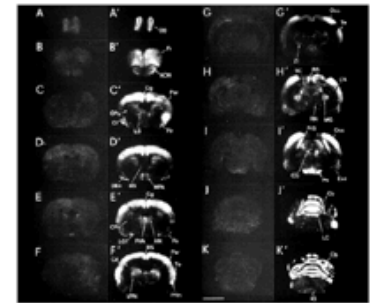


Neural Basis of Consciousness; Functions of Sleep

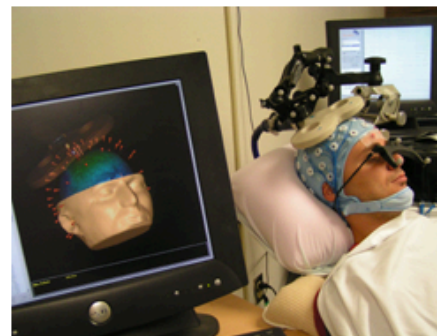
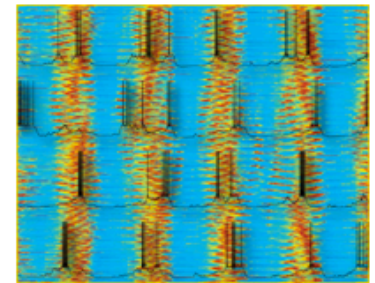
Giulio Tononi



http://tononi.psychiatry.wisc.edu/research_overview.html

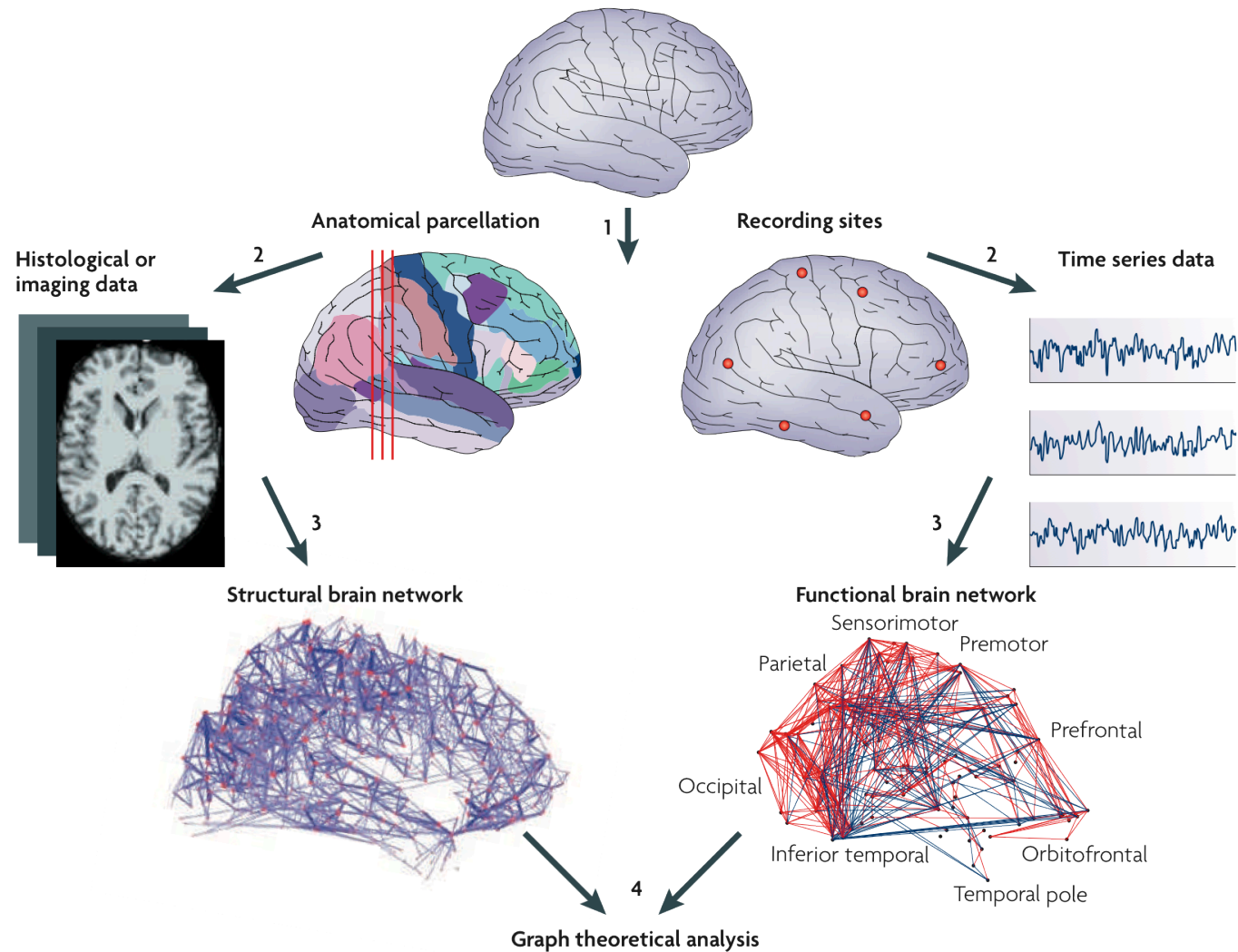


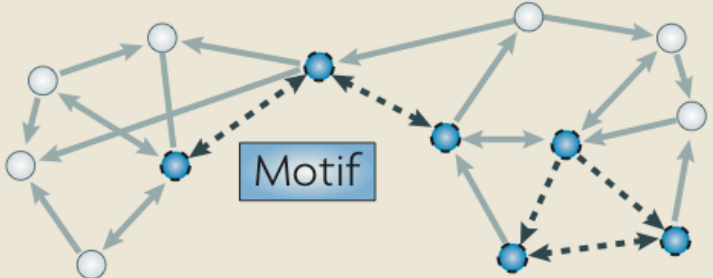
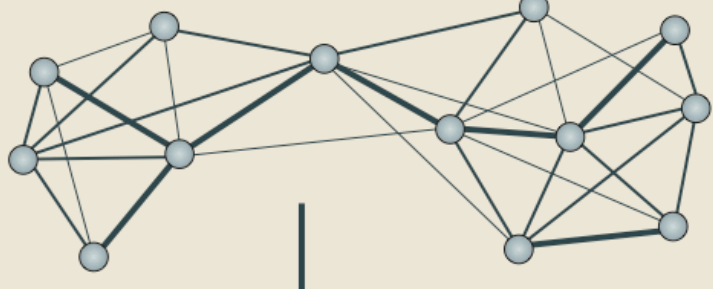
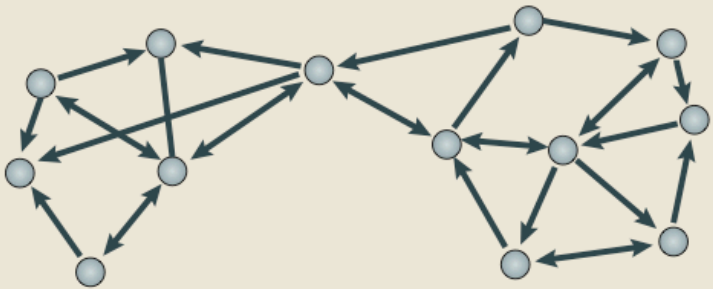
Our laboratories focus on two neurobiological problems – the mechanisms and functions of sleep and the neural substrates of consciousness. Both problems have considerable medical implications, especially for psychiatric disorders such as depression and schizophrenia.



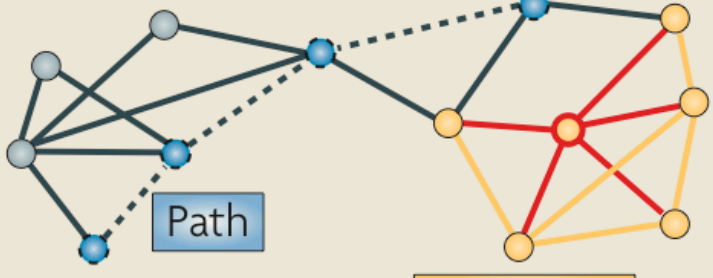
Complex brain networks: graph theoretical analysis of structural and functional systems

Ed Bullmore** and Olaf Sporns[§]





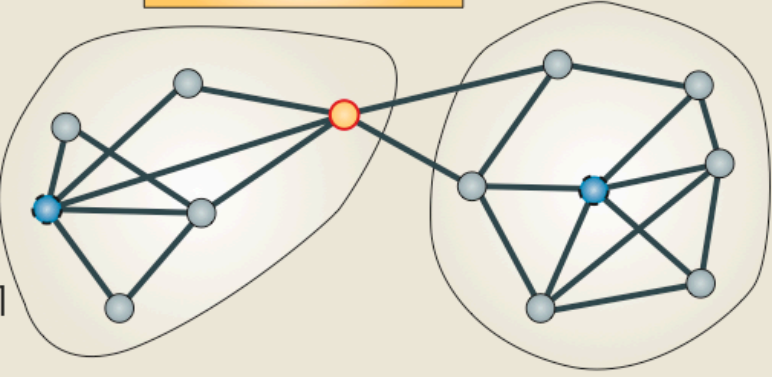
Threshold



Clustering

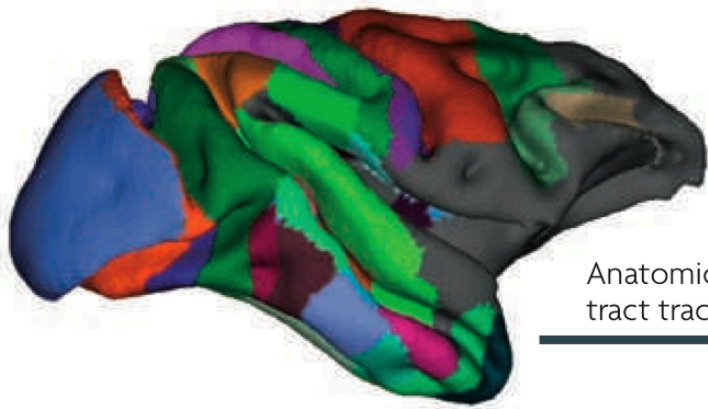
Connector hub

Community 1



Community 2

Provincial hub



Anatomical tract tracing

Structural brain network



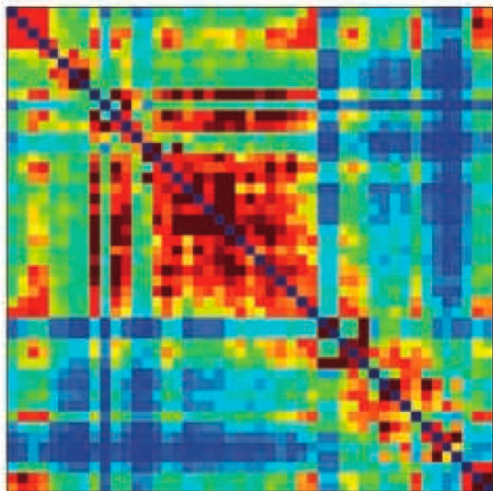
Coupling matrix and neural dynamics

Simulated electrophysiological time series

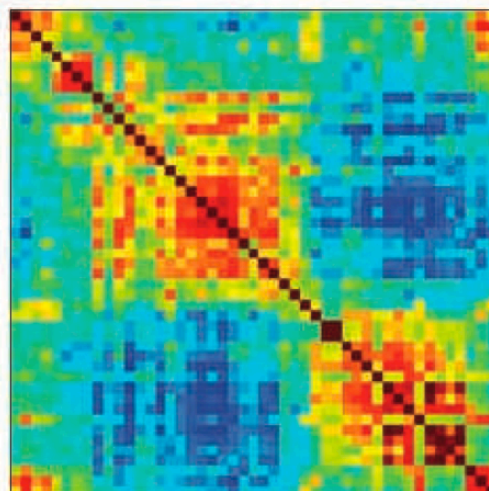
Simulated BOLD time series

Honey, Kotter, 2007

Functional brain network

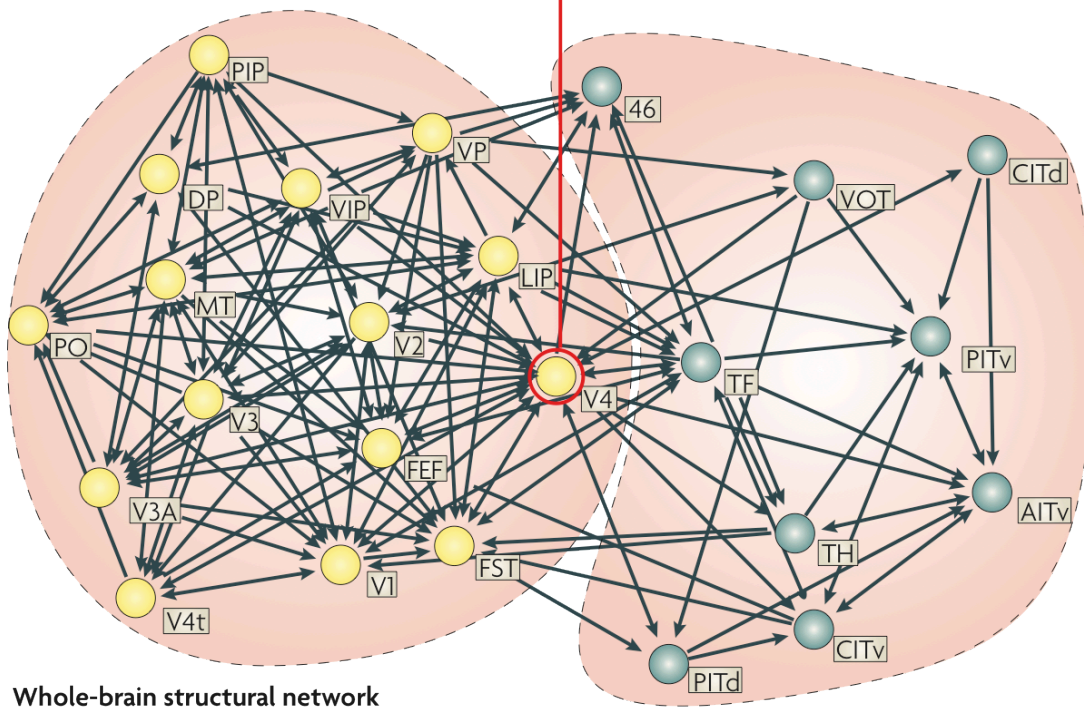
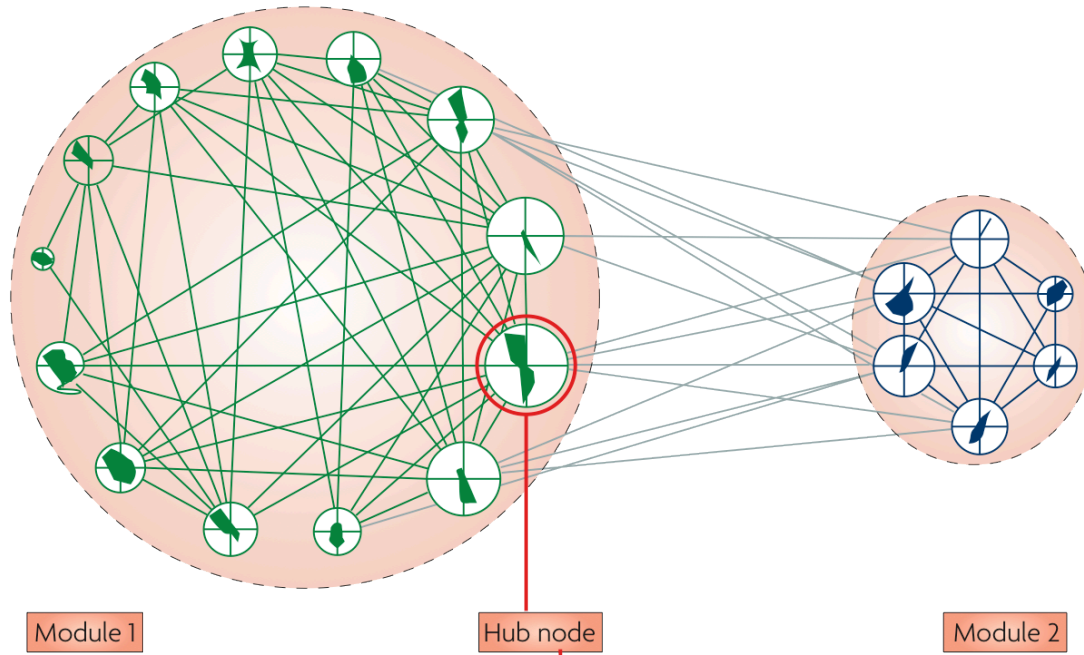


Mutual information



Cross-correlation

Cellular functional network



Whole-brain structural network

a Healthy volunteers

b People with schizophrenia

Degree ↑

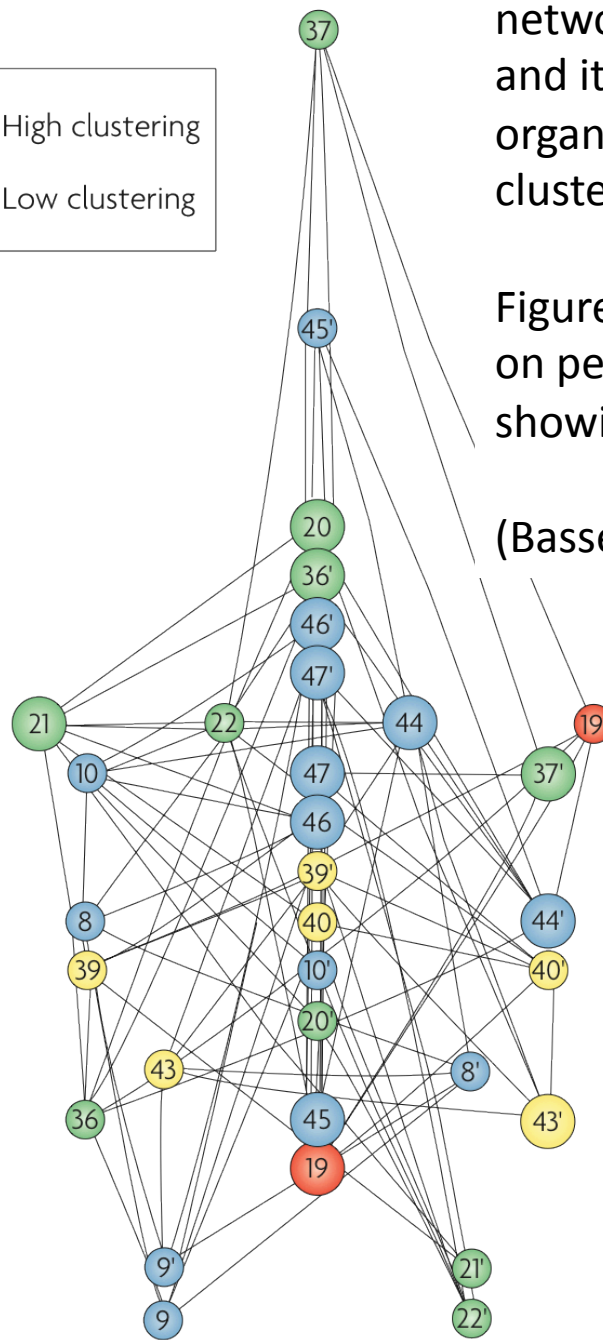
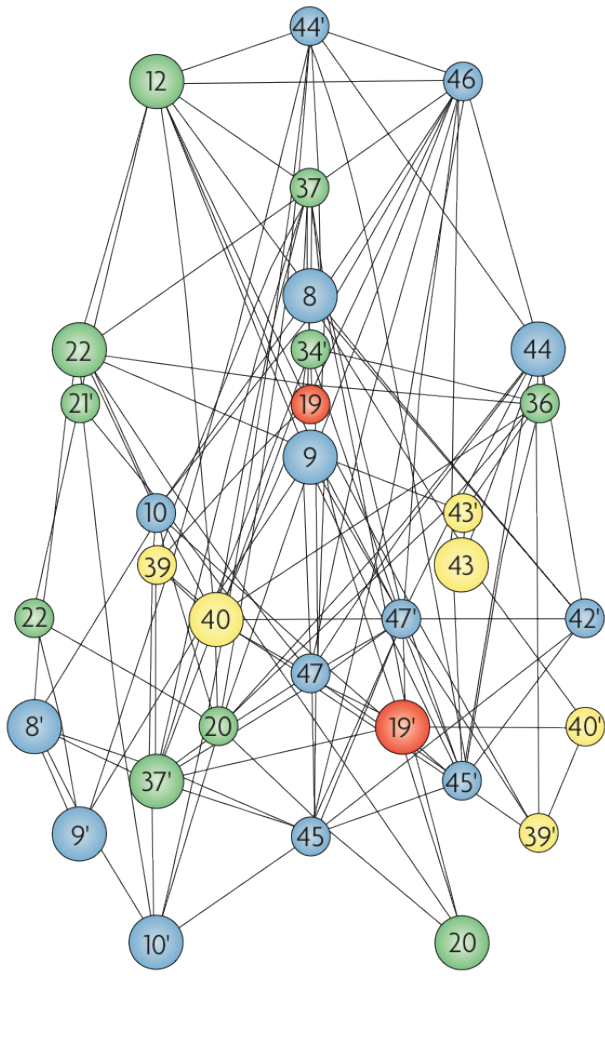
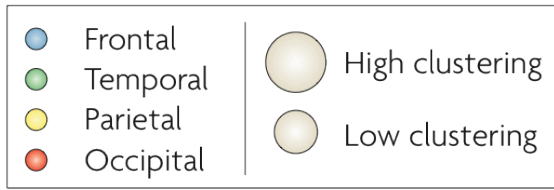


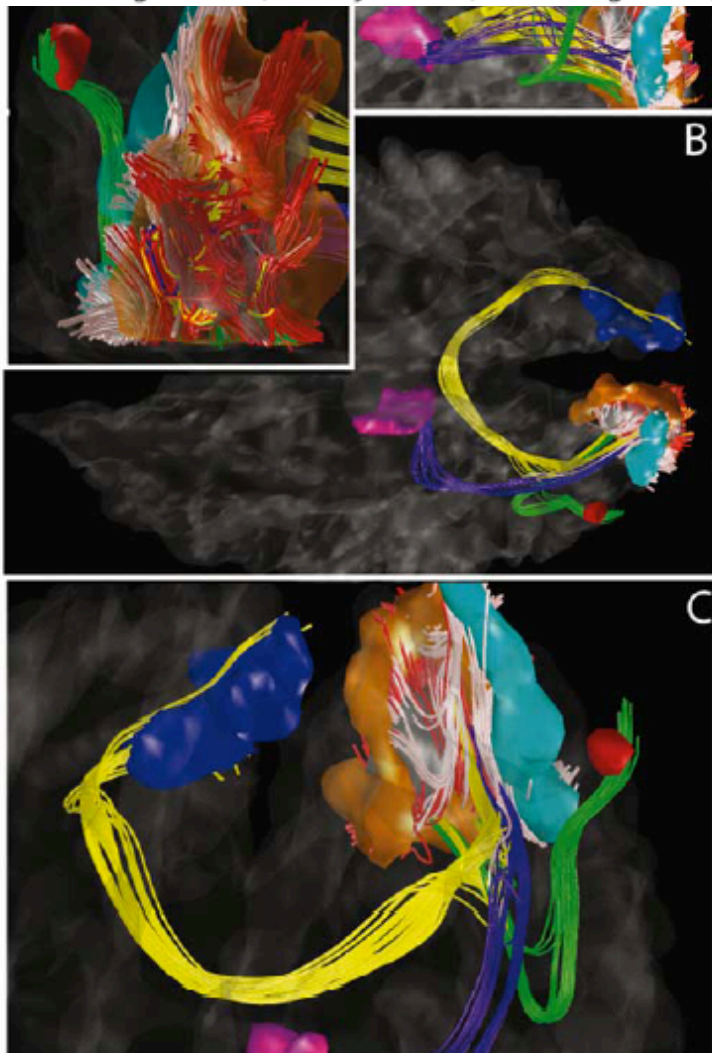
Figure a is the brain anatomical network of the healthy volunteers, and it shows a hierarchical organization characterized by low clustering of high-degree nodes.

Figure b is the equivalent network on people with schizophrenia, showing loss of this hierarchy

(Bassett, Bullmore et al. 2008).

Mapping Human Whole-Brain Structural Networks with Diffusion MRI

Patric Hagmann^{1,2*}, Maciej Kurant³, Xavier Gigandet², Patrick Thiran³, Van J. Wedeen⁴, Reto Meuli^{1*}, Jean-Philippe Thiran^{2*}



A complex system is: any system consisting of a number of components which give rise to the collective behaviour of the system by interacting with its environment in non-linear ways (even though there are examples of linear complex systems) (NECSI, 2008; CSCS, 2005; Rocha, 1999). For example, the brain is a complex dynamic system in which information is continuously processed and transferred to other interconnected regions with functional dynamics (Sporns et al., 2004, 2000). A system's complexity may be of one of two forms: disorganized complexity and organized complexity (Warren, 1948). In essence, disorganized complexity is a matter of a very large number of parts, and organized complexity is a matter of the subject system (quite possibly with only a limited number of parts) exhibiting emergent properties. **Disorganized complexity results from the particular system having a very large number of parts and the interactions of the parts can be seen as largely random.**

Do not underestimate the usefulness of degree and degree distribution as a measure of network complexity. This has to be the first step in quantifying a graph!

Most fundamental network measure is the degree of a node which is the total number of connections that link the node to the other nodes. Degree of a node can be directly computed from the adjacency matrix by adding all the binary values in each column of the matrix.

There are a lot of crappy network measures that are irrelevant or useless in extremely large network or brain network. Don't blindly expect all of them to work magically somehow.

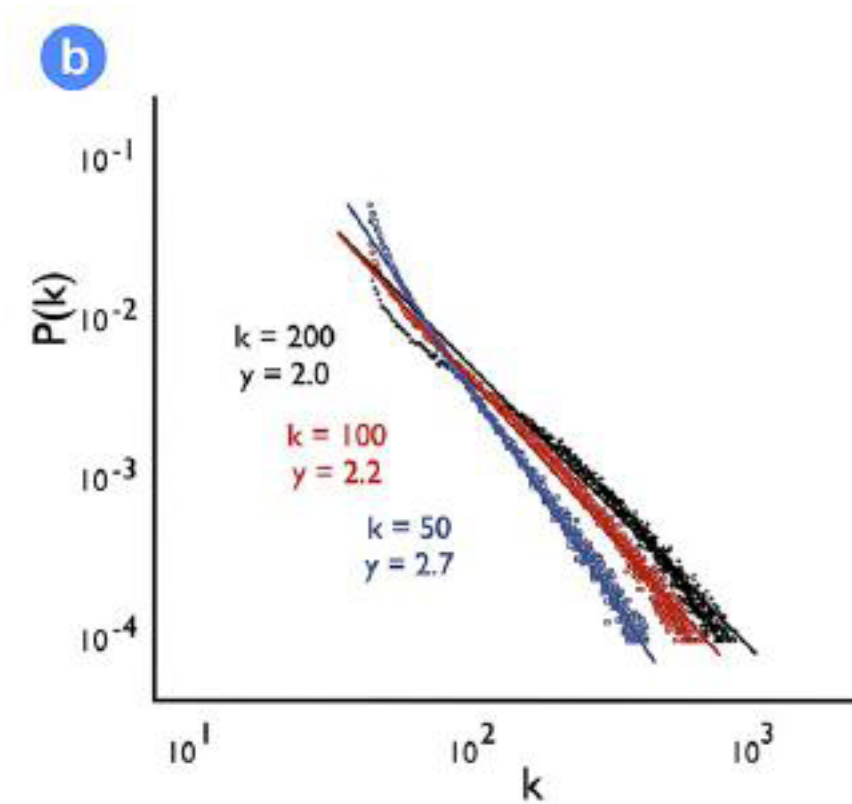
Comparing to the random network, brain network is known to have higher clustering coefficient, shorter path length and power law form of $P(k) \sim k^{-x^3}$. Based on these characters, brain networks are suspected to follow the pattern of **Small-world and scale-free networks**.

Small-world networks are characterized by a high level of clustering and a short average node-to-node distance (Watts and Strogatz, 1998) ← *This is pre-DTI study claim. Most likely an outdated statement that may not be true now.*

Scale-free networks are characterized by a connectivity distribution that follow $P(k) \sim k^{-x}$, indicating that most of the nodes have only a limited number of connections, but that a small number of so called hub-nodes have a large number of connections and are holding the network together (Barabasi and Albert, 1999; Grigorov, 2005)

Autistic children show increased local but reduced long-distance cortical–cortical reciprocal activity. It is also shown that autistic children have deficient corticocortical fibers (Hughes et al., 2007).

One can test the hypothesis of increased local connectivity by calculating the degree of each node and clustering coefficient (CC). If the degree of nodes and CC is higher in the autistic children in a certain region comparing to the normal control, then the hypothesis can be confirmed. For the reduced global connectivity, we can calculate path length and compare this to the normal population. If the path length of autistic children are significantly shorter than that of the normal control, then one can conclude that the connectivity between the sub-networks of the brain is reduced (i.e. modules of the brain are less connected). In normal population regions of right and left Thalamus, bilateral superior temporal lobe and anterior/posterior cingulated cortex and precuneus show high connectivity degree (M.P. van den Heuvel et al., 2008)



Connectivity Distribution $P(k)$ in M.P. van den Heuvel et al (2008).

Note: Graph is in logscale !

The complex network theory has originated from the graph theory in mathematics (Strogatz, *Nature*, 2001; Newman, *SIAM Rev.*, 2003; Barabasi and Albert, *Science*, 1999). To perform the complex network analysis for the structural connectivity, the following procedures are commonly executed. (1) Construction of brain networks from large-scale anatomical connectivity dataset has to be done first of all (Rubinov and Sporns, *Neuroimage*, 2009). Structural connectivity can be inferred from histological or Neuroimaging data like DTI. After this, one has to define the nodes and links of the network possibly by anatomical parcellation (Bullmore and Sporns, *Nature Reviews Neuro.*, 2009). In addition, weighted and/or directed links can be taken into account whenever possible. And then (2) various complex measure of brain connectivity can be applied to characterize properties of the network of interest, for example, modularity, resilience, and so on. The following figure well summarized all relevant concepts of the frequently used measure of the complex network (Rubinov and Sporns, *Neuroimage*, 2009).

The structural connectivity, by itself, has to meet the need of functional integration and segregation (Tononi et al., PNAS, 1994). Hence, a certain psychiatric or other clinical patients can exhibit over-connectivity and under-connectivity. To test it, measure of the functional integration and segregation, which corresponds to over- and under-connectivity, respectively, must be devised. The well-known measure for functional segregation is the clustering coefficient, which can be defined as the number of connections between the neighbors of a node divided by the maximum number of possible connections (Watts and Strogatz, Nature, 1998). For the functional integration, characteristic path length has been applied, which is the average shortest path length between all possible pairs of nodes (Rubinov and Sporns, Neuroimage, 2009). Thus, characterization of these or other measures enables us to determine whether the clinical population has a pathological network property. Many previous studies have done this to investigate underlying mechanisms of Alzheimer's disease (Supekar et al., PLoS Comput. Biol., 2008; Stam et al., Brain, 2008), schizophrenia (Liu et al., Brain, 2008), Seizures (Ponten et al., Clin. Neurophysiol., 2007), and other neurological and psychiatric diseases.

```
function C=clustering_coef_bu(G)
%C=clustering_coef_bu(G); clustering coefficient C, for binary undirected
graph G
%
```

```
%Reference: Watts and Strogatz, 1998, Nature 393:440-442
```

```
%
```

```
%Mika Rubinov, UNSW, 2007 (last modified September 2008)
```

```
n=length(G);
C=zeros(n,1);
```

Survival tip:

```
for u=1:n
```

```
    V=find(G(u,:));
```

```
    k=length(V);
```

```
    if k>=2;                %degree must be at least 2
```

```
        S=G(V,V);
```

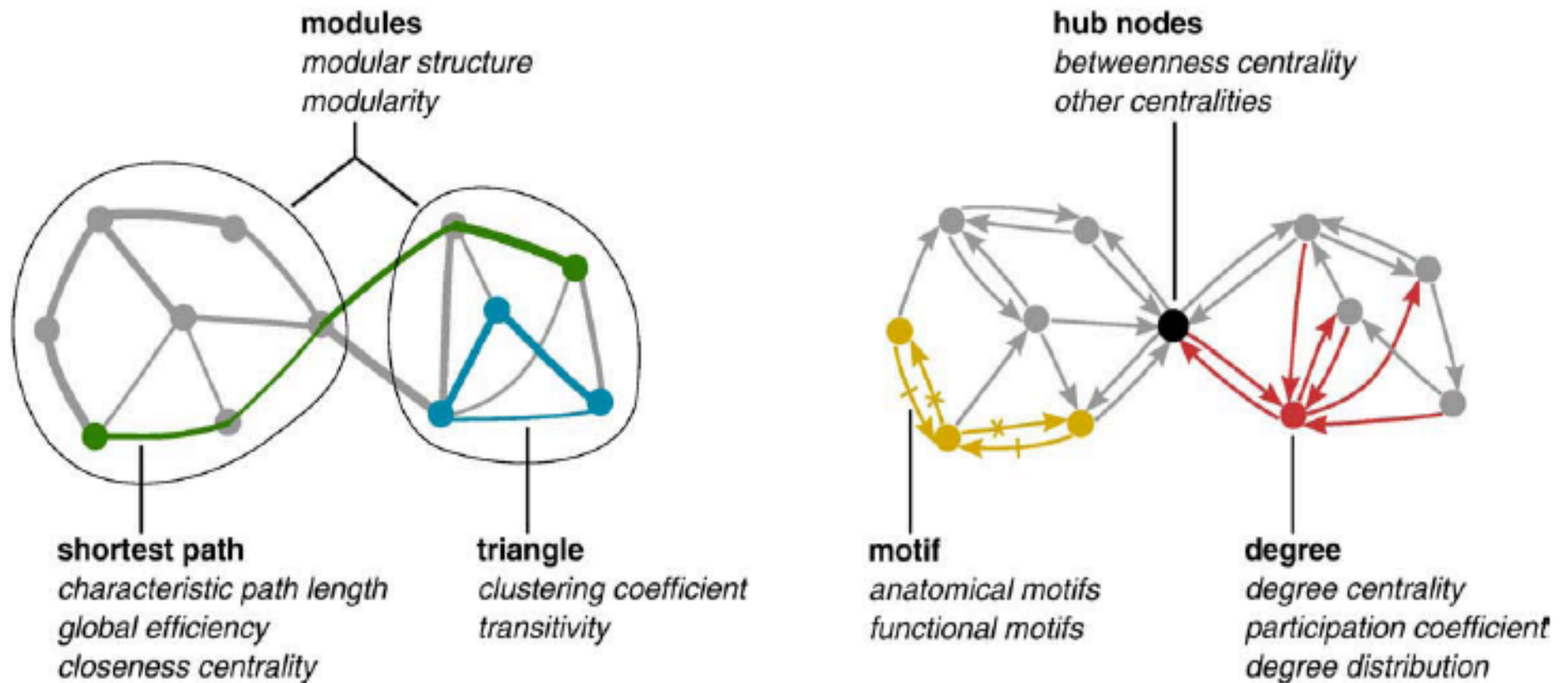
```
        C(u)=sum(S(:))/(k^2-k);
```

```
    end
```

```
end
```

*Reference, reference and
reference.*

Various network complexity measures



Rubinov and Sporns, Neuroimage, 2009

- 1) Node degree, degree distribution (Amaral et al. PNAS 2000, Barabasi et al. Science 1999)
- 2) Clustering coefficient (Watts et al. Science 1998, Milo et al Science 2002)
- 3) Hubs, centrality (Freeman et al. Sociometry 2977)
- 4) Modularity (Girvan et al. PNAS, 2002, Guimera et al, PNAS 205)

HW13 Solutions

Explain clearly what Wishart distribution is.
Randomly simulate 1000 Wishart distribution in MATLAB. Explain where Wishart distribution can be used in brain imaging.

No point given for any student who couldn't clearly connect to the description of Wishart distribution to the actual MATLAB code used.

Please don't even bother to submit things you don't understand. It is your job to convince me you clearly understand the material.

The chi-square distribution is formalized as

$$X^2 = \sum_1^k \left(\frac{X_i - \mu_i}{\sigma_i} \right)^2$$

where X_i is a normally distributed vector, μ_i is the mean of the vector, σ_i is the standard deviation of the vector, and k is the number of dimensions (or vectors).

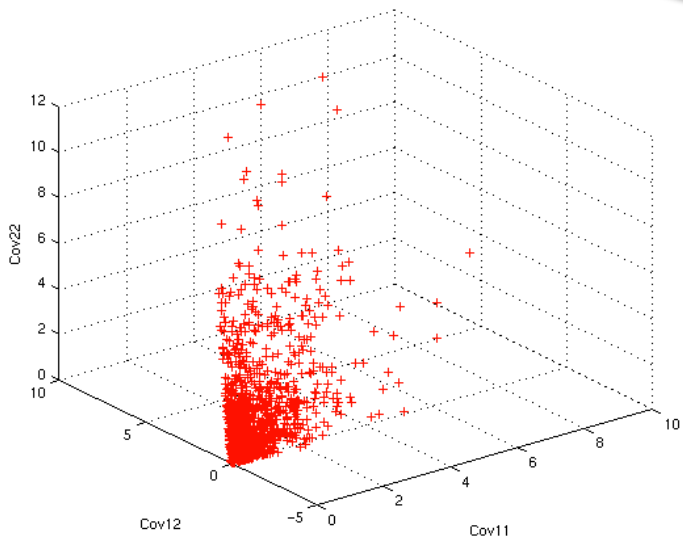
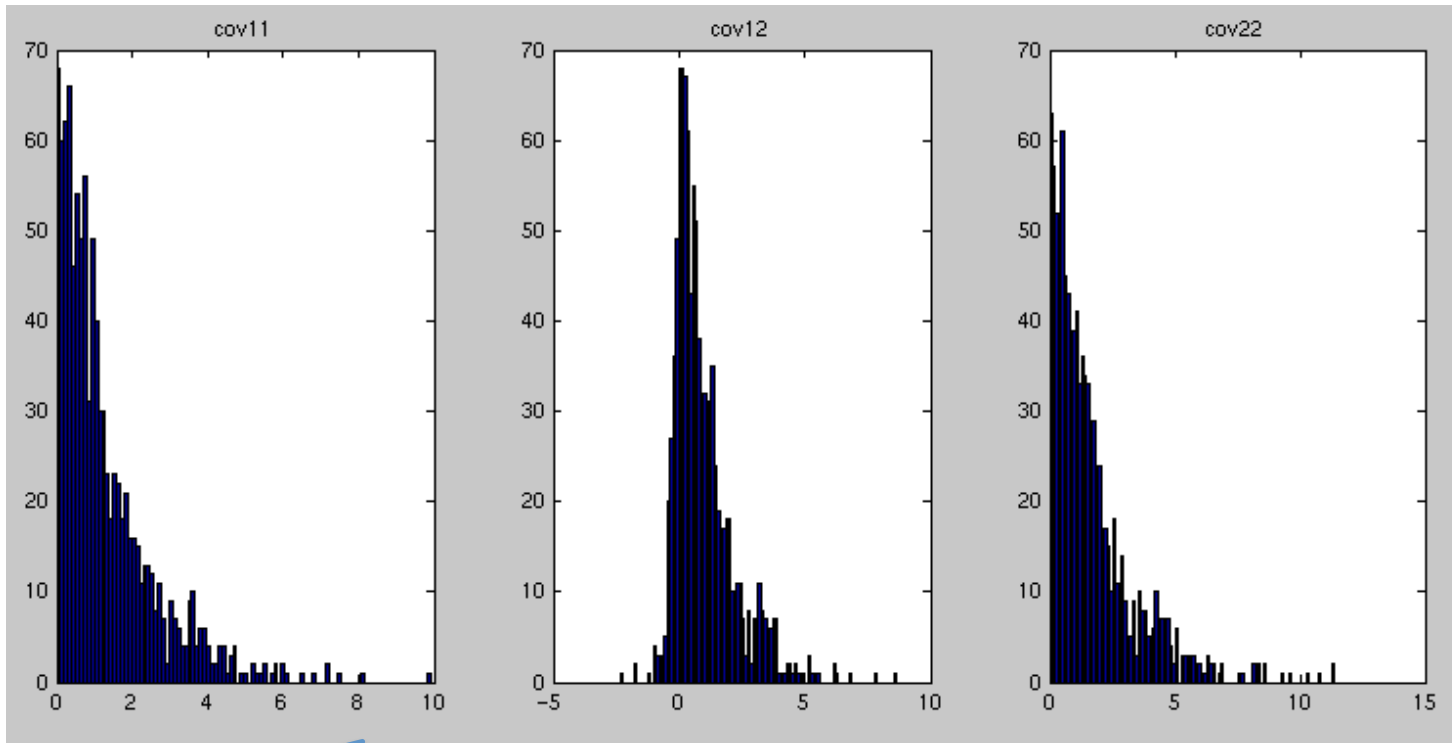
And the Wishart distribution is formalized as

$$\mathbf{S} = \mathbf{X}^T \mathbf{X} \sim \mathbf{W}_p(\mathbf{V}, n)$$

when \mathbf{X} is an $n \times p$ matrix, each row of which follows normal distribution in p -dimensions as

$$\mathbf{X}_{(i)} = (x_i^1, \dots, x_i^p) \sim N_p(\mathbf{0}, \mathbf{V})$$

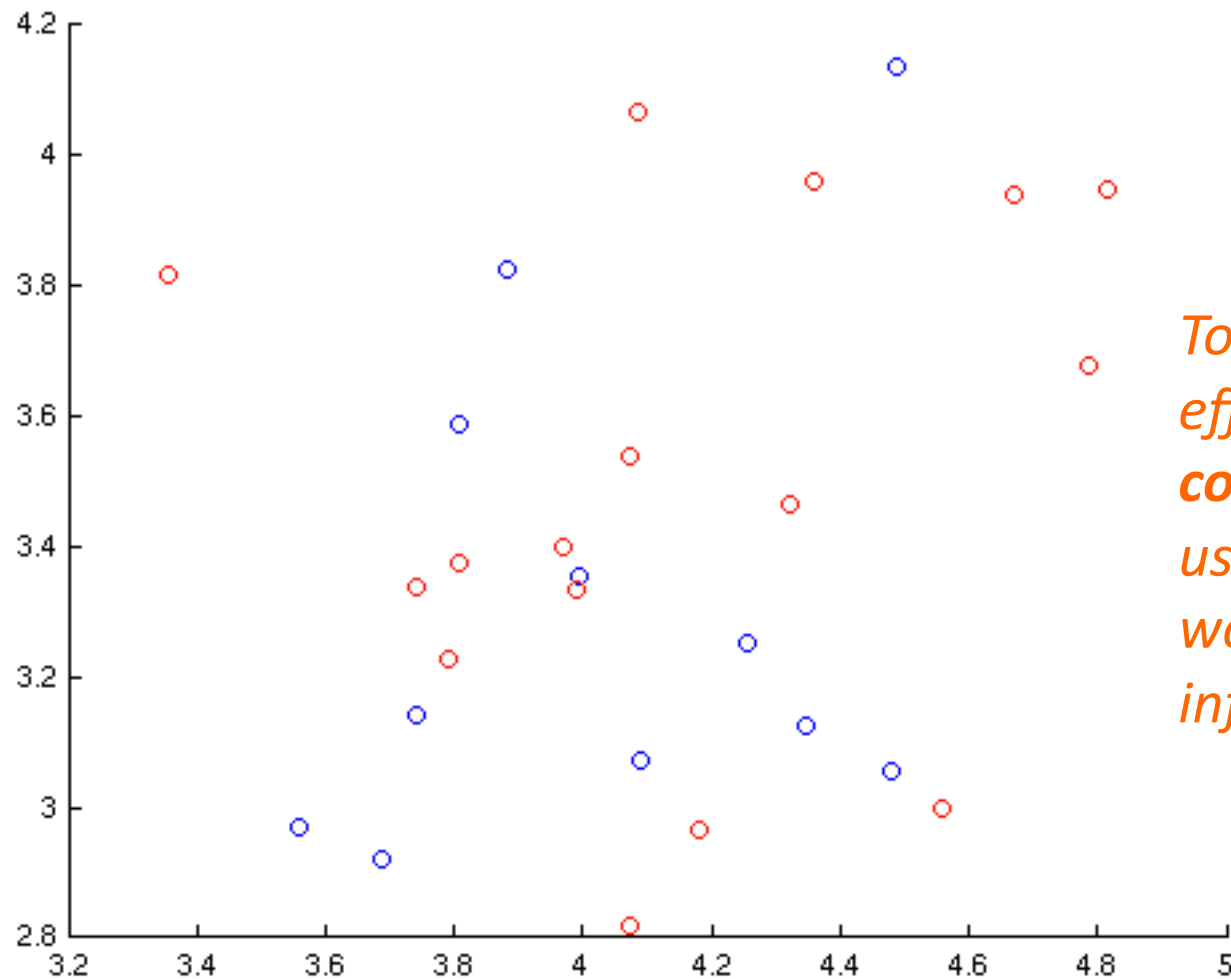
and the positive integer n is the number of degrees of freedom, \mathbf{V} is a positive-definite matrix for scale, sized $p \times p$.



Diagonal terms are related to Chi-square distribution

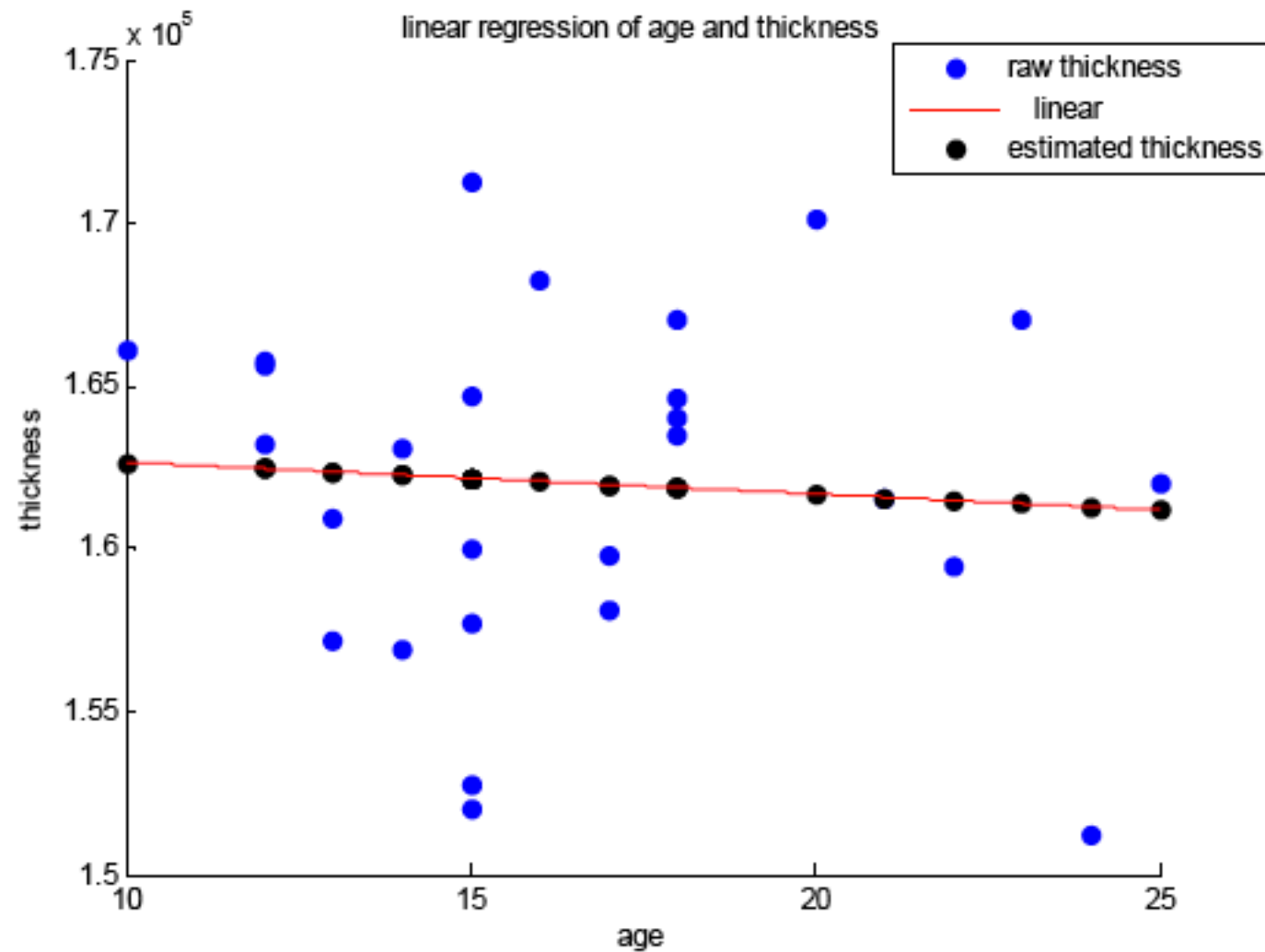
HW14 Solutions

Intercorrelation analysis of cortical thickness. Following Lerch et al. (2006. NeuroImage), compute the intercorrelation of cortical thickness and display the result using our autism data set. You can choose any seed vortex to construct the correlation map. Determine if there is any correlation difference between the groups.



*To incorporate age effect, **partial correlation** has to be used. Then how you would incorporate age information?*

Thickness of seed vertex (visual cortex, -22.5100, -101.2880, 16.3500) vs. target vertex (left parietal lobe -8.69, -55.29, 74.66) in Control (blue) and Autism (red).



By fitting $\text{thickness} = c_1 + c_1 \cdot \text{age}$ and obtaining the predicted thickness

Correlation on residual

$$\text{thick}_i = c1 + c2 * \text{age}_i + e_i$$

Correlation



$$\text{thick}_j = c1 + c2 * \text{age}_j + e_j$$

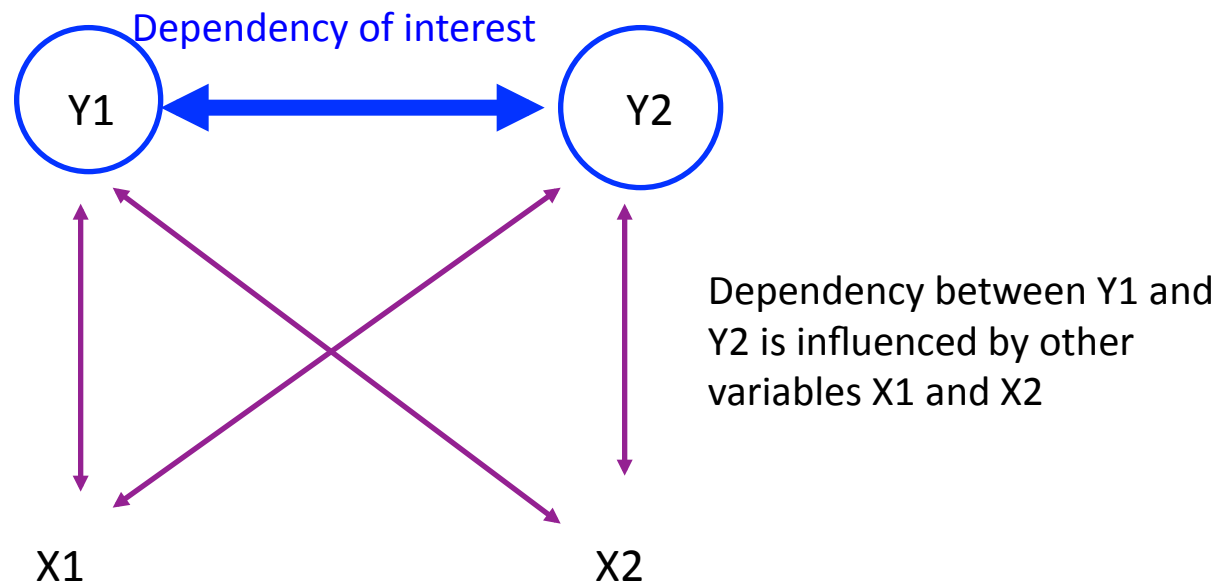
Partial Correlation



Are they same or different?

Partial correlation

Measure of dependency while removing the effect of other variables.



Read Chapter 2.11 of the textbook

Case study:

We are interested in relation between

Y_1 = cortical thickness

Y_2 = behavioral measure

Fact:

- Cortical thickness related to age (X_1)
- Cortical thickness related to brain size (X_2)

What we want:

$\text{Corr}(Y_1, Y_2)$ while accounting for X_1 and X_2

$$Y = (Y_1, Y_2), X = (X_1, X_2)$$

Covariance matrix:

$$\mathbb{V}(Y, X)' = \begin{pmatrix} \Sigma_{YY} & \Sigma_{YX} \\ \Sigma_{XY} & \Sigma_{XX} \end{pmatrix}$$

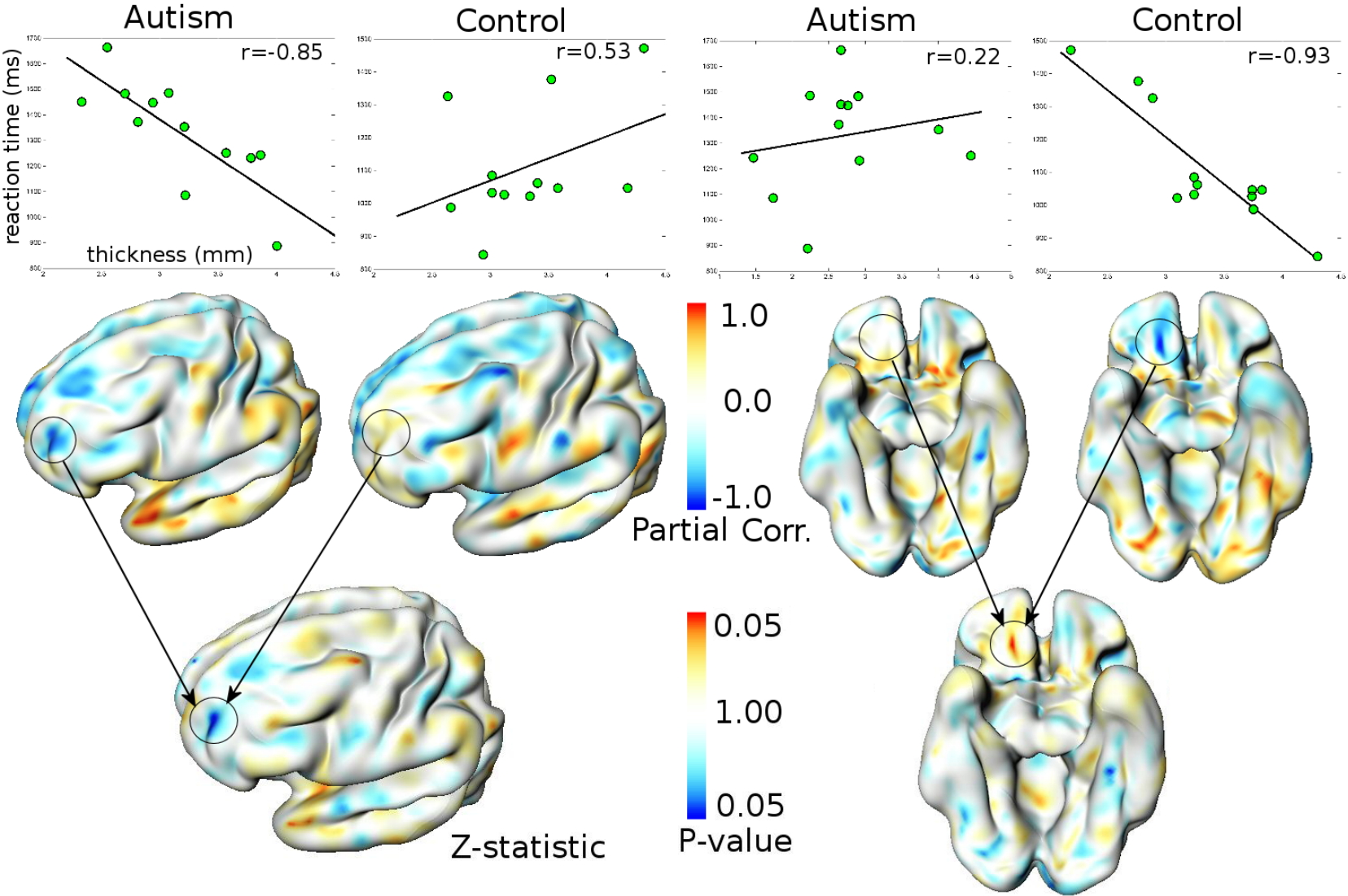
Partial covariance of Y given X:

$$\Sigma_{YY} - \Sigma_{YX} \Sigma_{XX}^{-1} \Sigma_{XY} = (\sigma_{ij})$$

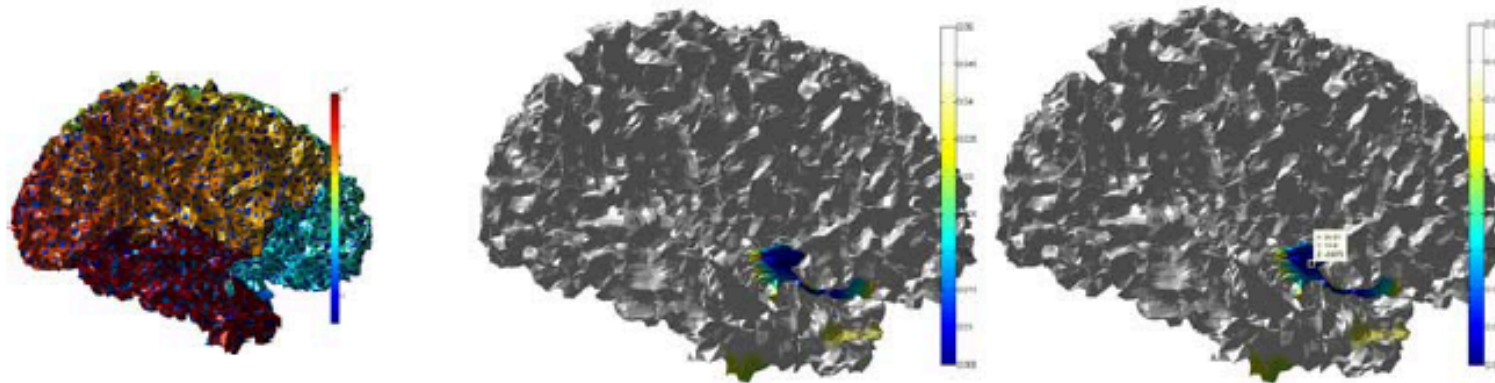
Under normality,
this is equivalent to the conditional covariance:

$$\text{Cov}(Y|X)$$

Correlation of emotion recognition response time and cortical thickness while accounting for age and brain size



Firstly, Designation of a seed vertex: I chose the seed vertex, where group differences are detected at a threshold of $p < 0.01$ (from previous HW8). Seed vertex is represented with x (30.5), y (18.6), z (-9.9) coordinates as below. Corresponding vertex number is 16071, right ventrolateral prefrontal cortex (BA47/45/44).



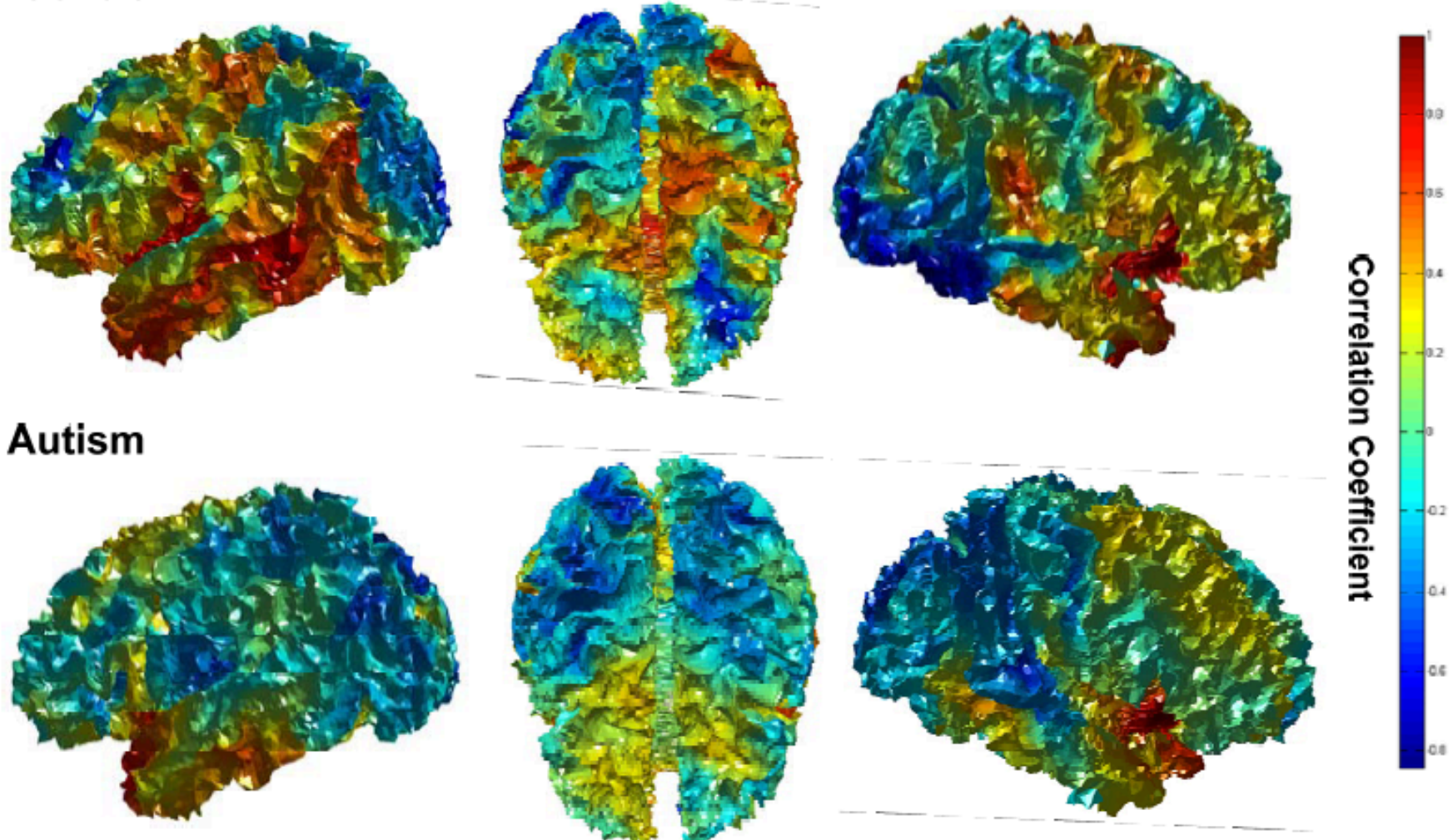
% Pearson correlation at seed point 16071

```
[rho1, pval1] = corr(control_t(:,16071), control_t(:,:));
```

```
[rho2, pval2] = corr(autism_t(:,16071), autism_t(:,:));
```

Can't possibly simpler than this!

Control



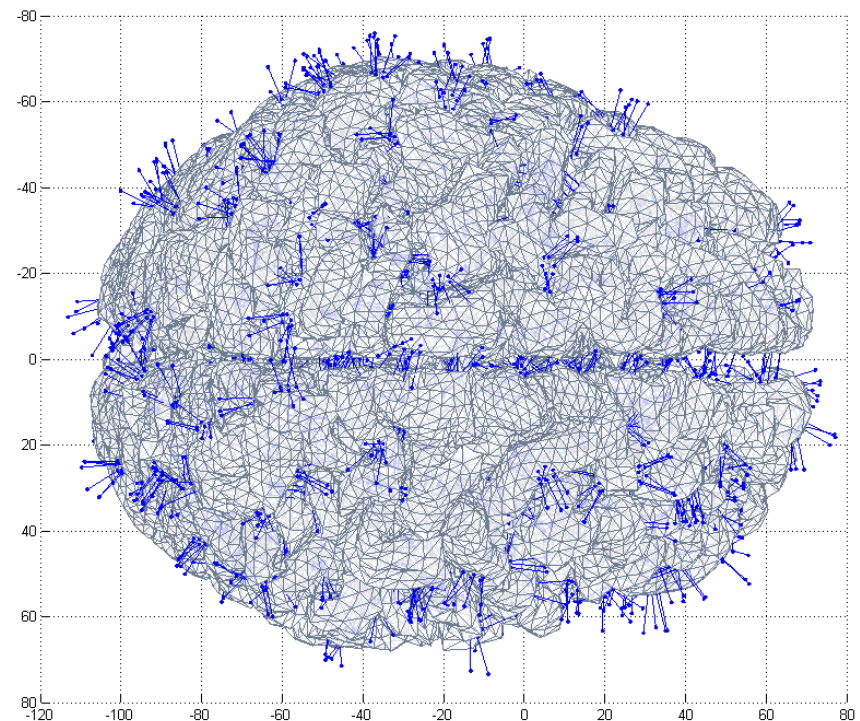
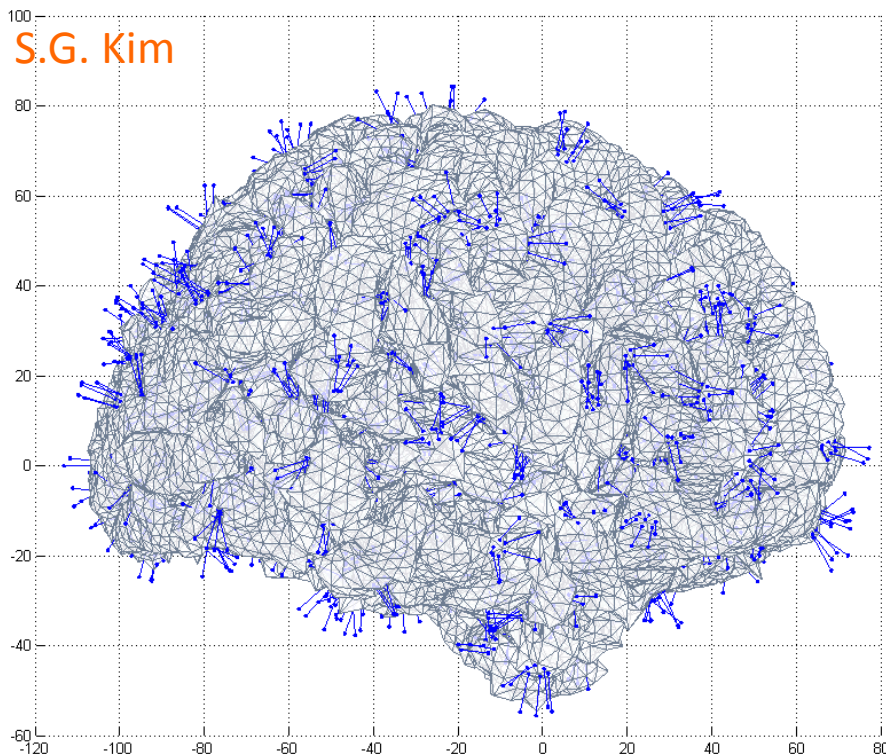
Specifically, seed vertex with right temporal region in autism shows decreased association than controls. This result partly provides supporting evidence that altered cognitive process is based in abnormality in prefrontal-limbic circuitry in autism (Courchesne et al 2004 *Curr Opin Neurol*).

How to perform test on correlation difference?

Random permutation test

Topic for Statistical Methods in NeuroImage Analysis in 2011

HW17: Estimate normal vectors on the above cortical surface without using PCA. Compare your method with PCA. Which one performs better? Other than fitting a quadratic surface, why estimating surface normal is important in brain imaging applications. Discuss.



Weighted average with respect to interior angles

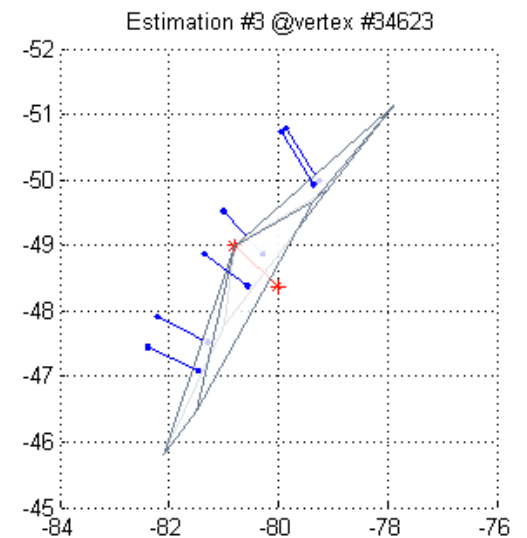
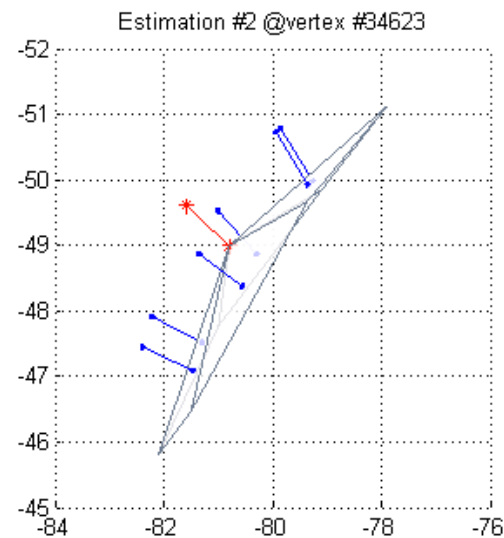
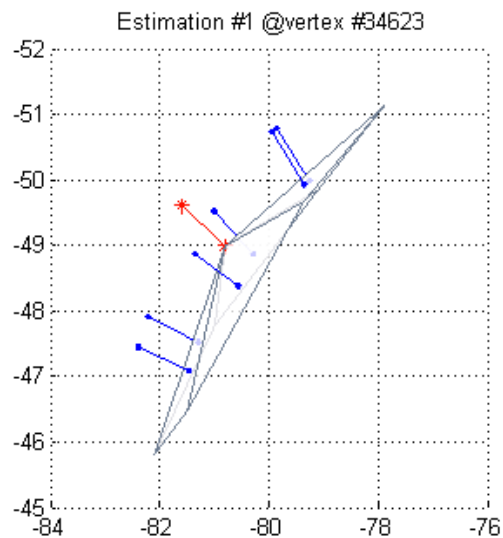
$$\mathbf{n}_j = \frac{\sum_{i=1}^m \varphi_i \mathbf{n}_i}{\sum_{i=1}^m \varphi_i}$$

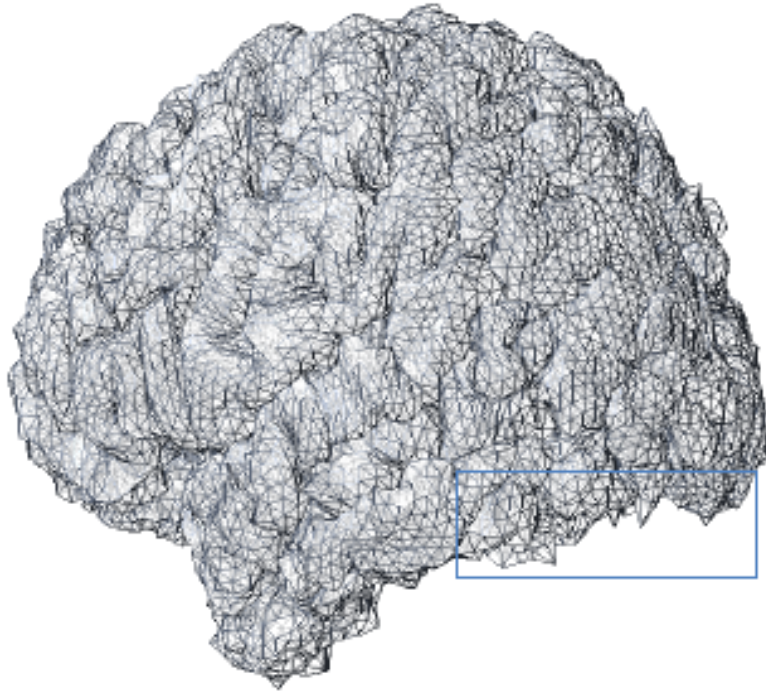
as Estimation #1,

Weighted average with respect to areas

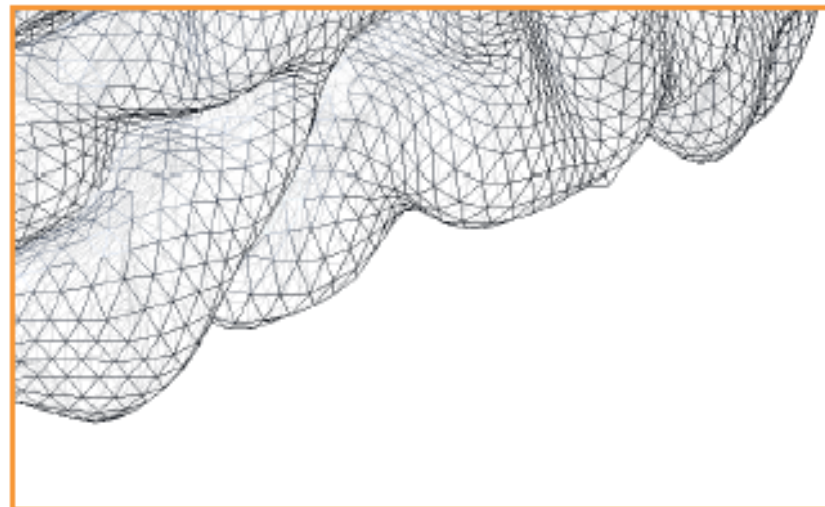
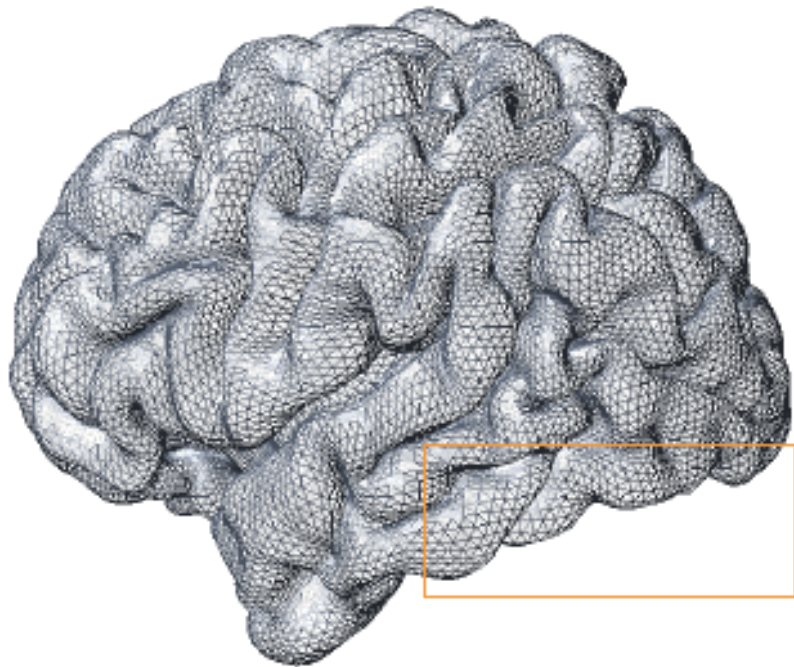
$$\mathbf{n}_j = \frac{\sum_{i=1}^m T_i \mathbf{n}_i}{\sum_{i=1}^m T_i}$$

as Estimation #2.





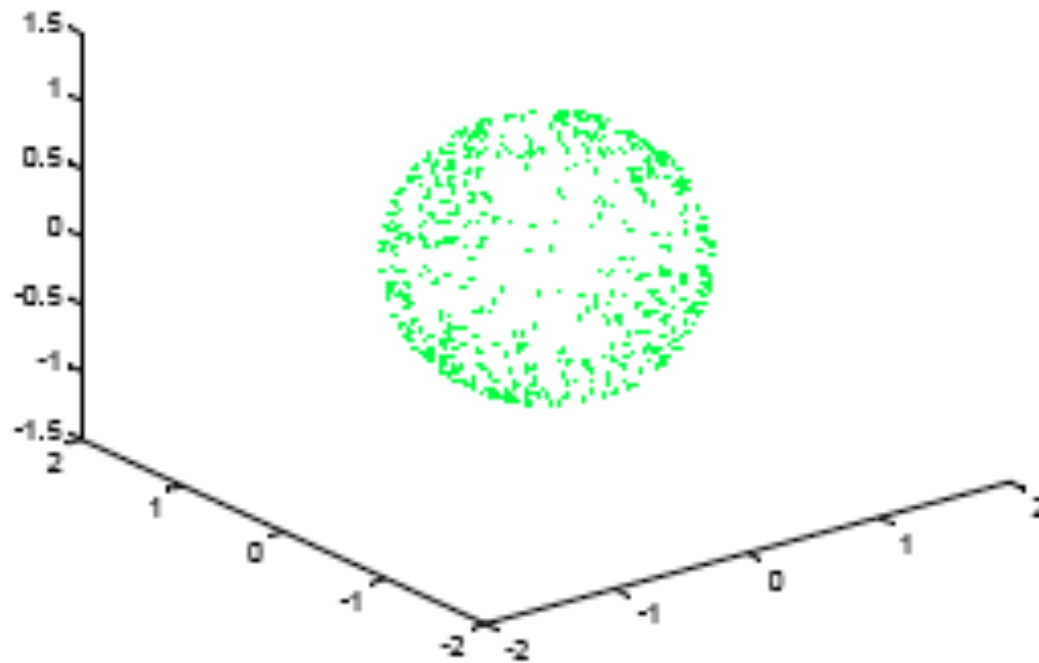
Mesh filtering improves the quality of surface.
Hence, it improves the normal vector estimation.



Validation

EunKyung Kim

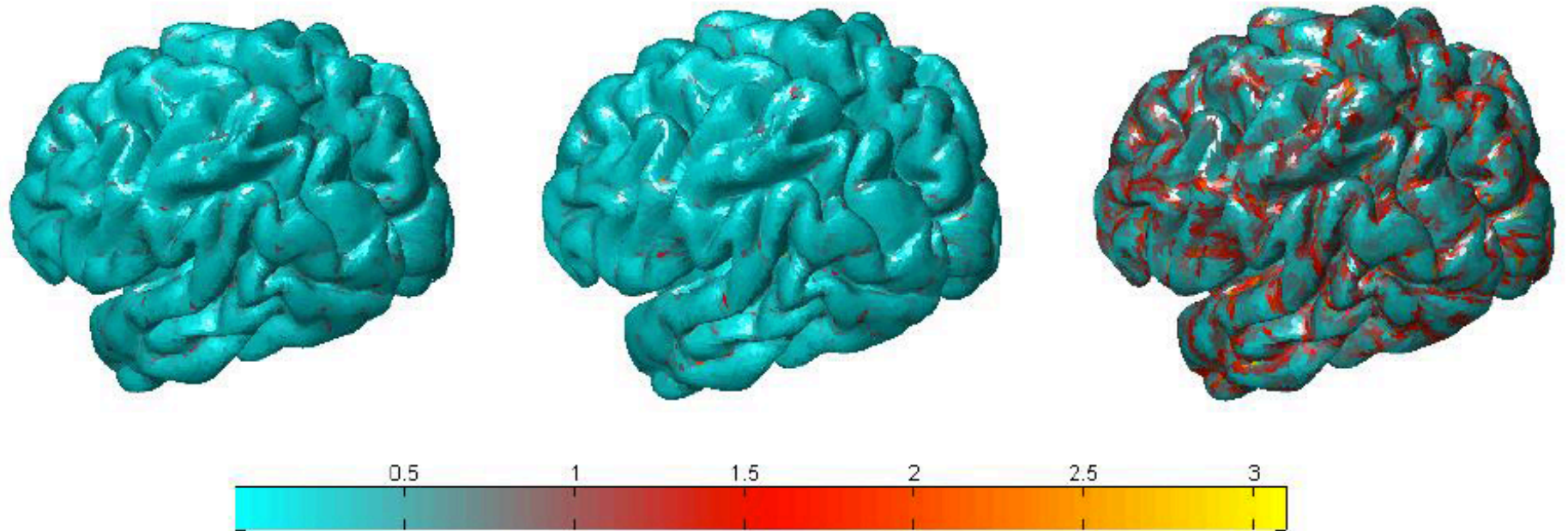
Validation against unit sphere where normal vectors are known analytically.



Measuring the difference between two normal vectors

$$|error_i^j| = \cos^{-1} \frac{\langle \mathbf{n}_i^j, \mathbf{s}_i^j \rangle}{\|\mathbf{n}_i^j\| \|\mathbf{s}_i^j\|}$$

where \mathbf{n}_i^j is the unit normal estimation using method j on vertex i on a noisy surface and \mathbf{s}_i^j the unit normal estimation using method j on vertex i on a smooth surface. The error map visualized on the smoothed surface in Fig. 12.



SeokJun Hong

1. Assume that there is a 2D plane which normal vectors \vec{n} is (a, b, -1) in 3D space and this plane can be expressed as an equation like,

$$aX + bY + c = Z$$

2. We have neighboring points per one center point and the three dimension coordination of these points form a matrix D (X, Y, Z).
3. For setting up the regression along the assumption, it could be expressed by,

$$\overbrace{D(:, 3)}^Y = \overbrace{[D(:, 1) \quad D(:, 2) \quad 1]}^X \begin{matrix} \beta \\ \left[\begin{matrix} a \\ b \\ c \end{matrix} \right] \end{matrix}$$

And the beta coefficient is calculated as a manner of OLS,

$$\beta = \text{inv}(X' \times X) \times X' \times Y$$

4. The unit normal vector of local surface consisting of a node set is

$$\frac{1}{\sqrt{a^2 + b^2 + 1^2}} (a, b, -1)$$

The normal vector is considered as a kind of sensitive feature to represent the unique property of local surfaces. For example, the well-known skull stripping tool, BET (fmrib oxford; www.fmrib.ox.ac.uk/fsl/bet2/index.html) calculates the normal vector for estimating the growth boundary such that the surface would be forced to be smooth and all vertices would be equally spaced [Stephen M. Smith, Hum Brain Map, 2002]. The normal vector also is used as the landmark feature to minimize the difference between the gradient points on image and this normal vector when performing surface-based registration. This minimization step finally achieves to register atlas surface to subject image in the research of [Zhiyong Xie et al, Medical Imaging 2006]. Actually traditional use of this normal vector predominates over the cortical thickness analysis. Although there might be better algorithmic definitions of thickness for accurately detecting cortical surface, the thickness is basically defined as the length from the inner/outer surface vertex to the outer/inner surface along the normal direction on the surface vertex [Tianming Liu et al, NeuroImage 2008].

The usefulness of estimating the normal vector is not limited to the structural study using anatomical T1 image. Recently several Diffusion Tensor Imaging (DTI) has studied the properties of principle direction drawn from Tensor Matrix based on the normal vector on the surface. For example, Hao Huang et al. has studied the anatomical properties of Human Fetal Brain using DTI and in this research, they calculate the normal vectors for measuring of the angle between the tensor primary eigenvector and the normal surface vector [Hao Huang et al, J Neurosci, 2009]. In contrast, there is the case that the principle direction of DT matrix around the surface boundary was intensively calculated for a better estimating the normal vectors, which is called as Surface-Normal Mapping using DTI [Evern Ozarslan et al, Biophysical J 2008].

Dajung Kim

CURVATURE INDICES: This is assigned to every surface triangle and quantifies the degree of surface convexity or concavity. One method to calculate curvature is to sum the projections of the centers of surrounding triangles onto the surface normal of each triangle. Positive CI reflecting convexity is 'gyral', while a negative or concave CI is 'sulcal'. The higher the absolute value of the CI, the 'tighter' the curve. Conversely, the lower the absolute value of the CI, the 'looser' the curve (Nopoulos et al, 2000; Bartesaghi and Sapiro, 2001).

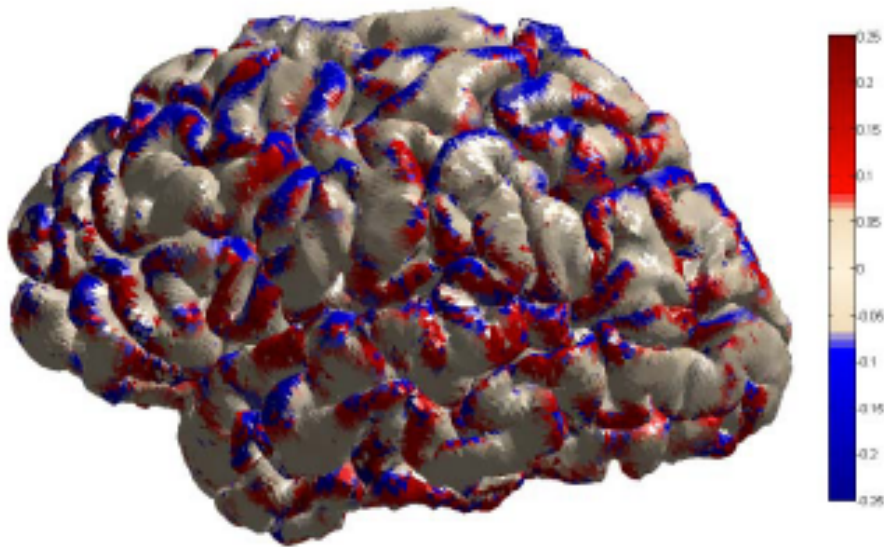
-CORTICAL DEPTH: This is calculated as the magnitude of the vector normals to each surface triangle, originating at the pial triangle surface and terminating at the gray/white surface (Nopoulos et al, 2000). This can account for cortical thickness (Andrade et al., 2001). Surface normal at each location is a prerequisite for principled cortical thickness measure (McDonald et al., 2008)

HW18: Either compute surface curvatures or come up with your own measure of surface bending/folding on the above cortical surface. Why cortical bending/folding is biologically important? What do you think is causing the cortical folding? Discuss.

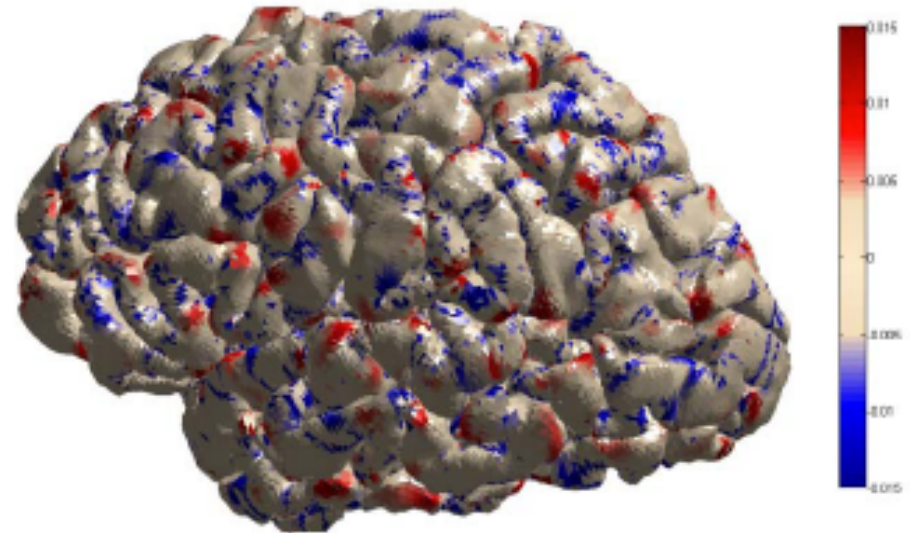
SeokJun Hong

Following the quadratic surface fitting method given in the textbook,

Mean Curvature



Gaussian Curvature



S.G. Kim

Following Cachia et al. (2003), the mean curvature estimation (H) can be computed as

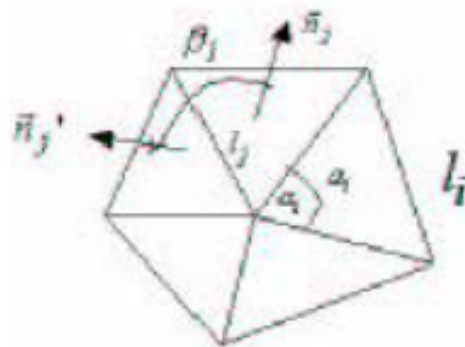
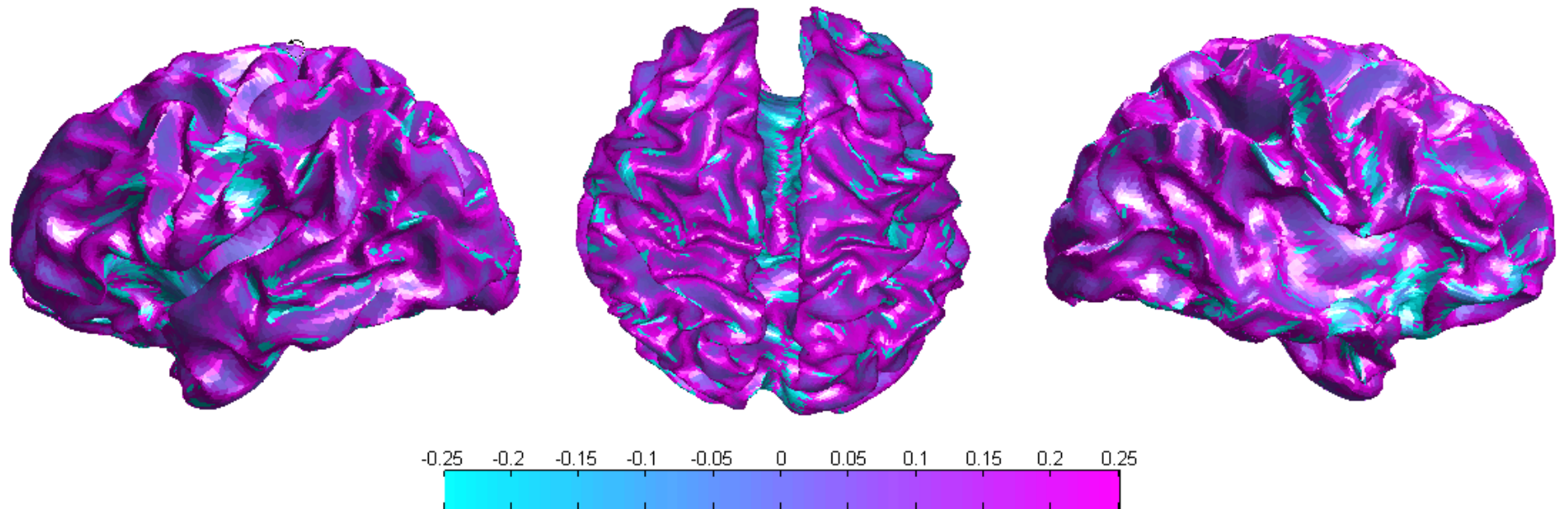

$$H = \frac{\frac{1}{4} \sum_j \beta_j l_j}{\frac{1}{2} \sum_i a_i - \frac{1}{8} \sum_i l_i^2 \cot(\alpha_i)}$$

Fig. 3. Approximation of the mean curvature from an irregular mesh [60]. α_i and a_i denote respectively the triangle angles and areas; β_j correspond to the dihedral angles between the normals n_j ; the edge lengths are noted l_i .



The meshes model the cortical surface of the brain consisting of gyri and sulci. We used these meshes to calculate the mean curvature (do Carmo, 1976) at thousands of points across the cortical surface. Mean curvature is an extrinsic surface measure and gives information about the change in normal direction along the surface (normals are vectors pointing outwards perpendicular to the surface). Mean curvature at a given point is defined as

$$T_{\text{curvature}} = \sum_{i=1}^n \left(\frac{(\tilde{x}_v - \tilde{x}_v) \cdot \tilde{N}_v}{B_v} \right)^2$$

where \tilde{x}^v is the centroid of its neighbors of vertex v , B_v is the average distance from the centroid of each of the neighbors, and I is the vector product operator

(MacDonald: A Method for Identifying Geometrically Simple Surfaces from Three Dimensional Images. PhD Thesis McGill University, Montreal).

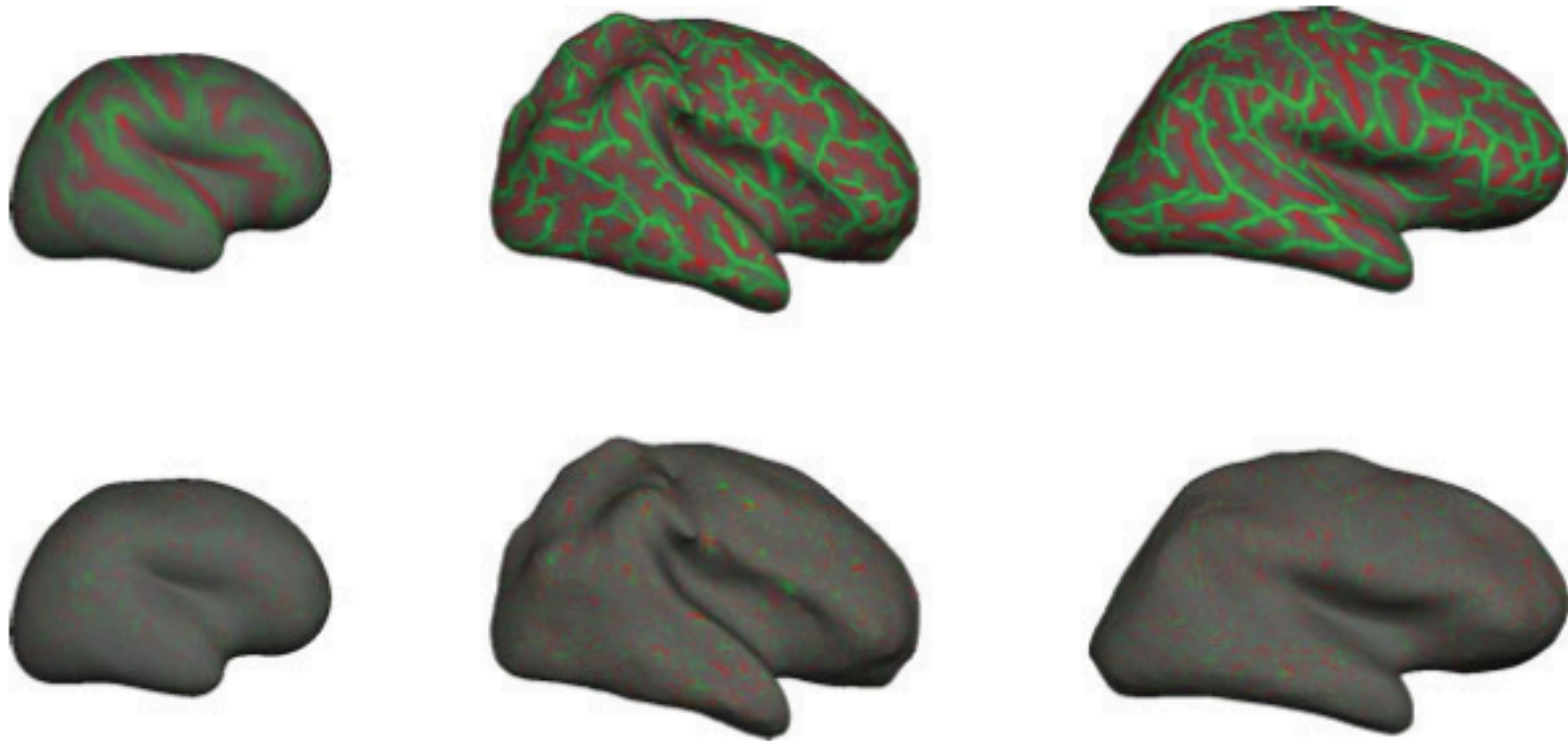


Figure 2. Projections of principal curvature functions k_1 (top) and k_2 (bottom) across entire brain surfaces. On left, the youngest neonate at 30.4 weeks CGA. In middle, the term neonate at 40.3 weeks CGA. On right, an adult subject. The complexity of the topological pattern of k_1 appears to peak around term and appears to represent the primarily cylindrical folds of the gyri/sulci. In contrast the topological variation of k_2 is at a higher frequency and appears to represent small local “bumps” or “dimples.” (Pienaar, 2008).

References

P. Rakic, Specification of cerebral cortical areas, *Science* 241 (1988), 170–176.

P. Rakic, A small step for the cell, a giant leap for mankind: A hypothesis of neocortical expansion during evolution, *Trends Neurosci* 18 (1995), 383–388.

D. C. Van Essen, “A tension-based theory of morphogenesis and compact wiring in the central nervous system,” *Nature*, vol. 385, no. 23, pp. 313–318, January 1997.

J. Régis, J.-F. Mangin, T. Ochiai, V. Frouin, D. Rivière, A. Cachia, M. Tamura, and Y. Samson, ““Sulcal root” generic model: A hypothesis to overcome the variability of the human cortex folding patterns,” Neurol. Med. Chir. (Tokyo), vol. 45, pp. 1–17, 2005.

What causes cortical folding:

What drives the cortical folding during the development process is not exactly known. However, several theories suggested that it is determined by tension of the wiring between the cortical areas (Van Essen, Nature, 1997), the different speed of growth in the cortical layers (Richman et al., Science, 1975), the subcortical cell generation (Kriegstein et al., Nat. Rev. Neurosci., 2006).

SooKyun Park

Kriegstein A, Noctor S, Martínez-Cerdeño V (2006) Patterns of neural stem and progenitor cell division may underlie evolutionary cortical expansion. Nat Rev Neurosci 7:883– 890.

Richman DP, Stewart RM, Hutchinson JW, Caviness JVS (1975) Mechanical model of brain convolitional development. Science 189:18 –21.

Rajimehr R, Tootell RB (2009) Does retinotopy influence cortical folding in primate visual cortex?. J Neurosci 20(36): 11149-11152.

Van Essen DC (1997) A tension-based theory of morphogenesis and compact wiring in the central nervous system. Nature 385:313–318.

The folding cortical surface has been traditionally an intriguing topic in the neuroscience field. Many researchers have studied about why the cortical surfaces are folded and bended during their development, which is so called as 'gyrogenesis' or 'gyrification'. Among many theories related to the 'gyrification', it is firmly entrenched that cortical surface folding is a process for maximizing the surface area, which could be considered as the amount of neuronal layer of neocortex, as constrained by limited brain volume and non deformable neighboring structures [David P. Richman et al., Science 1975]. However this sort of a simple reasoning seems to miss the core mechanism hidden in the gyrification.

Early genetic studies have suggested that the cortical buckling has partly determined by genetic factors. AJ Bartley et al have researched the cortical gyral patterns controlled by genetic factors using monozygotic and same-sex dizygotic twins. The result of their research has shown that genes give a considerable effect to variations in gyral patterns [Bartley et al, Brain 1997]. On the other hand, the theory of Mima and Mikawa has suggested that the gyrification pattern partly depends on nonuniform distribution of neuronal differentiation and neurite growth [Mima T., Mikawa T Dev Dyn 2004].

in addition to the genetic studies about gyrification, the mechanical modeling of actual forces and tension which make the cortical surface folded has been researched. In one research, a mechanical analysis of the elastic behavior of cortical surface during development has revealed that gyrification would be developed if the stress parameters, which were set up in their model, will be increased [David P. Richman et al., Science 1975]. Roberto Toro et al. have proposed the convolution of mammalian cortex is natural mechanical consequence of neuronal differentiation and growth through their simulation. They explained two fundamental mechanical properties which take participate in the cortical folding: one is 'elasticity' (a recovery of initial shape) and the other is 'plasticity' (permanent change of the shape). Through the computational simulation for showing the result about the effect of these mechanical properties on cortical surface, they have revealed that as the development of neuronal cell progresses, the convolutions become accommodated in the cortical layer due to the influence of non-isotropic forces [Roberto Toro, Yves Burnod, Cerebral Cortex 2005]. Plausible examples of such non-isotropic force and tension are cell division, cell migration, myelination, cortical connectivity, synaptic pruning and all of which may interact [Crino, P.B. & J. Eberwine J Neurosci Res 1997] [Cardoso C et al, Human Mutation 2002] [<http://en.citizendium.org/wiki/Gyrification>]

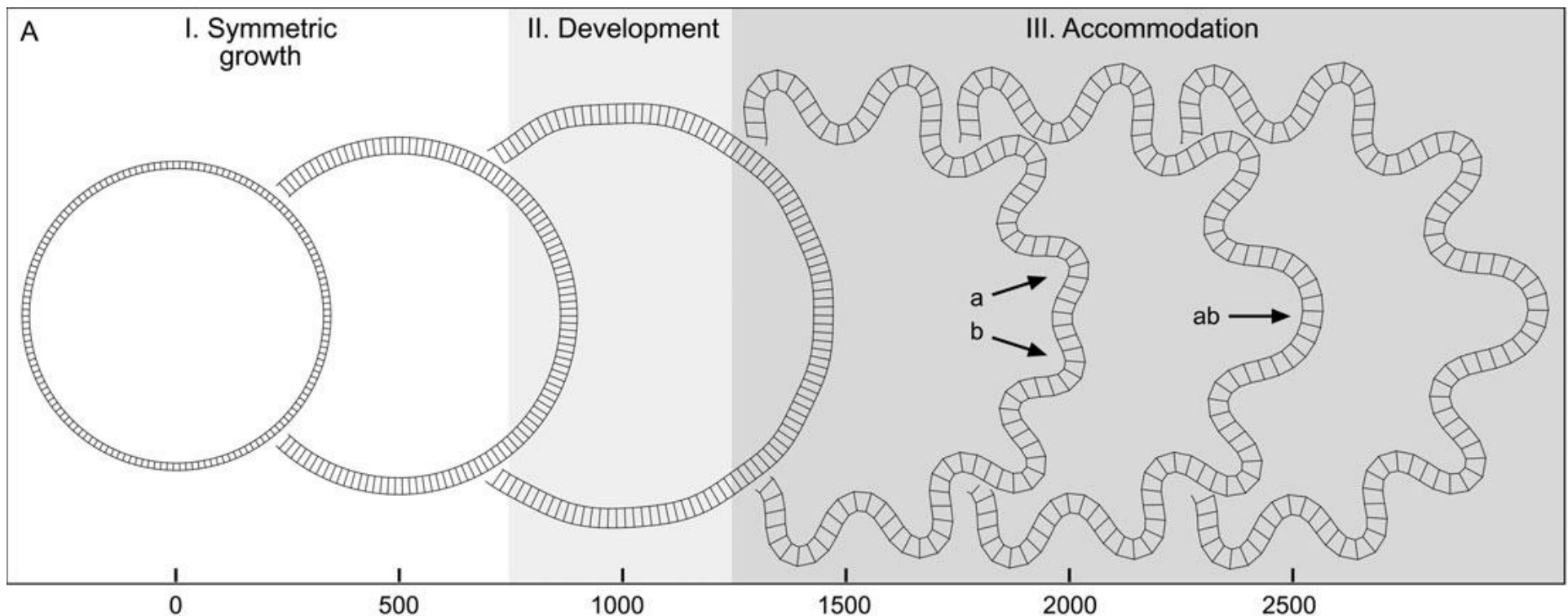
DaJung Kim

Congenital malformation of frontoparietal polymicrogyria from smaller number of convolutions in the cerebral cortex led to profound cognitive abnormalities (Rakic, 2004) Folding patterns have sexual difference (Luders et al., 2005). Patients with psychiatric disorder such as bipolar disorder, autism, which are suspected to neurodevelopmental disease, have abnormal gyrification in specific lobes (Mirakhur et al., 2001; Liao et al., 2008; Kates et al., 2009). Genetic determination (Rakic, 2004; Kippenhan et al., 2005) and/ or the differential effects of gonadal hormones during brain growth throughout lifetime are likely to affect the gender-specific emergence of local gyrification (Thompson et al., 2001).

Cortical folding started from 16 weeks in utero, and most cortical folding is principally defined in the late second and third trimesters of fetal life (Richman et al., 1975; Armstrong et al., 1995). Remarkable aspects of cortical development are that none of the constituent neurons are generated within the cortex. Rather, cortical neurons originated from ventricular and subventricular zones lining the cerebra cavity and then migrate to their proper laminar and settle in. This process depends on the transient scaffolding formed by shafts of elongated radial glial cells that span the fetal cerebral wall (Rakic, 1974; 1988).

Richman et al. (1975) reported greater expansion of outer vs. inner cortical layers cause gyrification. Another theory proposed by Rakic (1988) indicated that cortical folding results from intracortical connections. More recently, Van Essen (1997) suggested tension along axons produce gyri between strongly connected cortical regions and sulci between weakly connected weakly.

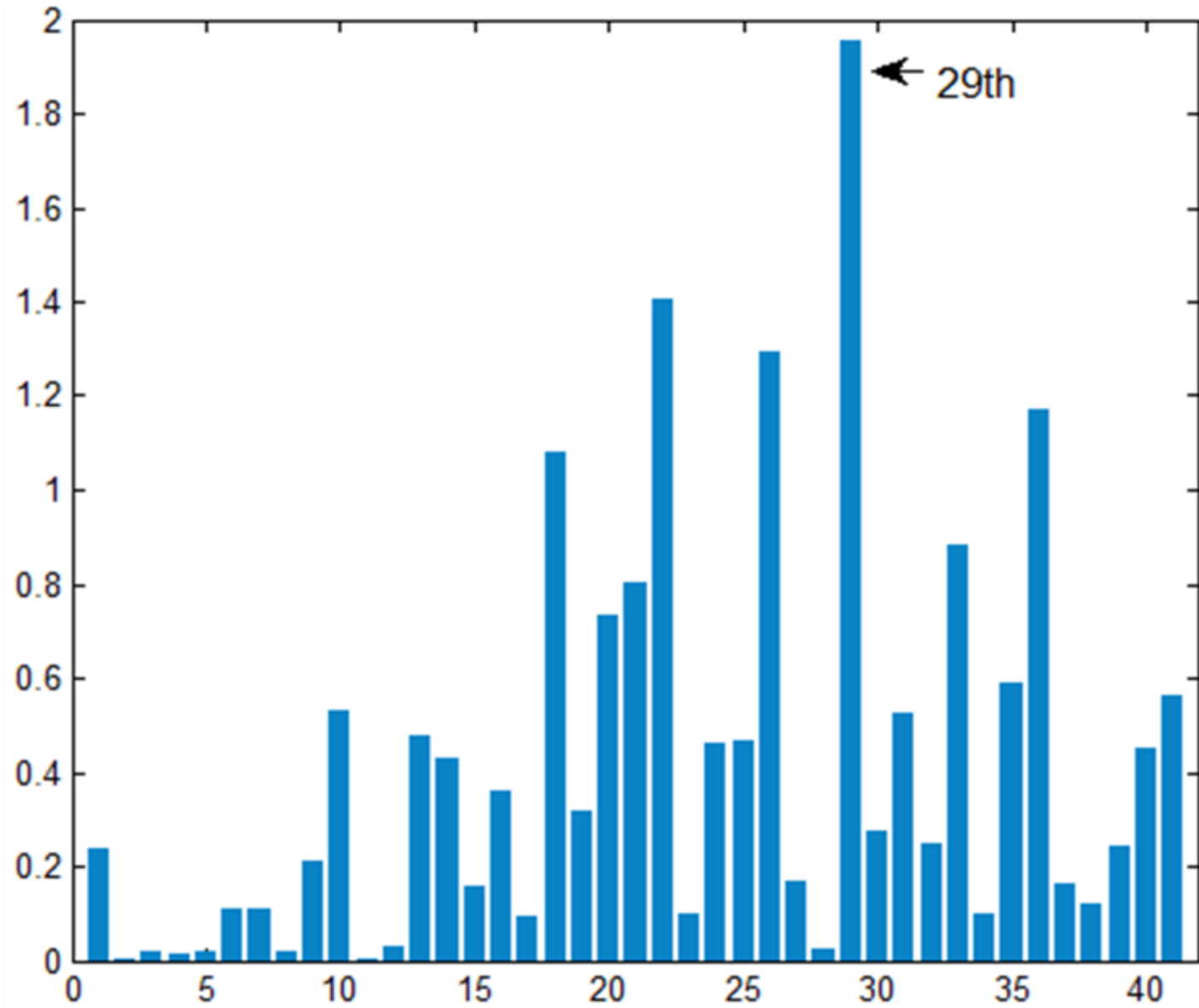
One hypothesis of the (primary) convolution is the result of cerebral cortex growth within the limitation of cranial volume. However, Toro and Burnod(2005) found that the convolutions are a natural outcome of cortical growth when they simulated their model for the development of cortical convolution



Development of convolution in model. As a results, the convolution was induced by convolution development itself. Three main steps are distinguished, symmetric growth, development, accommodation. In the last step, the convolutions (a, b) are fused into single one (ab).

HW19: Discriminate/classify cortical surfaces (autism vs. control) by using the spherical harmonic coefficients up to degree 40. Using only spherical harmonic coefficients, do you think you can localize the region of cortical shape difference? Discuss.

Hotelling's T square ($-\log_{10}P$)



HW20: Only using 5 spherical harmonic basis $Y_{lm}(0,0,\dots)$, $Y_{lm}(1,1,\dots)$, $Y_{lm}(2,2,\dots)$, $Y_{lm}(3,3,\dots)$, $Y_{lm}(4,4,\dots)$, write codes for performing the least squares approximation of estimating cortical thickness on a unit sphere. Find the best linear combination of 5 basis that give the smallest SSE among all possible combinations up to degree 60. Note: there are total 41^2 basis. So there are 41^2 choose 5 possibilities.

This is a problem you can't possibly solve using brute force approaches. Need to come up with either sampling or optimal branching strategy.

S.G. Kim

The computed SSE for this combination is $1.5128e+04$, and the computation 0.0394 seconds with Intel® Core™2 Duo CPU @ 2.99GHz with 2.00 GB RAM. Then the estimated calculation time would be $2.3359e+14$ seconds, i.e. 7 MILLION and 407.1 thousand YEARS.

HW21: Compute the Jacobian determinant.

S.G. Kim

$$\frac{\partial u_i}{\partial x_j}(\mathbf{X}_0) \cong \frac{u_i(\mathbf{X}_0 + \Delta \mathbf{x}_j) - u_i(\mathbf{X}_0)}{(\mathbf{X}_0 + \Delta \mathbf{x}_j) - \mathbf{X}_0} \text{ if } \mathbf{X}_0 \text{ is on the either edge of the field}$$
$$\cong \frac{u_i(\mathbf{X}_0 + \Delta \mathbf{x}_j) - u_i(\mathbf{X}_0)}{2((\mathbf{X}_0 + \Delta \mathbf{x}_j) - \mathbf{X}_0)} + \frac{u_i(\mathbf{X}_0 - \Delta \mathbf{x}_j) - u_i(\mathbf{X}_0)}{2((\mathbf{X}_0 - \Delta \mathbf{x}_j) - \mathbf{X}_0)} \text{ if } \mathbf{X}_0 \text{ is in the interior of the field}$$



This is the average of two different finite difference estimation. Improves the stability.

HW22: Determine if the Jacobian determinant of a deformation is normal or lognormal in distribution. Why is this an important problem in applications?

Jiwon Hur

Yanovsky et al. (2007) proposed an unbiased fluid image registration approach (Unbiased Registration Constraint). Contrary to classical methods for which the term unbiased is used in the sense of symmetric registration, unbiased means that the Jacobian determinants of the deformations recovered between a pair of images follow a log-normal distribution, with zero mean after log-transformation. The authors argued that this distribution is beneficial when recovering change in regions of homogeneous intensity, and in ensuring symmetrical results when the order of two images being registered is switched. The inverse-consistent property of the unbiased technique was shown in a validation study of the unbiased fluid registration methods (Yanovsky, 2008).

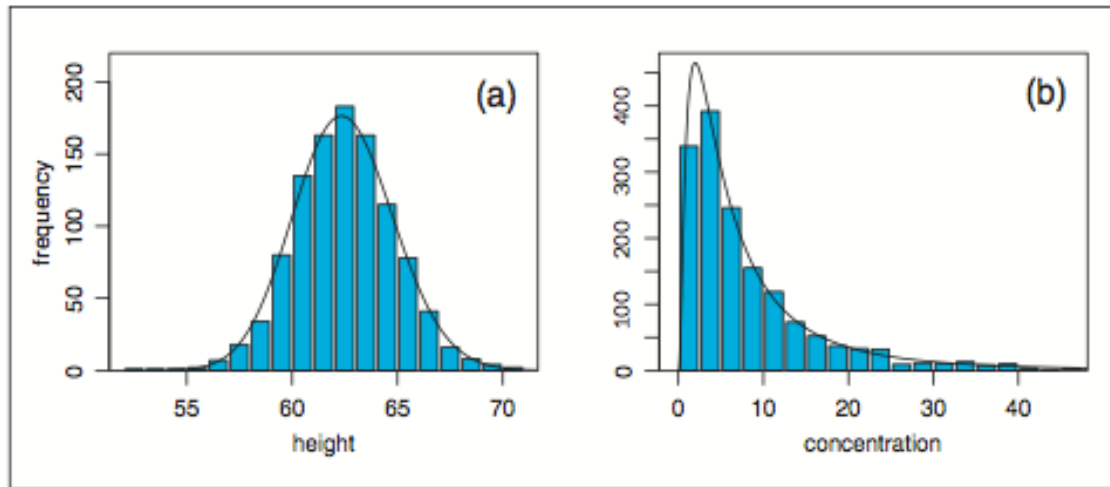


Figure 1. Examples of normal and log-normal distributions. While the distribution of the heights of 1052 women (a, in inches; Snedecor and Cochran 1989) fits the normal distribution, with a goodness of fit p value of 0.75, that of the content of hydroxymethylfurfural (HMF, $\text{mg}\cdot\text{kg}^{-1}$) in 1573 honey samples (b; Renner 1970) fits the log-normal ($p = 0.41$) but not the normal ($p = 0.0000$). Interestingly, the distribution of the heights of women fits the log-normal distribution equally well ($p = 0.74$).

I. Yanovsky, P. Thompson, S. Osher, and A. Leow, "Topology preserving log-unbiased nonlinear image registration: Theory and implementation," IEEE Conference on Computer Vision and Pattern Recognition, pp. 1–8, 2007.

I. Yanovsky, P. Thompson, S. Osher, and A. Leow, "Asymmetric and symmetric unbiased image registration: Statistical assessment of performance," IEEE Computer Society Workshop on Mathematical Methods in Biomedical Image Analysis, 2008.